12-2014

SURFACE MODIFICATIONS OF CAPILLARY-CHANNELED POLYMER (C-CP) FIBER STATIONARY PHASES: IMPROVING THE EFFICIENCY OF HIGHLY SELECTIVE ANALYTE SEPARATIONS

Abby Schadock-Hewitt
Clemson University, aschado@clemson.edu

SURFACE MODIFICATIONS OF CAPILLARY-CHANNELED POLYMER (C-CP) FIBER STATIONARY PHASES: IMPROVING THE EFFICIENCY OF HIGHLY SELECTIVE ANALYTE SEPARATIONS

A Dissertation
Presented to
the Graduate School of
Clemson University

In Partial Fulfillment
of the Requirements for the Degree
Doctor of Philosophy
Chemistry

---

by
Abby J. Schadock-Hewitt
December 2014

Accepted by:
R. Kenneth Marcus, Committee Chair
Kenneth A. Christensen
Jeffrey N. Anker
Philip J. Brown

ABSTRACT

High performance liquid chromatography (HPLC) is a fundamental methodology for the characterization and purification of macromolecules. Since its development in the 1970's, HPLC has significantly advanced its instrumentation and column technology to become a powerful analytical technique. A considerable amount of research focuses on advancements to the stationary phase, or solid support, on which molecules interact and separate. To overcome limitations of other phases that lead to poor mass transfer, slow speeds, and low efficiency, nonporous and superficially porous phases have been developed. Specifically, fiber based polymer stationary phases show great promise as stationary phases for protein separations.

The Marcus laboratory has investigated capillary-channeled polymer (C-CP) fibers as an HPLC stationary phase for the past decade. These novel shaped fibers have advantageous attributes including increased surface area over cylindrical cross section fibers, low cost, rapid mass transfer, and the ability to operate at high linear velocities without high pressure. The fibers are available in several base which allow for a wide variety of chemical interactions. What's more, surface modifications can allow for a broader range of chemical specificity. Therefore, the focus of this work is on adsorption-based surface modification of C-CP fibers.

First, modification with recombinant protein A ligand allowed for the capture and recovery of immunoglobulin G (IgG) antibody. This small scale study evaluated maximum protein A ligand density, the stability of the modification, and demonstrated the selective capture of IgG from a mixture with myoglobin (as a surrogate host cell protein) with minimal non-specific binding through the use of a sodium citrate (pH 4) wash buffer. IgG was recovered with high yield with a 0.1 M acetic acid elution buffer. The second modification involves the adsorption of head-group functionalized poly(ethylene glycol) lipids (PEG-lipids), where the lipid tail strongly adsorbs to the polypropylene surface and the hydrophilic PEG group extends away from the surface allowing for the functional ligand to interact with the analyte of interest. This modification was first evaluated as an initial proof-of-concept study, where biotin-PEG-lipid modified PP C-CP fibers were able to selectively capture streptavidin from a complex mixture that also contained a green fluorescent protein. Non-specific binding was minimized through the use of a 0.1 % PBS-Tween buffer. Next, a more in-depth study of surface loading characteristics determined maximum binding capacity when using FITC-PEG-lipid to modify the fibers. This modified surface was also exposed to several test solvents to reveal a highly robust surface modification. Finally, the mechanism of interaction between the lipid and the polypropylene was determined through modification with an environmentally sensitive probe, NBD. Fibers were modified with lipids containing an NBD group attached to either the head group or the fatty acid tail. Fluorescence imaging

revealed that the lipid tail intercalates into the PP structure to yield an efficient, robust surface modification. Overall, modifications of the polypropylene fiber surface show promise in increasing the efficiency of affinity separations.

DEDICATION

I dedicate this work to my remarkable Mum and Dad, whose unwavering guidance, support, and love has, without a doubt, sculpted me into the person I am today.

To my Mum, for instilling in me an amazing sense of self-worth, encouraging me to be the best that I can be, and, no matter what, always being only a phone call away.

To my Dad, for making me an artist, and being so proud of me when I chose chemistry as a vessel for my creativity. Your life lessons and words of wisdom will live on with me forever. RIP

To the rest of my family and my second family (The Jones) for their never ending encouragement, I am so thankful.

To Dr. Gregory S. Jones, for challenging me on every step of our journey and making this whole thing worth it.

ACKNOWLEDGMENTS

I would like to acknowledge my undergraduate research advisor, Dr. Frank Bright, and my graduate research advisor, Dr. Ken Marcus, for encouraging me to be the lab rat I am and granting me the opportunities to work in their respective labs. I thank Dr. Marcus for providing me with immense support throughout my graduate career, allowing for travel, collaboration and, most importantly, always challenging me to push past my limits.

Next, I would like to thank my colleagues at Clemson University, especially the Marcus Research Group. Specifically, Jennifer Pittman for her excellent and much appreciated guidance when I was just starting, and Ben Manard for always having my back and giving me quality advice. I appreciate all the friendship and support.

I would also like to acknowledge my committee members and the Clemson University Department of Chemistry.

I am also grateful for the financial support from the National Science Foundation Division of Chemistry under grant no. CHE-1307078.

TABLE OF CONTENTS

Table of Contents (Continued)

Page

Table of Contents (Continued)

Page

LIST OF TABLES

LIST OF FIGURES

List of Figures (Continued)

Figure Page

List of Figures (Continued)

Figure Page

List of Figures (Continued)

Figure Page

List of Figures (Continued)

Figure Page

CHAPTER ONE

INTRODUCTION

Introduction to Liquid Chromatography

Chromatography can be defined as a dynamic method of separation where the components of a mixture are separated due to their interactions between two phases, a solid phase (i.e. *stationary phase*) and a phase that moves relative to the stationary phase (i.e. *mobile phase*) [1,2]. When the mobile phase is a liquid, this process is termed liquid chromatography (LC). Russian researcher Mikhail Tswett developed the method of chromatography in the early 1900's as a way to separate the pigment compounds in leaf extracts. His sample, dissolved in a solvent, was placed at the top of an open glass column filled with particles (stationary phase). As more solvent (mobile phase) was added to the column, the sample passed down the column due to gravity. The pigments adsorbed to the stationary phase and instead of washing away, some retained strongly, while others that were retained weakly moved farther down the column. The sample components began to separate based on their chemical attraction to the particle stationary phase. Eventually, the components separated into individual bands, with each visible as a different color. Based on this discovery, Tswett used the term chromatography (Greek for "color writing") to describe the method [1,3].

While there are several different LC methods, it is most powerful when a column is used. In Tswett's early experiments, a glass column was used with gravity flow as the mechanism for fluid movement. In columns that are not meant to withstand high pressures, gravity or vacuum are the primary modes used to achieve fluid flow. However, with the development of smaller particles sizes, which improved separations, high pressures were necessary to create fluid flow. Thus, solvent pumps and columns were developed to withstand this increase in pressure [4]. In 1970, this variation of LC was termed high pressure liquid chromatography (HPLC) to explain chromatography using columns/stationary phases that generated 500 – 6000 psi of pressure. Throughout the 70's, as LC instrumentation and columns advanced and significant progress was made in chromatography of biomolecules, it was noted that "high pressure" was not always relevant, and so the technique became "high *performance* liquid chromatography" [4]. HPLC has grown into a multi-billion dollar industry; a necessary tool for the characterization, discovery, and manufacture of biomolecules used in research and development for biotechnology and pharmaceutical companies. The advances in HPLC over more traditional techniques have led to many advantages including speed, resolution, sensitivity, accuracy, and automation, among others. However, limitations including cost and complexity, and applications requiring better resolution and higher throughput, make HPLC a continuously developing field [4].

There are three major components of a chromatographic system that can be manipulated to improve separation performance; the mobile phase, the stationary phase, and the fluidics instrumentation. HPLC instrumentation involves a mobile phase passing through a solvent pump, an injection valve able to introduce the sample into the mobile phase with little-to-no disturbance of flow, and a detector. Advancements to instrumentation includes faster and more controlled flow and gradient rates, enhanced detector sensitivity, ease of use, automation, and overall higher throughput with new technologies [1,4]. The mobile phase can be manipulated in terms of liquid composition (additives, pH), flow velocity, and gradient composition and rate to improve the separation performance. Mobile phase and fluid flow parameters are optimized individually based on the sample and column, as the migration of analytes and their propensity for interaction with the stationary phase is dependent on these parameters. Probably the most important of the three major chromatographic system components is the stationary phase, which dictates the mechanism of retention and separation, and has been called “the heart of an HPLC” [4]. Physical column design is also important, as column length, column diameter, and column hardware (type of tubing and end fitting) can maximize resolution while minimizing analysis time, thus enhancing the quality of a separation [3]. But, the physical and chemical characteristics of a stationary phase are what ultimately determine column efficiency. For this reason, solid/stationary phases

will be discussed in depth later in this chapter. First, it is necessary to discuss the theoretical considerations of what is happening in a column during HPLC.

Separation Theory

As the separation of the components of a mixture is the goal of chromatography, resolution, or the amount of separation between two peaks, is an important factor. Resolution (R_S) is determined from the ratio of the distance between the peaks and their peak widths [4], defined quantitatively as:

$$R_S = \frac{2\Delta t_r}{w_1 + w_2} \qquad \text{Eq. 1.1}$$

where Δt_r is the distance between two peaks in terms of retention time (t_r) and *w* is peak width. Resolution is a combination of the retention, selectivity, and efficiency of a column. Retention of an analyte on a column is indicative of how strongly it is attracted to the stationary phase over the mobile phase. The capacity factor (k) is the measurement of the extent that an analyte is interacting with the stationary phase [4]. This is related to the partition coefficient (*K*), of the analyte between the stationary phase and mobile phase, according to equation 1.2:

$$k = K\frac{V_S}{V_M} \qquad \text{Eq. 1.2}$$

where V_S and V_M are the relative volumes of the stationary phase and the mobile phase at equilibrium. In other words, how long an analyte spends in the stationary phase, versus how long it spends in the mobile phase. Selectivity is the *relative* retention of analytes in a mixture, and is defined as the ratio of the capacity factors between two analytes [4], Equation 1.3:

$$\alpha = \frac{k_2}{k_1} \qquad \text{Eq. 1.3}$$

Selectivity is the basis for how well a stationary phase can distinguish between the components of a mixture. The more selective a stationary phase is, the better the separation will be due to an increase in resolution. Selectivity can be increased by changes in the physical and chemical structure of the stationary phase and the mobile phase. Selectivity is the most important parameter for successful chromatographic separations.

Another way to improve the resolution of a separation is by increasing efficiency. Here, efficiency is based on the dispersion of a single band of analyte, i.e. the peak width (*w*). To increase column efficiency, the broadening of a peak should be minimized in order to maximize the number of *theoretical plates* contained in a column. A *theoretical plate* (N) is a term given to describe individual segments of equal length that make up the total column length. This is

determined experimentally for a given peak using retention time and peak width at the base of the peak [5], shown in Equation 1.4:

$$N = 16\left(\frac{t_r}{w}\right)^2 \qquad \text{Eq. 1.4}$$

A column of length L will have a *height equivalent to a theoretical plate* (HETP, H). In Equation 1.5 it's shown that an efficient column will have a large N value and small HETP, as a higher number of theoretical plates gives a narrower peak width and yields better resolution [4].

$$H = \frac{L}{N} \qquad \text{Eq. 1.5}$$

The theory described above assumes that there is an equilibrium at each plate segment, but as this is not always true, a new equation was developed to account for the variety of parameters (rate of elution, diffusion of the analyte, paths for fluid flow, rate at which the solute equilibrates between stationary and mobile phases) that contribute to band broadening as fluid moves through a column. Plate height (*H*) is defined in Eq. 1.6 by the van Deemter equation [4,5]:

$$H = A + \frac{B}{u} + Cu \qquad \text{Eq. 1.6}$$

where u is the linear flow velocity and A, *B,* and *C* terms are constants that account for band spreading. Figure 1.1 shows a plot of each individual term in the van Deemter equation, demonstrating how each term independently affects plate height as a function of linear velocity, and how the three terms combine to form a van Deemter plot. The "*A*" term accounts for variation in the flow path that the analyte molecules travel. As shown in Fig. 1.1 the "*A*" term is independent of flow and is only a function of the particle size or channels in the packed bed. This term is minimized when there is uniform packing of a stationary phase.

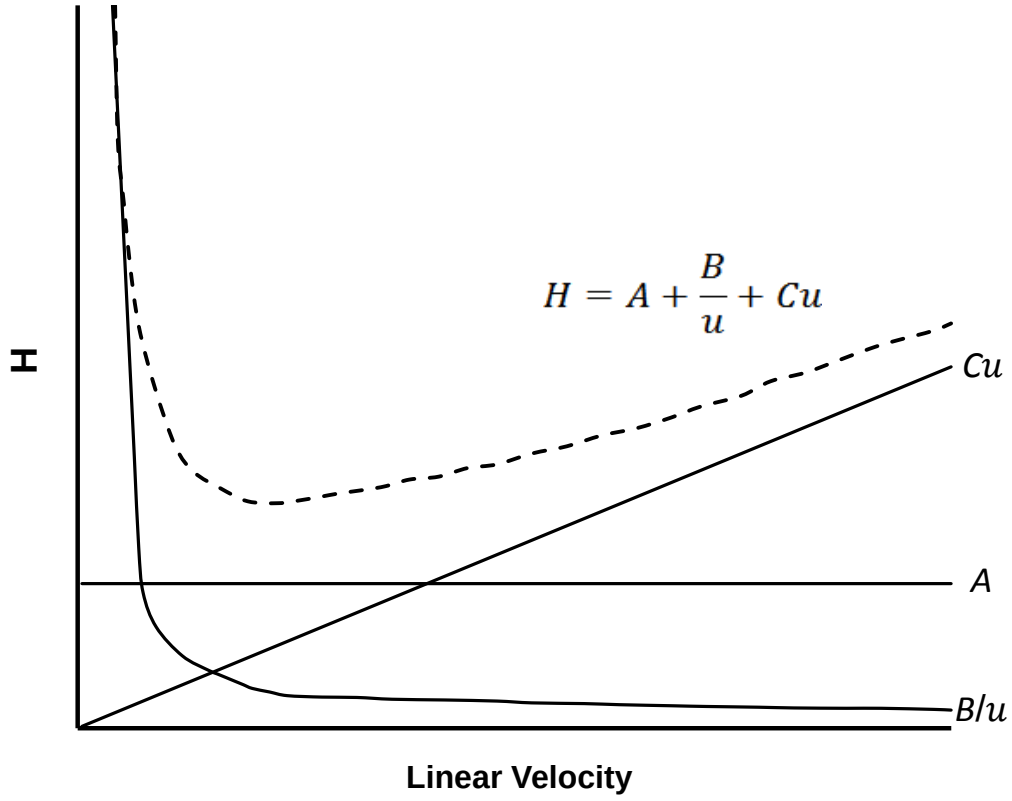

Figure 1.1 The three individual terms that contribute to band broadening due to a change in plate height (*H*) as a function of linear velocity [3] and the resulting van Deemter plot (**- - -**) showing the combination of the terms.

If there are inconsistencies in the packed bed both sample and solvent will move at different rates through the column due to increases in eddy diffusion (unequal flow patterns) and changes in laminar flow (flow retardation at the support wall). The "*B*" term is inversely proportional to linear velocity and describes how analyte molecules diffuse in the longitudinal (or axial) direction, in the bulk flow. As this type of diffusion increases with time, it contributes significantly more at low linear velocities. At higher linear velocities, molecules take less time to diffuse axially in the column and the contribution of the "*B*" term to plate height is significantly decreased. Finally, the "*C*" term takes into account the interaction kinetics between the stationary phase and mobile phase (i.e. mass transfer) in three ways: transfer of the molecules from the mobile phase to the stationary phase, adsorption/desorption of the molecule with the stationary phase, and how the molecule transfers from the stagnant mobile phase in a pore to the surface of the stationary phase. Obviously, the "*C*" term is complex and contributes the most to an increase in plate height, and thus band broadening, as flow velocity (u) increases. Development of improved support/stationary phases for HPLC that allow for a decrease in all three of these terms is highly desirable [4,5].

Stationary Phases in Liquid Chromatography

As stated above, the physical and chemical properties of a stationary phase affect many components of separations in HPLC including mass transfer rate, selectivity, and resolution. The stationary phase parameters that can be

optimized include particle size and shape, pore size and porosity, specific surface area, packing density, as well as the chemical characteristics including functional group density [3]. The traditional chromatography supports are silica and polymeric beads, with increasingly smaller sizes allowing for better separation efficiency. Silica is widely used due to high mechanical stability (can withstand high pressures), high control of size and porosity when synthesized, and the ease at which the particle surface can be derivitized. Yet, silica suffers many major disadvantages that include low chemical stability, a limited working pH range, and potential interactions between surface silanol groups and the analyte of interest. Polymer-based stationary phases, on the other hand, are chemically robust, durable, and remain stable over a wide pH range [3]. Polymer-based supports are not as commonly used as silica, however, due to several drawbacks. Polymeric packings are not as mechanically strong as silica, they absorb liquid easily and thus swell and shrink depending on the mobile phase used, and they have been found to be less efficient when compared to silica for small molecule separations [3]. However, for biomolecule separations, lower efficiency is not observed and their mechanical strength is suitable for the relatively low flow velocities used. For these reasons, polymeric phases with the advantages of silica, but with high stability and robustness, have been continuously researched and developed as HPLC stationary phases for protein separations [6,7].

As this dissertation is focused on protein separations, focus is placed on polymer-based stationary phases. Polymer packing materials include textiles [8,9], beads [10-12], and monoliths [13-16]. While textiles (or fibrous stationary phases) have not gained significant interest in the past, there is a clear rationale to why they make excellent stationary phases for macromolecule separations [6]. Polymer-based fiber stationary phases were first reported on for LC application by Kirby and Cates in 1983 [17], which looked at the separation of dye molecules on small segments of polyester (PET) fibers (staple phases) packed into a glass gravity column. Through this work, they were able to better understand how the structural (crystallinity) and physical properties of PET fibers affected dye adsorption, diffusion into the pore structure, and thus the separation process. Around the same time, it was also shown that whole (woven) textiles exhibited differing properties from staple fibers when packed into a column. Ladisch and coworkers [8,9,18-20] demonstrated the benefits of rolled fabrics for use in LC protein separations. Due to the continuous nature of the packed bed, high mass transfer rates and low backpressure were noted, with the separation chemistry based on the type of polymer textile chosen or the type of derivatization performed. The concept of aligned fibers, running in parallel down the length of a column was proposed by Kiso and coworkers in 1986 [21], who used cellulose acetate fibers packed in a fused silica capillary column. In this case, the space between the fibers forms an open capillary for fluid flow. Due to this channel structure, very low pressure drops were observed.

In an effort to expand upon the advantages of aligned fiber stationary phases, capillary-channeled polymer (C-CP) fibers have been extensively studied in the Marcus laboratory for HPLC [22-25] and solid phase extraction (SPE) [26,27] applications. C-CP fibers are melt-extruded from polypropylene (PP), polyamide (nylon 6), and poly(ethylene terephthalate) (polyester, PET) forming fibers with nominal diameters ~ 40 µm. These fibers are intriguing due to the eight capillary channels that run axially along the entire length of the fiber. When packed into a column the channels interdigitate, allowing for high packing densities as well as efficient use of space. This packing creates 1-5 µm open capillary channels that provide high surface area (compared to circular cross-section fibers of the same nominal diameter) needed for optimal interactions [28]. In terms of van Deemter "A-term" broadening, differing flow paths (eddy diffusion) in PP C-CP fiber columns have been found to be the dominant contributor to the HETP [24]. The capillary channels benefit fluid transport due to an inherent wicking of fluid along the length of the fiber, leading to operating backpressures < 2000 psi. The fibers have been found to have a limited porosity (~ 4 nm) on the size of proteins [29], and thus high velocities do not affect van Deemter "*C*-term" broadening due to a practically nonporous surface. In other words, mass transfer from the mobile phase to the surface of C-CP fibers is rapid due to a lack of molecular diffusion into and out of pores. It is important to note that the specific surface area for C-CP fibers tend to be 1-5 m^2/g, which is less than that of porous silica phases. For this reason, C-CP fiber stationary phases have shown

relatively poor performance in the separation of small molecules [30,31]. Instead, C-CP fiber use is geared towards macromolecule separations due to a lack of mass transfer limitations that allows for separations at high linear velocities (> 100 mm s^{-1}) and fast gradient rates with very high recovery and efficiency [23,32,33]. C-CP fibers are also very low cost and stable over a wide range of solvent and pH conditions. Cross-sectional micrographs of a single C-CP fiber and a packed column are shown below in Fig. 1.2.

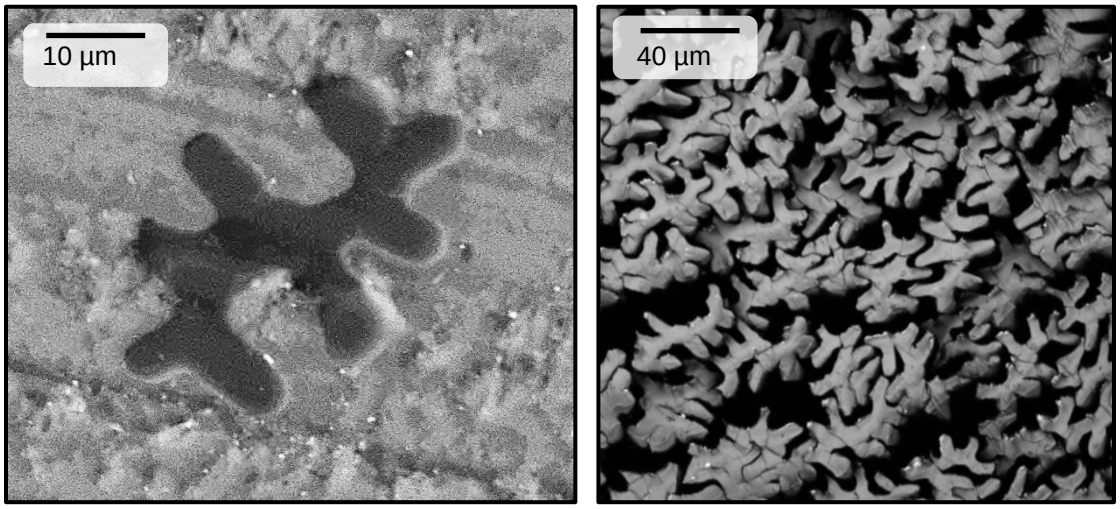

Figure 1.2 Micrographs of a single PP C-CP fiber (left) and of a PP C-CP fiber packed column (right).

Protein Separations

Understanding the role of proteins in cellular processes, drug discovery and development, biotechnology, and various others areas of life science, lies in the characterization of proteins. Proteomics, or the study of proteins and their biological functions, allows for the identification of disease biomarkers and

generates vital information. Due to the proteomes degree of complexity, advanced techniques to study and better understand proteins are continuously being developed [34]. As such, methods of protein purification have been continuously improving to allow for protein purification from a complex mixture in very few steps. Beyond proteomics research, drugs based on monoclonal antibodies (mAbs) and related proteins are becoming ever more prominent due to their therapeutic capabilities and contribution to the biopharmaceutical market. For example, the mAb market value is expected to reach 70 billion dollars by 2015 [35,36]. Currently, downstream processing, or purification of mAbs from the cell culture broths they were expressed in, is the bottleneck of this industry.

While many separation/purification techniques exist, HPLC is an attractive method, and the most commonly used, due to high speed, resolution, and general efficiency. The goal here is to purify a large batch of product in the smallest amount of time and while keeping costs low. There are several different modes of chromatographic separation that can be used for proteins including reversed-phase (RP), ion-exchange (IEC), hydrophobic interaction (HIC), size exclusion (SEC), and affinity chromatography (AC) [4,5,37]. As purification is of the utmost importance, several different modes of chromatography are often performed in sequence. While affinity chromatography has the ability to capture large amounts of the desired analyte with high selectivity and low nonspecific binding, affinity adsorbents are often expensive and thus used in smaller columns where repeat injections of sample are necessary to purify a large batch

[37]. IEC is commonly used as a first step to generate high resolution separations with high protein binding capacity. Compared to affinity stationary phases, IEC media is much more affordable and thus is used in larger columns that can handle larger volumes [37]. IEC and AC are the two modes of chromatography focused on in this dissertation.

Ion-exchange chromatography occurs due to the electrostatic attraction between proteins in the mobile phase and charged groups fixed on the stationary phase (or *ion exchanger*) [5,37]. The strength of the interaction (and thus, the quality of the separation) is based on the charge of the proteins and the ion exchanger and competition from other ions. When the stationary phase has cationic charged groups, it is called anion-exchange chromatography (AEC), and when the stationary phase has anionic charged groups, it is called cation-exchange chromatography (CEC). It is also possible for a surface to contain both negative and position charges, resulting in a zwitterionic surface. For proteins, net ionic charge is a function of pH and thus the pH of the mobile phase is used to influence retention and selectivity of the stationary phase. Ion exchangers are classified as either strong or weak and chosen based on the operating pH and the amount of selectivity required. Protein elution is based on pH or ionic strength gradients; as the number of competing ions in solution increases, proteins will begin eluting based on how strong their initial interaction with the stationary phase was (i.e. weaker interacting proteins will be eluted first). [5,37]

In affinity chromatography, an affinity ligand is bound to a solid support to form the stationary phase. An analyte of interest binds to the affinity ligand based on specific biochemical recognition between it and the affinity ligand [5]. This process is demonstrated in Fig. 1.3.

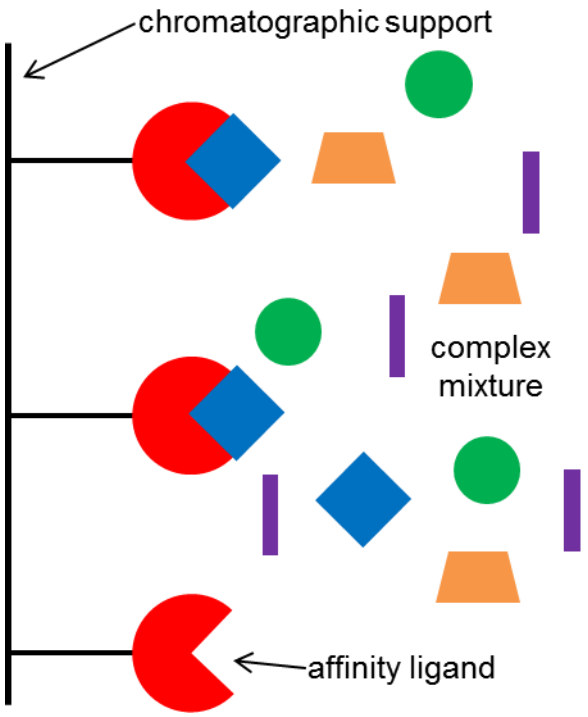

Figure 1.3 Example of affinity chromatography. Affinity ligands attached to a solid support selectively capture the desired analyte from a complex mixture.

AC is most often used to separate one analyte of interest from a mixture containing a multitude of different molecules. AC can also be used when an analyte of interest is tagged with a molecule or functional group that shows strong affinity for a ligand. Resolution mainly depends on the selectivity of the

immobilized ligand opposed to how the analyte migrates down the column [4]. After capture of the intended analyte, a wash step follows to remove any non-specifically bound species and ensure that the eluted fraction contains only the analyte of interest. A buffer that weakens the interaction between the affinity ligand and the protein, either by a conformational change or introducing a competing compound, is used for elution [4,37]. In affinity chromatography, binding capacity is limited by the amount of ligand immobilized to the support phase.

As has been stated, C-CP fibers have physical properties that make them highly suitable for protein separations. Nylon 6 C-CP fibers have naturally occurring end groups that allow for an ion-exchange surface that efficiently separates proteins. Taking this a step further, modifying the fiber surface to generate a species specific surface is highly practical. In this work, polypropylene fibers are used. Modification of PP fibers is done through hydrophobic adsorption to the polymer surface. Although these modifications are "only" based on adsorption, the modifications are found to be robust and stable across a wide variety of solvent environments. In this dissertation, analyte specific stationary phases are developed for affinity chromatography applications.

Summary

The current challenges faced in HPLC applications, as discussed above, are centered on ensuring a highly efficient separation in terms of speed, cost, throughput, and yield. Specifically, complex mixtures containing hundreds of different proteins require highly selective stationary phases to ensure adequate resolution in separation. The majority of work presented in this dissertation focuses on the chemical surface modification of C-CP fibers for the selective capture of proteins through affinity chromatography. The primary goal was to enhance the already advantageous physical characteristics of C-CP fibers by generating a species-specific, high surface density modification. This was possible by adsorption of a capture ligand onto hydrophobic polypropylene C-CP fibers, resulting in a robust modification due to strong hydrophobic interaction. Throughout this work, the physical properties of C-CP fibers are highlighted, and their application as species-specific affinity stationary phases is developed.

Chapter II, the only chapter to not involve a surface modification, rather, gives an introduction to C-CP fibers use for ion-exchange chromatography and how the extrusion process of forming nylon 6 beads into fibers can cause differences in their physical properties. A difference in chromatographic behavior between the two (presumably identical) nylon 6 fibers led to a closer look into the chemical and physical nature of the fibers. Testing included Fourier transform infrared spectroscopy (FTIR), differential scanning calorimetry (DSC), mechanical testing, MALDI-TOF mass spectrometry, the ninhydrin test, and

dilute solution viscometry. Differences in fiber perimeter, denier, and available surface area when packed into a column were also noted. The outcome of this work was published in the Journal of Applied Polymer Science (Schadock-Hewitt, A.J.; Pittman, J.J.; Stevens, K.A.; Marcus, R.K., *J. Appl. Polym. Sci.*, 2012, 128, 1257-69) and reprinted with permission from John Wiley and Sons, Inc.

Chapter III involves the modification of polypropylene C-CP fibers with a recombinant protein A ligand as an affinity stationary phase for the capture of immunoglobulin G (IgG) antibody. IgG, needed in high quantities and high purity, can be selectively captured by the protein A ligand and thus protein A affinity chromatography is the most commonly used methods of IgG purification. This study was done in an initial, small analytical SPE micropipette tip format so that solvent, protein, and antibody use was minimal. The surface modification with protein A was optimized to generate the highest ligand capacity. Performance of the stationary phase was evaluated through exposure to a mixture of human IgG and myoglobin. Capture and recovery were determined with absorbance measurements of collected eluents. Results were published in The Journal of Separation Science (Schadock-Hewitt, A.J.; Marcus, R.K., *J. Sep Sci.*, 2014, 37(5), 495-504), and reprinted with permission from John Wiley and Sons, Inc.

Chapter IV describes the modification of PP C-CP fibers with head group functionalized poly(ethylene glycol) (PEG)-lipids. A PEG-lipid molecule contains a fatty acid lipid tail that strongly adsorbs to the hydrophobic PP surface, and a hydrophilic PEG moiety that orients itself towards the more polar mobile phase

allowing for the head group (functional group) to be free in solution. PEG-lipids used to modify a surface have been termed lipid-tethered ligands (LTLs). In this proof-of-concept experiment, PP fibers were modified with a Biotin-PEG-lipid and used to capture streptavidin from a pure solution and a complex cell broth. When compared to methoxy-PEG-lipid modified PP C-CP fibers and unmodified PP C-CP fibers, only Biotin-PEG-lipid modified fibers showed a high specificity for streptavidin, with the two controls showing little-to-no non-specific binding. These results were published in Analyst (Schadock-Hewitt, A.J.; Pittman, J.J.; Christensen K.A.; Marcus R.K., *Analyst*, 2014,139, 2108-2113), reproduced with permission from The Royal Society of Chemistry.

In Chapter V, the initial proof-of-concept modification of PP C-CP fibers with head group functionalized PEG-lipids is expanded on. Here, ligand binding characteristics were studied with breakthrough curves and frontal analysis across a range of lipid concentrations and mobile phase flow rates. Generation of a linear adsorption isotherm highlights the efficient mass transfer and fluid transport properties of C-CP fibers. Dynamic binding capacity and maximum capacity were determined. Additionally, exposure of the lipid-modified PP C-CP fibers to several solvents revealed a chemically robust system, as only 50% acetonitrile and 100% hexanes were able to disrupt the surface adsorption. The conclusions show a lipid tethered ligand (LTL) system. The results were published in the Journal of Separation Science (In press, DOI:

10.1002/jssc.201400807), reprinted with permission from John Wiley and Sons, Inc.

Chapter VI the PEG-lipid surface modification is further investigated in order to understand the mode of adsorption of the lipid tail to the polypropylene surface; either with the fatty acid tail resting along the fiber surface or intercalating into the bulk PP fiber. Lipids labeled with the environment-sensitive 7-nitro-2-1,3-benzoxadiazol-4-yl (NBD) fluorophore were used to modify the PP C-CP fiber surface, with NBD covalently attached to the head group (NBD PE or the acyl chain (acyl NBD PE). Changes in fluorescence behavior, examined through fluorescence microscopy, reflected if the ligand was free in the solvent environment or embedded into the fiber polymer matrix. These results allow us to better understand this surface modification. Results have been submitted to The Journal of the American Chemical Society.

References

[1] J.C. Giddings, Unified Separation Science, John Wiley & Sons, INC, New York, NY, 1991.

[2] W. Corporation, J.C. Arsenault, P.D. McDonald, Beginners Guide to Liquid Chromatography, Wiley, 2014.

[3] U.D. Neue, HPLC Columns Theory, Technology, and Practice, Wiley-VCH, New York, 1997.

[4] R.L. Cunico, K.M. Gooding, T. Wehr, Basic HPLC and CE of Biomolecules, Bay Bioanalytical Laboratory, Richmond, CA, 1998.

[5] S.R. Mikkelsen, E. Corton, Bioanalytical Chemistry, John Wiley and Sons, Inc., Hoboken, New Jersey, 2004.

[6] R.K. Marcus, Journal of Separation Science 31 (2008) 1923.

[7] R.K. Marcus, Journal of Separation Science 32 (2009) 695.

[8] Y. Yang, A. Velayudhan, C.M. Ladisch, M.R. Ladisch, Journal of Chromatography A 598 (1992) 169.

[9] K. Hamaker, S.-L. Rau, R. Hendrickson, J. Liu, C.M. Ladisch, M.R. Ladisch, Industrial & Engineering Chemistry Research 38 (1999) 865.

[10] V. Smigol, F. Svec, J.M. Fréchet, Anal Chem 66 (1994) 2129.

[11] B. Gong, L. Li, J. Zhu, K. Qiang, L. Ren, J Sep Sci 28 (2005) 2546.

[12] B. Ara, Z. Chen, J. Shah, M. Rasul Jan, L. Ye, Journal of Applied Polymer Science 128 (2012) 315.

[13] F. Svec, J Sep Sci 27 (2004) 747.

[14] R.D. Arrua, T.J. Causon, E.F. Hilder, Analyst 137 (2012) 5179.

[15] A. Jungbauer, R. Hahn, Journal of Chromatography A 1184 (2008) 62.

[16] K.K. Tetala, T.A. van Beek, J Sep Sci 33 (2010) 422.

[17] R.D. Kirby, D.M. Cates, Textile Research Journal 53 (1983) 586.

[18] C.M. Ladisch, Y.Q. Yang, Textile Research Journal 62 (1992) 481.

[19] K. Hamaker, J.Y. Liu, C.M. Ladisch, Biotechnol. Progress 14 (1998) 21.

[20] C. Li, C.M. Ladisch, Y. Yang, R. Hendrickson, C. Keim, N. Mosier, M.R. Ladisch, Biotechnol. Prog. 18 (2002) 309.

[21] Y. Kiso, K. Jinno, T. Nagoshi, J. High Resolute Chromat. Chromat. Comms. 9 (1986) 763.

[22] R.K. Marcus, W.C. Davis, B.C. Knippel, L. LaMotte, T.A. Hill, D. Perahia, J.D. Jenkins, J. Chromatogr. A 986 (2003) 17.

[23] R.D. Stanelle, C.A. Straut, R.K. Marcus, Journal of Chromatographic Science 45 (2007) 415.

[24] K.M. Randunu, S. Dimartino, R.K. Marcus, J Sep Sci 35 (2012) 3270.

[25] A.J. Schadock-Hewitt, J.J. Pittman, K.A. Christensen, R.K. Marcus, Analyst 139 (2014) 2108.

[26] D.S. Fornea, Y. Wu, R.K. Marcus, Analytical Chemistry 78 (2006) 5617.

[27] B.T. Manard, R.K. Marcus, J Am Soc Mass Spectrom (2012).

[28] J. KNOX, M. GILBERT, Journal of Chromatography 186 (1979) 405.

[29] Z. Wang, R.K. Marcus, J Chromatogr A 1351 (2014) 82.

[30] R.D. Stanelle, L.C. Sander, R.K. Marcus, J Chromatogr A 1100 (2005) 68.

[31] R.D. Stanelle, M. Mignanelli, P. Brown, R.K. Marcus, Anal Bioanal Chem 384 (2006) 250.

[32] D.M. Nelson, R.D. Stanelle, P. Brown, R.K. Marcus, American Laboratory 37 (2005) 28.

[33] R.D. Stanelle, R.K. Marcus, Analytical and Bioanalytical Chemistry 393 (2009) 273.

[34] M.R. Wilkins, R.D. Appel, J.E. Van Eyk, M.C. Chung, A. Görg, M. Hecker, L.A. Huber, H. Langen, A.J. Link, Y.K. Paik, S.D. Patterson, S.R. Pennington, T. Rabilloud, R.J. Simpson, W. Weiss, M.J. Dunn, Proteomics 6 (2006) 4.

[35] J.H. Chon, G. Zarbis-Papastoitsis, N Biotechnol 28 (2011) 458.

[36] P.A. Marichal-Gallardo, M.M. Alvarez, Biotechnol. Prog. 28 (2012) 899.

[37] J.-C. Janson, Protein Purification: Principles, High Resolution Methods, and Applications, Wiley, 2011.

CHAPTER TWO

EXTRUSION-BASED DIFFERENCES IN TWO TYPES ON NYLON 6 CAPILLARY-CHANNELED POLYMER (C-CP) FIBER STATIONARY PHASES AS APPLIED TO THE SEPARATION OF PROTEINS VIA ION EXCHANGE CHROMATOGRAPHY

Introduction

Nylon is among the most common commercially used synthetic fibers, having a wide range of textile and industrial applications[1-4]. Nylon is advantageous over other textile polymers due to its robustness, chemical versatility, dyeability, unique wettability (high hydrophilicity), as well as overall chemical and thermal stability. These features lead to the use of nylon in a variety of chemical manipulations such as a protein immobilization support in the form of membranes[5,6], and particles[7,8] for chemical separations and fluorescence measurements. Nylon-based materials have also been used in the form of nanofibrous membranes for water filtration, effectively isolating 90% of 0.5 μm particles from flowing streams[9]. While there are several chemical forms of nylon, nylon 6, named for the 6 carbons between each amide in the polymer backbone, is used most often as a chemical support due to its more open and random structure, allowing for more rapid and uniform functionalization. Nylon 6 (poly(∑-caprolactam)) is an AB type linear polyamide, formed through the aqueous polymerization of the cyclic amide caprolactam. For the above applications,

nylon 6 is relatively cheap when compared to similar supports, is readily available, has an active surface for interactions with analytes of interest, and provides for ready surface chemical modification for attachment of species-specific ligands. As a drawback, nylon 6 precipitated to form bead supports must be activated to generate the desired amine and carboxyl groups on its surface; however, most membranes and fibers require no such pre-treatments prior to use.

It seems advantageous to develop a nylon fiber support that can also be used as a stationary phase for high performance liquid chromatography (HPLC) separations, requiring no pre-treatment, with the ability to effectively separate several proteins in a mixture. Marcus has reviewed the application of fibrous stationary phases in liquid chromatography, where common traits include low materials costs, ease of column fabrication, presentation of diverse surface chemistries, efficient fluid mass transit through columns, and effective solute mass transfer to and from the stationary phase surface through convective diffusion processes[10,11]. In this laboratory, we are currently focused on the characterization of capillary-channeled polymer (C-CP) fibers utilized as a combined support/stationary phase for protein separations by HPLC. These fibers exhibit a higher surface area versus circular cross section fibers due to their unique shape, consisting of eight capillary channels that run axially down the length of the fiber. In terms of biomolecule separations, the fibers are essentially non-porous and exhibit very efficient mass transfer properties; as

such, effective separations can be performed at high linear velocities (>25 mm s^{-1}) with low backpressures (<1500 psi).

C-CP fibers have been studied extensively and have been applied in many different chromatographic modes including reversed-phased (RP), ion exchange (IEX), hydrophobic interaction (HIC), and mixed-mode chromatographies[10-18]. These different modes are readily affected through the choice of the base polymer identity among polypropylene (PP), poly(ethylene terephthalate) (polyester, PET), and nylon 6. In 2003, Marcus *et al.* first demonstrated the combined support/stationary phase ability of PP and PET C-CP fibers in reversed-phase separations of polyaromatic hydrocarbons (PAHs), organic and inorganic lead, amino acids, and lipids[12]. PP and PET C-CP columns, when compared with a commercially available C_4-derivatized silica column for the separation of proteins, showed increased repeatability of peak width and retention time, greater recoveries, and the potential for ultrafast separations[13,14] . Rapid protein separations were further studied with optimal peak resolution achieved with a 2.1 mm i.d. PET column at a flow rate of 7 mL/min[15]. Smaller i.d. PP microbore columns (1000 mm in length) were shown to achieve high column efficiency while maintaining relatively low backpressures[16]. Most recently, nylon 6 C-CP columns were shown to effectively separate proteins at comparatively high linear velocities (~21 mm/s) by a mixed-mode IEX/RP chromatography[17] and excellent resolution with fast analysis times achieved by HIC[18]. Overall, C-CP fiber columns have continuously been shown

to provide high efficiency separations at high linear velocities and high recoveries in comparison to derivitized silica phases which are the industry standards[15].

The nylon 6 C-CP fibers are similar to commonly used membrane and bead-form supports because they are cheap, easily made, and readily available[2-4]. Unlike analogous polyamide particles, nylon 6 fibers do not require activation to generate surface functional groups. When nylon 6 bulk polymers are extruded into fibers various degradation processes lead to a discontinuity of the polymer chains, exposing the amine and carboxyl surface functional groups. It is these end groups that contribute to the hydrophilicity of the surfaces (allowing for effective hydrophobic interaction separations) and provide cationic and anionic sites to affect ion exchange separations as described here[18]. The nylon 6 C-CP fibers enable electrostatic interactions between the charged amino acids making up the outer portions of a protein molecule and the charged end groups ($-NH_3^+$ and $–COO^-$) of the amide polymer. The mixed-mode nature of separation involves additional interactions between hydrophobic portions of proteins with the alkyl chains making up the polymer backbone. An underappreciated aspect of the use of nylon 6 as an extraction/chromatographic support is the level of "surface tunability" that can be affected due to the zwitterionic nature of the end groups. As such, nylon 6 C-CP fibers can be used for both anion- and cation-exchange separations based on the solvent pH, as illustrated in Fig. 2.1. As indicated, the nylon 6 surface is cationic in nature at low pH (making it useful for anionic exchange), with the surface charge being a net negative at pH> 8

(allowing for separations based on cation exchange). Not unlike other types of chromatographic stationary phases, HPLC separations on C-CP fiber columns are first dictated by the chemical nature of the fiber surfaces as this determines the types and strengths of the protein-surface interactions. The specific fiber shape, perimeter, denier and column packing density in turn affect the column hydrodynamics and the available surface area for interaction. Even in the case of identical monomers, subtle differences may be manifest due to inconsistencies in the base nylon 6 polymers used for fiber extrusion.

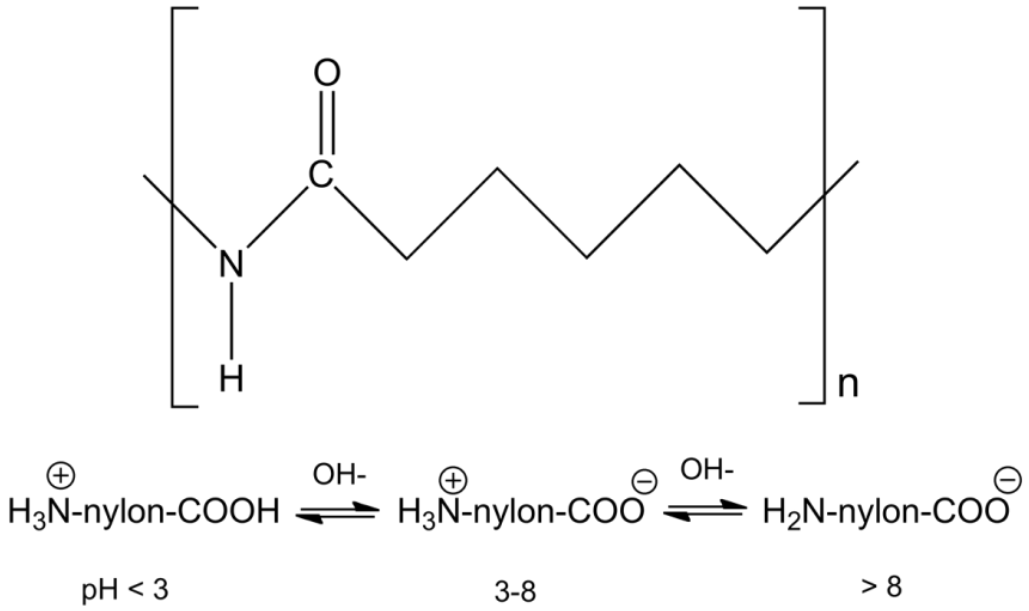

Figure 2.1 Nylon 6 monomer structure and the effects of pH on the end group functionality

It is known that nylon performance (in general) is based on a variety of properties, including amide content (molecular weight), crystallinity, and melting

point. Due to their linear discerned symmetry, nylon 6 fibers show high crystallinity that varies based on extrusion processes[19]. We describe here a comprehensive evaluation of the chemical and physical attributes of two nylon 6 C-CP fiber stocks (referred to as nylon 6A and nylon 6B) which affect their performance in the ion exchange chromatography separation of a simple three-protein suite of ribonuclease A, cytochrome c, and lysozyme. Attenuated total reflectance Fourier transform infrared spectroscopy (ATR-FTIR) and differential scanning calorimetry (DSC) provide insight into the base polymer and amorphous/crystalline structure of the nylon 6. MALDI-TOF mass spectra of the surface of fibers dissolved in trifluoroethanol (TFE) also provide confirmation of the identities of the base monomers. Mechanical properties discerned from tensile testing allow for information regarding the fiber extrusion process. Relative viscometry of the fibers was measured and used to calculate a number average molecular weight. As a final test, end group densities were quantitatively determined by a reaction with ninhydrin, which causes a photometrically measureable color change in the presence of amide groups, and serves to complement MALDI data, relating molecular weight and end group density. As a whole, this insight into the physical and chemical characteristics of C-CP fibers alludes to a greater understanding of their properties and future performance optimization. Regardless of the actual identity of the materials evaluated here, the results point to the need to critically evaluate the roll of

differing base polymers and fiber extrusion conditions in the ultimate chemical character of the fiber surfaces, and thus their separation qualities.

Experimental

Chemicals, Reagents, and Standards

HPLC-grade acetonitrile (ACN) and HPLC-grade methanol, used to clean the fibers, and 2-propanol (isopropanol) and ethanol, used in the ninhydrin reaction, were obtained from Fisher Scientific, (Pittsburgh, PA, USA). Milli-Q water (18.2 $M\Omega cm^{-1}$) derived from a Millipore water system (Billerica, MA, USA) was used for fiber rinsing and preparation of TRIS-HCl buffer, ammonium chloride (NH_4Cl) salt solutions, and all other aqueous-based solutions. 1M TRIS-HCl, pH 8.0, was purchased from Teknova (Hollister, CA, USA) and diluted appropriately into 20 mM TRIS-HCl, pH 8, employed as mobile phase, buffer A. 1 M NH_4Cl in 20 mM TRIS-HCl was used as the elution buffer, buffer B. A standard three-protein stock solution was prepared in 20 mM TRIS-HCl buffer at pH 8.0, at a concentration of 0.25 mg mL^{-1} for each protein. The suite included ribonuclease A (RNase A) (MW = 13.7 kDa), cytochrome c (cyto c) (MW = 12.4 kDa), and lysozyme (MW = 14.3 kDa), all having isoelectric points (pI) above the physiological pH = 7.4, and so referred to as basic. The protein solutions were stored at 6° C. Pyridine, propionic acid, sodium propionate, 2-methoxy-ethanol, ε-aminocaproic acid, and ninhydrin, all used in the ninhydrin reaction, and the 2-

(4-Hydroxyphenylazo)benzoic acid (HABA) and sinapic acid (SA) matrix species for MALDI-MS, and the 2,2,2-trifluoroethanol (TFE) used to dissolve fibers prior to MALDI-MS analysis, were purchased from Sigma Aldrich (Milwaukee, WI, USA).

Physical Property Considerations and Column Preparation

Nylon 6 C-CP fibers were obtained from the Clemson University School of Materials Science and Engineering (Clemson, SC, USA) (nylon 6A) and Fiber Innovations Technology (FIT, Johnson City, TN, USA) (nylon 6B). Bundles of fibers were prepared and pulled through 0.8 mm i.d., 200 mm long fluorinated ethylene propylene (FEP) tubing (Cole-Parmer, Vernon Hills, IL, USA) as previously described to form microbore format C-CP fiber columns[12,13]. The perimeter, weight, denier, and total surface area are provided in Table 2.1. The fiber perimeter was determined through a mathematical program using the SEM cross-section images of the fibers (Fig. 2.2). The denier per filament (dpf) was determined by calculating fiber weight in grams per 9000 meters.

Table 2.1 Physical property differences between nylon 6 C-CP fibers

Sample	Filaments / Yarn	DPF	Perimeter (μm)	Surface Area/ Column (cm^2)	Average Mass/Column (mg)
Nylon 6A	30	2.67	207.5	373.5	7.76 ± 0.02
Nylon 6B	25	7.74	270.7	189.5	8.25 ±0.02

Bobbins of nylon 6A were wound as 30 filaments per fiber bundle, while nylon 6B has 25 filaments per fiber. Based on previous results[13] , the nylon 6 C-CP fiber columns were packed to yield interstitial fractions of $\varepsilon_i \cong 0.6$ (i.e. ~60% void volume). In this case, 900 nylon 6A fibers and 350 nylon 6B fibers were pulled through the FEP tubing, respectively.

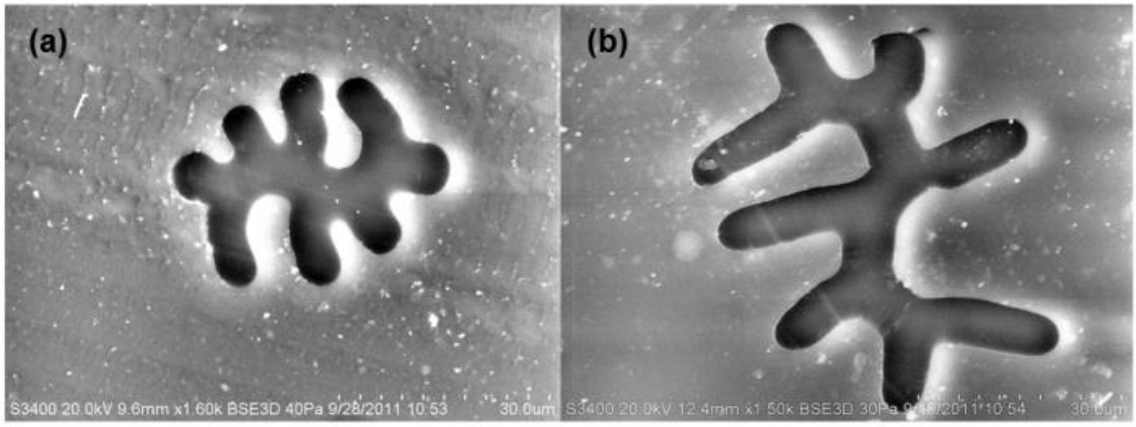

Figure 2.2 SEM cross-sectional images of nylon 6 C-CP fibers (a) nylon 6A and (b) nylon 6B

The actual column void volumes were determined by injection of an unretained compound, uracil (0.1 mg mL^{-1})[20]. The total surface area of fibers, reported in Table 2.1, was calculated by multiplying column length, fiber perimeter, and the number of individual filaments in the column. Once pulled through the column, the fibers were trimmed with a surgical scalpel to be flush with the tubing ends. Before performing separations, columns were completed with end fittings (Valco Instruments, Houston, TX, USA) and PEEK unions (VWR International, West

Chester, PA, USA), allowing for connection to the HPLC system for fiber/column washing. Successive wash solutions beginning with 100% ACN, followed by 100% hexane, 100% isopropyl alcohol, and finally 100% DI-H_2O, were pumped through the capillary column (1 mL min^{-1}). Each solvent was flushed until a stable baseline absorbance signal was achieved for at least 10 min.

Chromatographic System and Operations

The chromatographic system consisted of a Dionex (Sunnyvale, CA, USA) Ultimate 3000 with a model LPG-3400SD pump, a WPS-3000TSL autosampler, and a VWD-3400 RS variable wavelength UV-VIS absorbance detector, operated at 216 nm. The Dionex Chromeleon software was used to generate data for the chromatograms, and further analysis was done through Microsoft (Seattle, WA, USA) Excel. C-CP fiber columns were washed, prior to experimental runs, with 100% acetonitrile until a stable baseline absorbance is reached, then 100% milli-Q water until a stable baseline value was achieved, and finally equilibrated with 100% 20 mM TRIS-HCl (buffer A) while the baseline remained stable. Each protein mixture injection was performed at 2 mL min^{-1} 100% buffer A with a 2 minute equilibration between injections. No difference was seen in chromatograms when a hold time of 1 minute was added before gradient initiation and when it was not. Optimal protein elution was found at a gradient of 0-50% 1M NH_4Cl in 20 mM TRIS-HCl in 2 minutes. In doing so, the proteins are sequentially eluted through a displacement mechanism wherein the cationic groups of the proteins are substituted by the increasing ammonium ion (NH_4^+)

content in the mobile phase. While single chromatograms are presented to illustrate the separation characteristics of the respective fibers, triplicate repetitions do indeed yield agreements in retention times of better than 5 %, relative.

Scanning Electron Micrographs

Micrograph cross-sectional images of nylon 6A and nylon 6B were taken on a Hitachi S-3400-N (Hitachi Scientific Instruments, Pleasanton, CA, USA) scanning electron microscope (SEM) system. Single fibers were mounted vertically, suspended in a resin, and one end cut smooth with a RMC Powertome X (Boeckler Instruments Inc., RMC Products, Tucson, AZ, USA) microtome before being mounted on a standard stainless steel SEM platform using double-sided graphite tape in a near-vertical position. Images were taken at an accelerating voltage of 20 kV with image magnifications of 1500−1600x.

Attenuated Total Reflection FTIR (ATR-FTIR) Spectroscopy

ATR-FTIR measurements were performed on washed and air-dried nylon 6 C-CP fibers using a Thermo-Nicolet Magna 550 FTIR spectrometer equipped with a single bounce Thermo-Spectra-Tech Foundation Series Diamond ATR with a 50° angle of incidence. The fibers were force-pressed onto the diamond crystal to ensure maximum contact. Generated spectra were an accumulation of 16 scans

with a resolution of 4 cm^{-1}. Data analysis and processing was performed using OMNIC ESP software, Version 6.1a.

Differential Scanning Calorimetry (DSC)

A TA Instruments (New Castle, DE) MDSC 2920, equipped with a nitrogen cooling system was used to test the thermal properties of the fibers. Approximately 2 mg of the respective C-CP fibers were washed and air-dried prior to sealing in an aluminum pan. In quenching experiments, samples were initially heated from 0-300 °C at a rate of 20 °C min^{-1}. At 300 °C the cell temperature was held constant while the sample was removed and quench-cooled on a stainless steel bar cooled with liquid nitrogen. After the cell was re-equilibrated to room temperature, the quenched sample was re-introduced. The second DSC analysis was performed identically to the first, with heating from ~25-300 °C at 20 °C min^{-1}. DSC was also performed without quench cooling to confirm melting temperature and heat capacity. The acquisition software used was TA Instruments Thermal Advantage, Version 1.1A. Data was analyzed using TA Instruments Universal Analysis 2000, Version 3.9A. Samples of each fiber type were run in triplicate for each DSC process.

Matrix Assisted Laser Desorption Ionization Time-of-flight Mass Spectrometry (MALDI-TOF-MS)

MALDI analysis was performed on a Bruker Daltonics (Billerica, MA, USA) microflex LRF, MALDI-TOF mass spectrometer in the positive ion (160 ns delay), reflectron mode. The system is equipped with a nitrogen laser (337 nm) operating at a pulse rate of 60 Hz. A 72% laser power was used throughout the studies, with the spectra presented being a summation of 300 laser shots per position. A mass range of 260 – 3000 m/z was suitable. Fibers were tested in triplicate as TFE-dissolved samples as a means to assess the "original" polymer/monomer identities. In this case, 1 µL of the sample was sandwiched between two 1 µL drops of HABA as the matrix; each drop was pipetted onto the target and left to dry before addition of the subsequent layer.

Mechanical Properties

The mechanical properties, such as the modulus, tenacity, and extension at break of the washed and air-dried fibers were determined from their load elongation curves. Tensile testing was performed using an Instron 5582 (Canton, MA, USA). ASTM2256 was utilized to obtain the elongation, modulus and tenacity of the yarn samples. A gauge length of 25 mm was employed for yarn testing and the cross head speed set such that fiber breakage occurred in 20 ± 2 seconds. 10 samples of each yarn were analyzed and the average and standard deviation was calculated for elongation, modulus, and tenacity in each case.

Dilute Solution Viscometry

The relative viscosity (RV) of each fiber sample was determined in 90% formic acid at 25°C using an Ostwald viscometer size B. A 1% solution (wt/wt) was prepared for both nylon samples and the flow time compared to that of pure solvent. The flow times were recorded until the measurements were reproducible to ± 0.2sec. The RV was calculated using the following equation:

$$RV = t / t_0 \qquad [1]$$

where t is the average flow time of the test solution and t_0 is the average flow time of the neat solvent.

Ninhydrin Analysis Technique

The amine end group content was determined through the ninhydrin technique, as described by Knott and Rossbach[21]. Fiber samples were prepared in the same manner as for column preparation, using 20 mg of each fiber type and the same series of solvents (ACN, hexane, isopropyl alcohol and DI-H_2O), followed by air-drying prior to analysis. Each sample was placed in a 50-mL round-bottom flask with 1 mL of 10% isopropanol, 1 mL of 10% pyridine, and 2 mL of a reagent solution of 9.3 mL propionic acid, 20.18 g sodium propionate, 50 mL methylcellosolve, and 2 g of ninhydrin filled to 100 mL with water. The flask was stoppered and the mixture heated for 30 minutes in a boiling water bath. 20 mL of 50% ethanol was added to the mixture and the flask was shaken then left to sit for 15 minutes. The fibers were removed from the mixture and pressed at

the end of a syringe to ensure that the vast majority of liquid was removed. The liquid remaining in the flask was quantitatively transferred into a 100-mL volumetric flask and filled to the mark with water. Each fiber type was analyzed in triplicate with a $2x10^{-6}$ M solution of ε-aminocaproic acid analyzed in parallel to the fibers as a calibrant. A reaction containing no fibers or ε-aminocaproic acid was used as a blank with the quantitative absorbance measurements performed at the λ_{max} = 570 nm.

Results and Discussion

Physical characteristics of fibers/columns

As described previously, the respective fiber columns were composed to yield interstitial fractions of $\varepsilon_i \cong 0.6$. In considering the capillary tubing (200 x 0.8 mm i.d.), creating this interstitial fraction required 30 column lengths of nylon 6A fiber, with 30 filaments per fiber bundle giving a total of 900 fibers running lengthwise down the column. For the larger nylon 6B, which has 25 fibers per bundle, only 14 column lengths or 350 total filaments were required to yield very similar void volumes. In terms of total fiber mass, the 900 nylon 6A fibers weighed 7.76 mg, and the 350 fibers of nylon 6B weighed 8.25 mg. However, while there is more total polymer fiber in the latter column, a more important figure of merit in terms of chemical separations is the accessible surface area, at which chemical

interactions can occur. To be clear, on the size scale of proteins, the pore sizes in these extruded fibers are such that only “surface” interactions are occurring. SEM imaging, shown in Fig. 2.2, reveals the relative size and perimeter differences of the fibers. Shown on the same 30-µm scale, nylon 6B (Fig. 2.2b) takes up almost 2X the area of nylon 6A (Fig. 2.2a), also having deeper, wider channels. In support of the obvious visual difference, nylon 6B is ~25 % larger in perimeter than nylon 6A, as noted in Table 2.1. Although nylon 6B has a larger perimeter than nylon 6A, the total surface area in the column based on the number of fibers needed for efficient column packing tells the opposite story, as the total available fiber surface area for the nylon 6A column is nearly twice that of the higher dpf fiber column. In dealing with interactions that occur primarily on the fiber surface, this insight is significant when considering chromatographic separation qualities. On a first-principles basis, a column with 2x greater surface area suggests a higher propensity for solute-surface interactions affecting high separation efficiencies.

Protein Separation

The protein mixture of ribonuclease A, cytochrome c, and lysozyme was first separated on the nylon 6A C-CP fiber packed column using a mobile phase of 20 mM Tris-HCl buffer at pH 8, with an optimized gradient program of 0 – 50% 1M ammonium chloride in 20 mM Tris-HCl over 2 minutes at a flow rate of 2 ml min^{-1}. The chromatogram in Fig. 2.3a displays an efficient separation with fully

resolved peaks in elution order of RNase A at 0.58 min, cyto c at 0.78 min, and lyso at 1.21 min. Protein identity was confirmed by single-solute injections. This order is reflective of each protein's isoelectric point (pI) (RNase A pI = 8.7, cyto c pI = 10.0, lysozyme pI = 11.0), which hints at the density of the charged groups available on the protein as a function of the mobile phase pH. At pH 8, all three proteins have a net positive charge, and are thus displaced by the increasing ammonium ion concentration. While the net charge of the protein is not fully descriptive of the retention characteristics of the proteins, it does suggest that RNase A is the least retained due to the small ratio between its pI and the solvent pH, being the least cationic (i.e. having the smallest number of protonated surface amine groups) of the three proteins. The elution order thus (loosely) follows the number of cationic/acid groups at pH = 8.

Figure 2.3b shows the separation of the same three-protein suite on a nylon 6B C-CP fiber packed column under the same gradient conditions as for nylon 6A. Resolved peaks from cyto c and lyso are seen at shorter retention times of 0.66 and 1.03 min, respectively, while RNase A is mostly unretained, and is seen as a continuation of the solvent/injection peak at t_0 ~0.05 min. The broad band from t ~ 0.13 – 0.50 min. suggests that any RNase A retention was due to hydrophobic interactions and very little electrostatic interaction occurred with the nylon 6B surface.

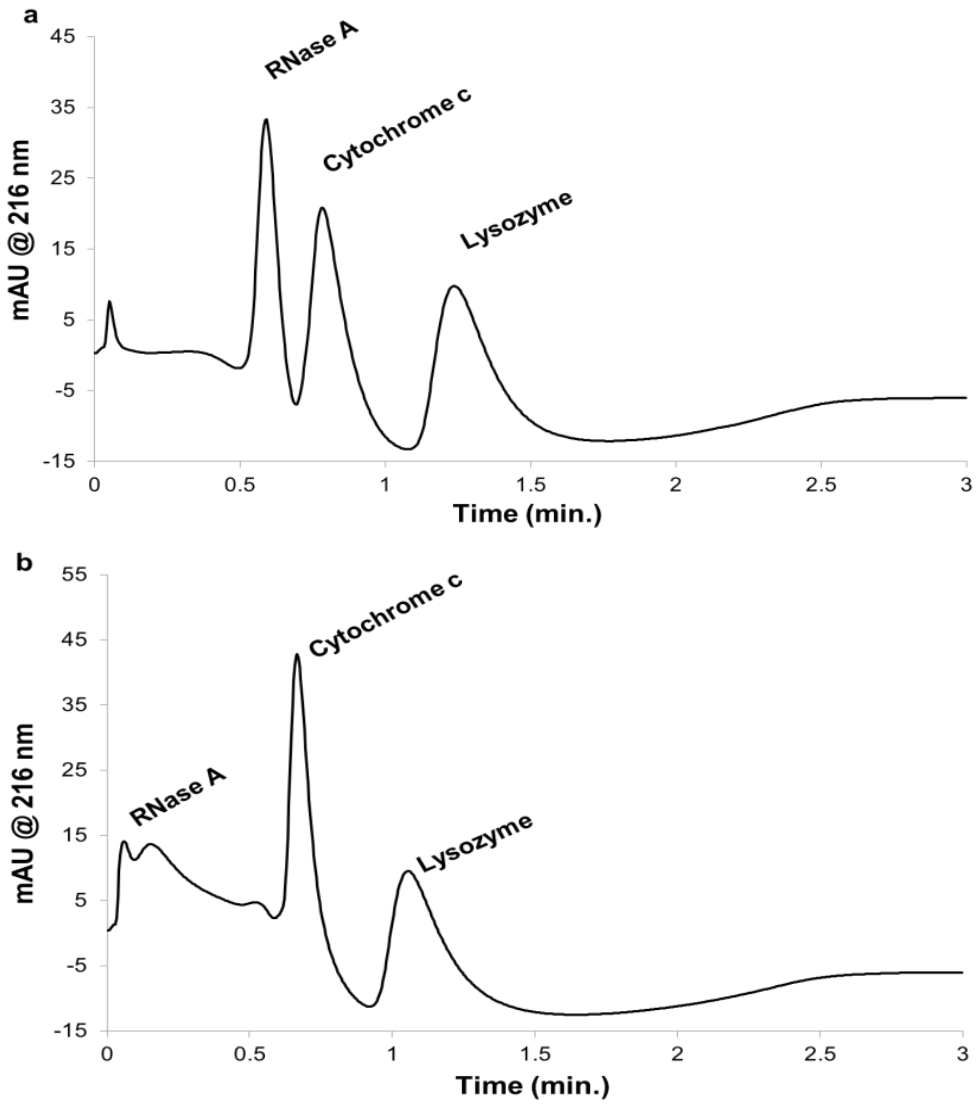

Figure 2.3 Separation of ribonuclease A, cytochrome c, and lysozyme on (a) nylon 6A C-CP and (b) nylon 6B C-CP fiber columns (gradient conditions in text).

In practice, even if the protein has a net charge of 0 (i.e., pH = PI), this only implies that there are an equal number of positive and negative charges, with the equilibrium value determined by the precise pH. Also important here, is the fact

that even in the absence of any protein or surface charge, there are hydrophobic interactions which may affect some level of retention, if only slightly. The combination of loss of RNase A retention and the shorter retention times for cyto c and lyso points to an overall loss of surface activity; i.e. access to a lower surface charge density. In comparing Figs. 2.3a and b, it is curious that two forms of nylon 6 fibers produce such different chromatograms. It is understood that physical differences manifest in the column hydrodynamics might affect the quality of the protein elution profiles (principally peak widths and shapes), but such differences would not affect the chemical nature of the separations in terms of degree of column retention. As much of the chemical/physical information about the fibers was unknown, it was important to delve deeper into the cause of these chromatographic differences on seemingly chemically equivalent materials. The studies described here are directed at gaining greater levels of understanding as to how extrusion and molecular weight based differences may affect the chemical nature of what *should be* an identical separation.

Chemical and physical structural characterization

FTIR

As a first step, it was necessary to confirm the basic chemical identity of the two fibers under study. More specifically, characteristic amide, amine, and carboxyl groups present in the nylon 6 fibers are easily identified through FTIR spectroscopy. FTIR is an essential method for polymer characterization, and the

availability of reference nylon FTIR spectra make comparisons easy. Fourier transform infrared spectra were taken for nylon 6A and nylon 6B; included in Appendix A, Fig. A-1. Characteristic nylon 6 bands are seen for both. An N-H stretch band is seen from 3356 – 3180 cm^{-1} and the C=O (amide I) stretch band is seen from 1682 – 1579 cm^{-1}. A C-N stretch, N-H bend (amide II) band is seen from 1579 – 1483 cm^{-1}. An amide II overtone is seen at 3105 – 2989 cm^{-1}. C-H stretches are seen from 2976 – 2771 cm^{-1}. The amide III band is seen from 1272 – 1191 $cm^{-1.}$ The C-C skeletal stretches are seen from 1192 – 1000 cm^{-1}. Comparison of these spectra with known nylon 6 absorbance bands served only to confirm that each fiber was made from a nylon 6 base polymer[22,23]. Accordingly, as nylon 6A was extruded on-site we are absolutely confident that its source was nylon 6. Likewise, we are able to confirm that the nylon 6B C-CP fiber *was not* made from a nylon 6,6 base polymer (as one obvious alternative) due to the similarity between the two FTIR spectra; further testing described here supports this fact as well.

Thermal Analysis

The thermal characterization of the fibers was carried out via two modes of differential scanning calorimetry (DSC) to determine if crystallinity differences existed between the samples. Crystallinity might be expected to impact separations in terms of access to the subsurface regions of the fibers. As seen in Fig. 2.4, a broad endothermic peak observed between 5 and 60 °C, which may

be attributed to water loss, and unfortunately masked any information regarding the existence of a glass transition temperature (T_g).

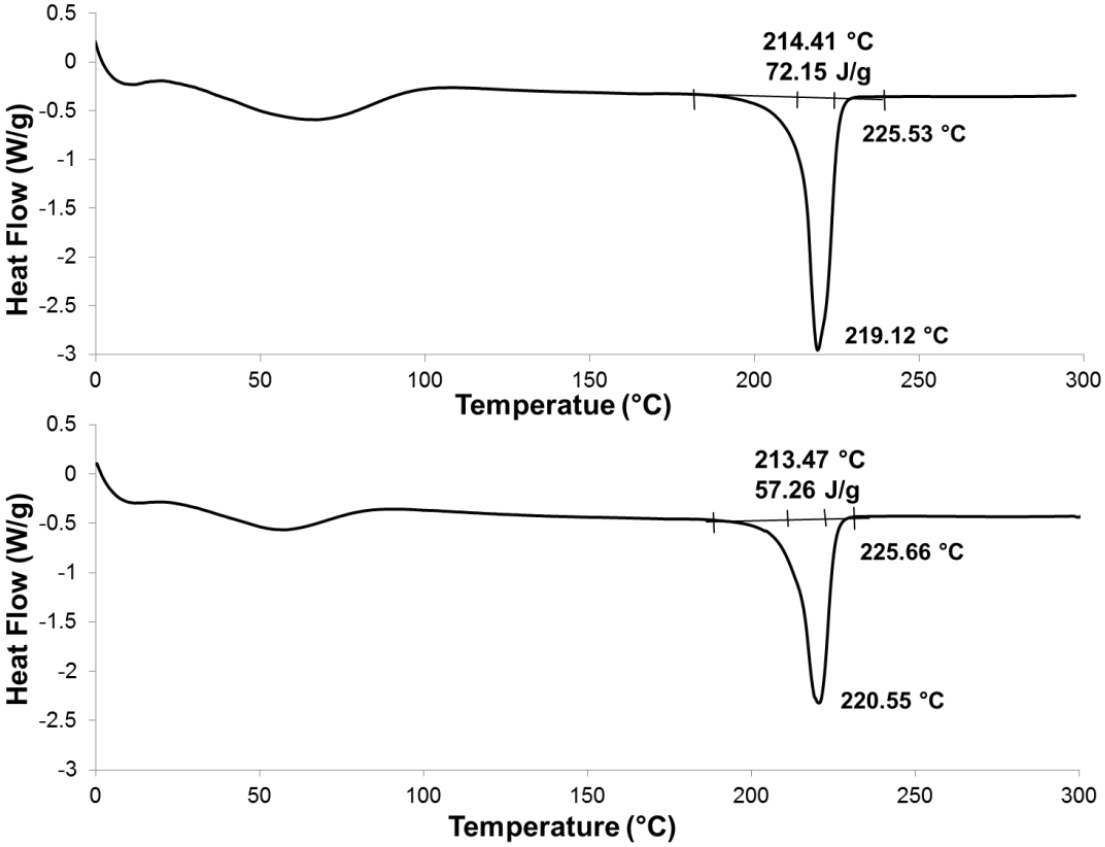

Figure 2.4 Direct DSC curves of (a) nylon 6A and (b) nylon 6B C-CP fibers.

At T_g, the amorphous regions of a semi crystalline polymer change from a glassy state to a rubbery one. In other words, the polymer reaches a point where there is enough energy for the chain to begin to rotate around its bonds. To obtain an amorphous glassy material prior to DSC analysis, solid fibers are first melted and then quench-cooled. In this case, the transition from glassy to rubbery can be

seen as both materials display very similar thermal characteristics as seen in Fig. A-2 of Appendix A. A step change in heat capacity occurs as the temperature rises. In S2a, T_g is seen from 6.5 – 42.1 °C and likewise in S2b from 9.1 – 44.7 °C for the two nylon fiber types. Based on this data, the T_g peaks should have occurred in the region of 40 °C in Fig. 2.4. No significant difference was observed in the initial DSC thermograms regarding the onset, offset, and midpoint temperatures of the melting exotherms with all three values lying in the expected range for nylon 6. The heat of melting (ΔH_m) was calculated by integrating the area under the melting peaks (Fig. 2.4), which were found to be 72.15 J/g and 57.26 J/g for nylon 6A and nylon 6B respectively. The percent crystallinity of each sample was then calculated using the following equation using theoretical heat of fusion for 100% crystalline nylon 6 of 230 J/g,[24]

$$\% \text{ crystallinity} = (\Delta H_m / \Delta H_c) \times 100 \qquad [2]$$

where ΔH_m = heat of melting and ΔH_c = cold crystallization energy.

In this case, the DSC of neither sample reflected a cold crystallization peak, and so the values obtained from the integration of the melting endotherms were the sole input values. The degrees of crystallinity obtained were, 31.4 % for nylon 6A and 24.9% for nylon 6B. This was anticipated, as the denier per filament of the two samples were 2.64 and 7.74 for nylon 6A and nylon 6B, respectively. Lower denier fibers typically undergo more severe wind up conditions (i.e. higher wind up speed and tension), and so more crystallinity would be imparted to the smaller fibers. The 20% higher crystallinity in nylon 6A

in comparison to nylon 6B gives insight into a potential to tailor fiber properties based on the extrusion process. In agreement with the IR data, when in their amorphous form after rapid quenching from the melt and subjection to the same DSC heating regime, nylon 6A and nylon 6B both indicated thermal transitions characteristic of nylon 6, having T_g at approximately 40 °C, a crystallization temperature (T_c) at 68 °C, and a melting temperature (T_m) at 220 °C (Fig. 2.4). This similarity in the thermal behavior via DSC did not highlight significant potential differences between the samples other than the crystallinity.

MALDI-TOF-MS

MALDI-MS was performed to provide insight into possible molecular weight differences between the two nylon 6 samples. In principle, the polymer molecular weight should be some reflection of the number of end groups available per unit area. While solid fiber analysis is uncommon, there is also little literature addressing MALDI-MS of nylon 6 fibers due to its insolubility in most common solvents such as tetrahydrofuran. To get around this, in some cases, a finely ground powder of sample and matrix is pressed into a pellet and analyzed in that form[25]. However, it is noted that this method was not accurate for end group determination, as disruption of end groups can occur during sample preparation. The groups of Montaudo [26,27] and Park[28] report fully dissolving nylon 6 samples in trifluoroethanol (TFE) prior to MALDI analysis. They were able to obtain accurate mass values and end group distributions for several nylon

6 samples. MALDI mass spectra were obtained on the dissolved nylon 6A and nylon 6B samples in an effort to ascertain the likelihood of them being extruded from the same molecular weight polymers. Figure A-3 of Appendix A displays the MALDI-TOF mass spectra of samples that were fully dissolved in TFE prior to application to the MALDI target. While nylon 6B yielded a somewhat higher overall intensity, the *m/z* values for both spectra show nearly identical structure. Seen is a uniform oligomeric distribution having mass differences of ~113.1 Da between the respective families of peaks. This value is expected, as it is the molecular weight of the nylon 6 monomer (Fig. 2.1), with the multiplets of peaks corresponding to oligomers having different numbers of monomer units. More specifically, the major peak in each multiplet represents ions of the form -[-NH-(-CH_2-)$_5$-CO-]$_n$- •••Na^+ (113.1 x n + 23), with a peak one mass unit of greater of the general form H-[-NH-(-CH_2-)$_5$-CO-]$_n$-•••Na^+ (113.1 x n + 1 + 23). The previously cited works attribute the lower-mass peak to polymer containing cyclic oligomers.[26-28] In each series, there is a substantial signal for a species 16 Da above the major peak, representing an ion of the form -[-NH-(-CH_2-)$_5$-CO-]$_n$-O-•••Na^+ (113.1 x n + 16 + 23). For both samples, the most intense peaks correspond to oligomers with n = 9 - 13, with no appreciable chemical differences observed between the two dissolved fiber types. The similarity displayed again confirms that the molecular base structure of these two nylons is the same.

Mechanical Testing

To investigate further the differences between the extruded C-CP fibers, tensile testing was performed. The response curves of Fig. A-4 of Appendix A reflect the amount of positive strain (tensile) the respective fibers could withstand before breaking. Nylon 6B, on average, withstood a higher load (breaking strength, gf) than nylon 6A. The resulting average elongation, tenacity, and modulus of ten individual fiber tensile tests are given in Table 2.2. Both fiber samples yielded levels of elongation of ~12%. The values for both modulus and tenacity are significantly different as would be expected when considering the difference in deniers of 2.67 and 7.72 for nylon 6A and nylon 6B respectively. The higher denier sample, in this case nylon 6B, has lower tenacity and modulus, which is a direct result of the spinning process already alluded to.

Table 2.2 Comparison of mechanical properties of samples

Sample	Elongation (%)	Tenacity (g/den)	Modulus (g/den)
Nylon 6A	12.60 ± 1.57	2.87 ± 0.16	29.12 ± 2.44
Nylon 6B	12.39 ± 0.71	1.30 ± 0.07	19.89 ± 1.26

In order to achieve low denier fibers the wind up speeds are greater and as such more orientation and crystallinity is imparted to the filaments. Hence, much improved mechanical properties are achieved due to the increased alignment and proximity of the polymer chains with one another. These data coupled with that obtained via DSC support this observation.

Determination of Relative Viscometry

The viscosity of dilute polymer solutions is considerably higher than that of the pure solvent. Any observed viscosity increase is dependent on the solvent, the temperature, the molecular chain length, and the polymer concentration. The number average molecular weight $(\overline{M})_n$ of nylon 6 is related to the number average degree of polymerization, $(DP)_n$, as follows

$$(\overline{M})_n = 113.16\ (DP)_n \qquad [3]$$

Where 113.16 is the molecular weight of caprolactam.

It is possible to use RV as a measure of molecular weight using the following empirical relationship[29]

$$(DP)_n = 95.70\ (RV-1) \qquad [4]$$

Relative viscosity values of 2.08 and 2.33 were obtained giving corresponding $(\overline{M})_n$ values of 11,695 and 14,403 for nylon 6A and nylon 6B respectively. Clearly a polymer with lower average molecular weight, in this case nylon 6A, will also have a greater number of end groups per unit fiber mass available for chemical interactions. In agreement with the MALDI-MS spectra, nylon 6B has a longer repeating polymer chain and less available end groups to contribute to protein interactions.

Determination of Amino End Group Content

As a final test, the quantification of end groups available on each fiber sample was determined. As described previously, the separation of proteins on nylon 6 C-CP fibers is due to both hydrophobic interactions with the nylon 6 backbone and electrostatic interactions with charged end groups on the fiber surface, having an equal number of amino and carboxy groups. The reaction of primary amines (which *de facto* are end groups) with ninhydrin allows for the quantitative determination of the amino end groups on the fiber. This ninhydrin method, introduced by Knott and Rossbach[21] in 1980, compares a reaction of ninhydrin and the sample fibers with a reaction of ninhydrin and ε-aminocaproic acid, which is an intermediate in the polymerization of nylon 6, resembling the nylon 6 monomer unit. When ninhydrin is in the presence of amino groups, it binds to nitrogen to produce a bluish-purple compound, called Ruhmann purple; the more intense color produced, the greater number of amino end groups are present. This method was chosen over other common methods, such as acid/base titrations, due to the ability to differentiate between primary amine end groups and other basic groups. The number of amino groups can be quantitatively determined from a Beer's Law plot of absorbance values versus concentration of standard, neat ε-aminocaproic acid solutions. The sensitivity of this method is due to the reaction medium, which causes the fibers to swell, ensuring that a greater extent of the fiber matrix is reacted.

The results of the ninhydrin reaction determinations (in terms of μmol amino groups per gram of fiber) are presented in Table 2.3. In this case, nylon 6A yields around 25% more amine functionality per unit fiber mass than nylon 6B.

Table 2.3 Amino end group content determined by a reaction with ninhydrin (2,2-Dihydroxyindane-1,3-dione)

Sample	Amino End Group Content (μmol/g)
Nylon 6A	76.6 ± 1.19
Nylon 6B	62.0 ± 1.79

Extending this value to the relative amount of fiber mass per column leads to the conclusion that overall the number of amine groups in the nylon 6A column is approximately 16% greater than the number in the nylon 6B column. As noted, the ninhydrin solvent system is designed to penetrate the porosity of the fiber matrices, while the size of these proteins (with radii of gyration of ~4 nm) prohibits their entering the natural fiber porosity. Thus, the relevant charged sites are only those that exist on the fiber surface. Therefore, the 16% higher mass-based end group density, coupled with the ~ 2x higher fiber surface area per column combine to very effectively yield greater levels of retention based on ionic interactions.

From a correlation of the ninhydrin results with the relative viscometry and MALDI-MS spectral data, it is strongly suggested that the nylon 6A fibers were

extruded from a base polymer having somewhat shorter oligomer lengths, meaning a shorter chain of nylon 6 monomers between end groups. This supports its comparability with the spectral data of dissolved, amorphous samples, and allows for more end groups to be present per unit of fiber mass. Nylon 6B, was extruded from a base polymer having longer oligomer length, contributing to its high molecular weight peaks in the solid state mass spectra and the lower density of amine end groups.

Conclusions

A range of physical and chemical tests has been implemented to compare two nylon 6 C-CP fiber stocks that exhibited different chromatographic behavior. The nylon 6A C-CP fiber-packed column allowed for a highly efficient separation of a three-protein suite using a steep gradient at a flow rate of 2 mL min^{-1} with all proteins eluting in less than 2 minutes. Under the same conditions, the nylon 6B C-CP fiber-packed column was unable to fully-retain ribonuclease A, with the cytochrome c and lysozyme components also showing reduced retention. Investigation into the physical structure of the fibers and columns revealed differences in the absolute shape, perimeter/surface area, and denier. Chemical, thermal, and mechanical testing showed differences in crystallinity, strength, molecular weight, and number of amine end groups between the fiber types. In general, while is seems clear that the two fibers are extruded from nylon 6 polymers, based on the FTIR and DSC testing, the solid-state MALDI data, in

combination with the thermal and viscometry measurements, suggest a process in manufacture of the base nylon 6 polymer, whereby longer oligomer chains are affected. The higher-numbered oligomers present in nylon 6B result in fewer end groups per unit fiber mass. A smaller number of surface end groups yields less efficient surface ionic interactions for protein retention, thus the weakly retained ribonuclease A is likely only interacting through hydrophobic means.

Much of the previous work with C-CP fibers was undertaken fully realizing that fiber extrusion conditions would affect the fiber shape, denier, etc., which dictate the column hydrodynamic characteristics. The studies described here point clearly to the importance of base molecular weight and fiber extrusion conditions in affecting the physical and chemical nature of polymer fibers that otherwise originate from identical monomers. It is believed that the knowledge of these effects will allow for a much more thorough understanding of the C-CP fiber platform and optimized paths forward.

Acknowledgments

This material is based upon work supported by the National Science Foundation Division of Chemistry under Grant No. 1011820 (co-funded by the MPS/CHE, ENG/CBET, and EPSCoR). The technical expertise in the acquisition of the FTIR and DSC data by Ms. Kim Ivey of the Clemson University School of Materials Science and Engineering is gratefully acknowledged.

References

1. Putscher, R. E.; Saunders, J. H. in Kirk-Othmer Encyclopedia of Chemical Technology; Grayson, M., Ed.; John Wiley & Sons, Inc.: 1982, p 328.
2. Lewis, D. M. in Synthetic Fibre Materials; Brody, H., Ed.; Ed. Longman Group, Essex, UK: 1994.
3. Brody, H., Synthetic Fibre Materials; Longman Scientific & Technical, 1994.
4. Fourne, F., Synthetic Fibers; Hanser/Gardner Publications, Inc.: Cincinnati, Ohio, 1999.
5. Escandar, G.; Gomez, D.; Mansilla, A.; de la Pena, A.; Goicoechea, H., Anal.Chim. Acta 506, 161 2004.
6. Peralta, C.; Fernandez, L.; Masi, A., Microchem. J. 98, 39 2011.
7. Pahujani, S.; Kanwar, S.; Chauhan, G.; Gupta, R., Bioresour. Technol. 99, 2566 2008.
8. Yang, F.; Weber, T.; Gainer, J.; Carta, G., Biotechnol. Bioeng. 56, 671 1997.
9. Aussawasathien, D.; Teerawattananon, C.; Vongachariya, A., J. Membr. Sci. 315, 11 2008.
10. Marcus, R. K., J. Sep. Sci. 31, 1923 2008.
11. Marcus, R. K., J. Sep. Sci. 32, 695 2009.

12. Marcus, R. K.; Davis, W. C.; Knippel, B. C.; LaMotte, L.; Hill, T. A.; Perahia, D.; Jenkins, J. D., J. Chromatogr. A 986, 17 2003.

13. Nelson, D. M.; Stanelle, R. D.; Brown, P.; Marcus, R. K., Am. Lab. 37, 28 2005.

14. Nelson, D. M.; Marcus, R. K., Analytical Chemistry 78, 8462 2006.

15. Nelson, D. M.; Marcus, R. K., Protein Pept. Letts. 13, 95 2006.

16. Stanelle, R. D.; Mignanelli, M.; Brown, P.; Marcus, R. K., Anal. Bioanal. Chem. 384, 250 2006.

17. Stanelle, R. D.; Straut, C. A.; Marcus, R. K., J. Chromatogr. Sci. 45, 415 2007.

18. Stanelle, R. D.; Marcus, R. K., Anal. Bioanal. Chem. 393, 273 2009.

19. Stepaniak, R.; Garton, A.; Carlsson, D.; Wiles, D., J. Polym. Sci. Part B-Polym. Phys. 17, 987 1979.

20. Neue, U. D., HPLC Columns: Theory, Technology, and Practice; Wiley-VCH: New York, 1997.

21. Knott, J.; Rossbach, V., Angew. Makromol. Chem. 86, 203 1980.

22. Rotter, G.; Ishida, H., J. Polym. Sci. Part B-Polym. Phys. 30, 489 1992.

23. Huang, L.; Allen, E.; Tonelli, A., Polymer 40, 3211 1999.

24. Wunderlich, B., Macromolecular Physics Volume 3: Crystal Melting; Academic Press, 1980.

25. Skelton, R.; Dubois, F.; Zenobi, R., Anal. Chem. 72, 1707 2000.

26. Montaudo, G.; Montaudo, M.; Puglisi, C.; Samperi, F., Macromolecules 28, 4562 1995.

27. Montaudo, G.; Montaudo, M.; Puglisi, C.; Samperi, F., J. Polym. Sci. Part A-Polym. Chem. 34, 439 1996.

28. Choi, H.; Choe, E. K.; Yang, E. K.; Jang, W.; Park, C. R., Bull. Korean Chem. Soc. 28, 2354 2007.

29. Gupta, V. B.; Kothari, V. K., Manufactured Fiber Technology; Chapman and Hall: London, UK, 1997.

CHAPTER THREE

INITIAL EVALUATION OF PROTEIN A-MODIFIED CAPILLARY-CHANNELED POLYMER FIBERS FOR THE CAPTURE AND RECOVERY OF IMMUNOGLOBULIN G

Introduction

The industry for therapeutic monoclonal antibodies (mAbs) is continuously growing due to the demand for their use in biopharmaceuticals. In 2009, mAb-based therapeutics represented $38 billion of the $99 billion total biopharmaceutical global market and included five of the ten top-selling products [1]. Antibody production from recombinant cell cultures has increased from < 1 g L^{-1}, to 5 g L^{-1} that is common today [2,3], with reports on the 10 g L^{-1} scale [4]. For initial capture of mAbs from the cell culture supernatant, protein A affinity chromatography is the method of choice due to the high selectivity of the Fc region of IgG for the recombinant protein A ligand, a well characterized affinity system [5,6]. However, with several polishing steps required after capture, current downstream processing costs can add up to 80% of total antibody manufacturing costs [1]. With safety and efficacy a top priority, focus has been shifted to the improvement of downstream processing. Successful endeavors would address the current production bottleneck of performing purification steps in a fast, cost-effective way while still yielding a high amount of pure antibody.

Current commercial protein A sorbents are available on a variety of supports including agarose, polystyrene, porous glass, and macroporous polymers [7-9]. The method of protein A immobilization varies for each sorbent and includes CNBr or epoxy coupling, amine and thio-ester linkages, and other proprietary covalent binding methods to ensure a nearly irreversible immobilization. However, these sorbents are often very expensive and suffer from flow rate limitations in terms of high backpressures, media compression, and limited mass transfer rates. While packed-bed chromatography continues as the mainstay for antibody separations, Gottschalk suggests that the next few years will reveal an expansion of novel protein A supports to yield cost-effective methods having lower overhead costs while maintaining or improving process throughput and yields [3].

Introduced here is a method of protein A affinity chromatography utilizing polypropylene (PP) capillary-channeled polymer (C-CP) fibers as a support phase. These fibers have previously been investigated in this laboratory for applications in HPLC [10-13] and SPE [14-16] protein separations. Their advantages include highly efficient fluid movement and a low porosity surface, resulting in the ability to perform separations at high linear velocities (>75 mm s^{-1}) with low back pressures (<20 psi cm^{-1}) without sacrificing chromatographic quality [17]. Efficient fluid movement is due to their unique shape, consisting of eight capillary channels running down their length [18]. When packed into a column format, the fibers interdigitate and align to form single micron-sized

channels. The high linear velocities in narrow channels combine with the nonporous nature of the fibers [19] to yield very favorable mass transfer characteristics for rapid and efficient protein separations. C-CP fibers are also robust over a wide pH range and are extremely cost efficient when compared to commercial products.

Beyond the native surface chemistries of polyester, nylon-6 and PP C-CP fibers, there is a diversity of surface modifications that can be employed to impart greater selectivity to the fiber support phases, while maintaining the advantageous fluidic properties of C-CP fiber columns. For example, a SPE medium has been generated from polyester C-CP fibers modified with polyacrylic acid that has the ability to bind metal ions from aqueous solution [15]. More recently, a novel surface modification strategy based on the adsorption of head group-modified PEG-lipids has been [20]. In this approach, the highly hydrophobic lipid tails adsorb to PP fibers, while the PEG linkers are effectively solvated and present the capture head group to the solute-containing stream. The basic concept of this immobilization chemistry was demonstrated with a biotinylated PEG-lipid to construct an affinity phase for the capture of streptavidin labeled with Texas Red (SaV-TR) for on-fiber detection. Very high levels of selectivity were realized in for the capture of streptavidin-tagged proteins produced in a fermentation broth.

In this work we report the initial evaluation of IgG capture on protein A-modified PP C-CP fibers. A micropipette tip format has been employed as in

previous SPE applications (Fig. 3.1) [14-16]. This format allows for conservation of fiber, sample, and solvent, as well as allowing for solution introduction by centrifuge, providing a relatively quick and simple surface modification test bed.

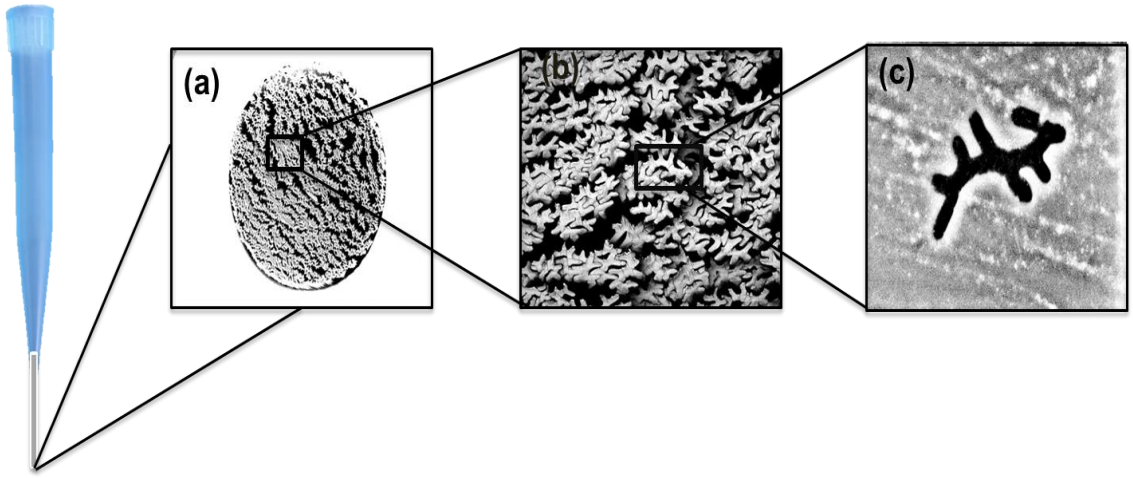

Figure 3.1 Photograph of a C-CP fiber tip attached to a micropipette tip with successive SEM cross section images of greater magnification showing a) C-CP fiber packed tip with a cross section diameter of 760 μm (entire image width of 1.3 mm), b) zoomed in view of a C-CP fiber packed tip with an image of 260 μm, and c) a single PP fiber with an image width of 90 μm.

PP C-CP fiber surfaces are modified by adsorption of native recombinant *Staphylococcus aureus* protein A (rSPA). Optimization of the surface coating process and assessment of the stability of the adsorbed rSPA layer under a variety of common solvents and buffers is reported. Myoglobin is used as a representative of modest-sized proteins that are typical of cell culture products in terms of unwanted binding to the stationary phase in a mixture with the target antibody. A BSA block step and an intermediate wash step were evaluated toward prevention of non-specific adsorption on the hydrophobic base fiber

surface. Finally, a variety of common IgG elution strategies were evaluated to determine the most promising means of recovery. Overall, this investigation provides support for the evolution toward preparative-scale protein A-modified C-CP fiber columns as a means to minimize current bottlenecks in IgG capture and purification.

Materials and Methods

Chemicals and Reagents

HPLC-grade ACN and methanol, acetic acid, and phosphoric acid were all purchased from Fisher Scientific (Pittsburg, PA). Milli-Q water (18.2 $M\Omega\,cm^{-1}$) derived from a Millipore water system (Billerica, MA) was used for fiber rinsing and preparation of all buffers and aqueous solutions. rSPA was obtained from Syd Labs, Inc. (Malden, MA) and was prepared to necessary concentrations (0.05 – 1 mg mL^{-1}) in phosphate buffered saline (PBS) consisting of 140 mM NaCl, 10 mM Na_2HPO_4, 1.8 mM KH_2PO_4, and 2.7 mM KCl at pH 7.4 (Sigma Aldrich, Milwaukee, WI). Stability of the rSPA-modified surface was tested with PBS solutions (pH 3 – 12), 100% ACN, 50% methanol, 0.01 M HCl, and 0.01 M NaOH. Purified IgG from human serum and myoglobin from equine heart (Sigma Aldrich, Milwaukee, WI) were prepared to necessary concentrations (0.05 – 2 mg mL^{-1}) individually and as a 4:1 mixture in a load buffer of 20 mM di-basic sodium phosphate and 150 mM sodium chloride. BSA was obtained from Sigma Aldrich

(Milwaukee, WI) and prepared to a 0.2 mg mL^{-1} in PBS. Glycine, di-basic sodium phosphate, sodium acetate, and disodium citrate, all obtained from Sigma Aldrich (Milwaukee, WI), were evaluated as intermediate wash buffers (pH 5) and elution buffers (pH 3). All solutions discussed here were tested on both the native C-CP fiber surface and the rSPA-modified surface to determine stability and the extent of interactions.

C-CP Fiber Tip Construction and Preparation

Polypropylene (PP) C-CP fibers were manufactured by and obtained from the Clemson University School of Materials Science and Engineering (Clemson, SC). Fiber tip construction begins by packing capillary chromatography columns with PP C-CP fibers that have been rinsed with ACN, methanol, and milli-Q water [21]. It has been previously shown that optimal macromolecule separations occur with C-CP fibers columns having an interstitial fraction of $\varepsilon_i \cong 0.6$ [21]. To achieve this value, 600 PP C-CP fibers were pulled into 300 mm, 0.8-mm i.d. fluorinated ethylene polypropylene (FEP) capillary tubing (Cole Parmer, Vernon Hills, IL). In the studies presented here, columns were constructed with $\varepsilon_i = 0.63$, having less than 5% variability to ensure uniformity over the course of the experiments. After packing, capillary columns were subject to radial compression by manually pulling through a 0.6-mm i.d. glass capillary. The columns were fit to an HPLC system and further conditioned with ACN and Milli-Q water for 15 minutes each at 1 mL min^{-1}. The column was cut into 2.54 cm segments with an

additional 4 mm gap left at one end allowing for the tubing to be press-fit onto the end of a low-retention 1-mL micropipette tip (Redi-Tip, Fisher Scientific, Pittsburg, PA). This fiber tip format has been described previously and successfully applied in our laboratory for SPE [14-16]. The weight of fiber stationary phase per 2.54-cm tip is 4.0 ± 0.1 mg. Figure 3.1 provides successive viewpoints of the C-CP fiber tip structure, from the assembled SPE tip down to the single-fiber level.

C-CP Fiber Tip Modification

All solution exposure to the fiber-packed tips was done through centrifugation spin-down at 1900 relative centrifugal force (RCF) (Clinical 50, VWR, West Chester, PA) for 1 to 4 minutes, depending on the fluid volume applied. The PP C-CP fiber tips were first equilibrated with 1 mL PBS at pH 7.4. In determining an optimal load concentration, rSPA solutions were made in a range of 0.1 mg mL^{-1} to 1 mg mL^{-1} and loaded in 0.1 mL aliquots. In determining an optimal load volume, 0.1 mg mL^{-1} rSPA was loaded in 0.1 mL – 1 mL aliquots. rSPA load volumes were cycled through tips four times to ensure uniform surface modification. Lastly, PBS was applied as a wash step in an equal volume to that of the rSPA load step. After modification, tips were stored individually in PBS and kept at 2 – 6 °C. The chemical stability of the rSPA surface was evaluated by spinning 0.9 mL of the various test solutions through tips, with the results

reported as percent rSPA removed. Each tip was used within one week of modification.

Capture and Elution of IgG

Initially, individual 0.1 mL solutions of 0.1 mg mL^{-1} IgG and 0.1 mg mL^{-1} myoglobin were centrifuged through native and rSPA-modified PP C-CP fiber tips for comparison. The surface-blocking step involved passing of 0.9 mL of 0.2 mg mL^{-1} BSA through the tips. The above process was repeated with a 4:1 IgG:myoglobin mixture. Intermediate wash buffers were evaluated with 1.8 mL volumes via centrifugation. The wash buffers included 0.1 M loading buffer, 0.5 M sodium acetate, and 0.5 M sodium citrate. Six IgG elution buffers were examined, with 0.9 mL of each buffer initially centrifuged through tips. The elution buffers included 0.1 M acetic acid, 0.1 M glycine, 0.5 M sodium acetate, 0.1 M disodium citrate, and 0.1 M citric acid buffer. Cleaning-in-place (CIP)/regeneration was evaluated with 0.01 M NaOH + 1 M NaCl.

Protein Quantification

Solutions centrifuged through the C-CP fiber tips were collected individually. UV-Visible absorbance response functions for rSPA, IgG, myoglobin, and BSA were used to determine protein concentrations in these solutions. Measurement was done with a Tecan GENios absorbance microplate reader (Tecan US, Inc. Durham, NC) utilizing a Costar UV-transparent 96-well

microplate. The amount of protein adsorbed to the fiber surface was calculated by subtracting the concentration observed in the load and wash volumes from the initial concentration of the load volume. The absorbance of rSPA was determined at 230 nm, BSA was determined at 280 nm, and the absorbance of the individual IgG and myoglobin solutions were determined at 280 and 405 nm, respectively. In order to determine the individual protein concentrations in a 4:1 IgG:myoglobin mixture, an absorbance ratio method was employed involving the simultaneous solving of Beer's Law with two equations and two unknowns. For this method, the ratio of absorbance of the analytes at the isoabsorptive point (where they both absorb, 280 nm), and the absorbance maximum of one of the components (myoglobin, 405 nm) was evaluated to determine their individual concentrations in the mixture. This calculation utilizes Beer's law and the following formula:

$$C_{IgG} = \frac{\left((A_1)(a_{y2}) - (A_2)(a_{y1})(b)\right)}{\left((a_{x1})(a_{y2}) - (a_{y1})(a_{x2})(b^2)\right)}$$

$$C_{myo} = \frac{\left((A_2)(a_{x1}) - (A_1)(a_{x2})(b)\right)}{\left((a_{x1})(a_{y2}) - (a_{y1})(a_{x2})(b^2)\right)}$$

Where,

C_{IgG} = concentration of IgG

C_{myo} = concentration of myoglobin

b = cell path length

a_{x1} = absorptivity of IgG at 280 nm

A_1 = absorbance of mixture at 280 nm

A_2 = absorbance of mixture at 405 nm

a_{y1} = absorptivity of myoglobin at 280 nm

a_{y2} = absorptivity of myoglobin at 405 nm

a_{x2} = absorptivity of IgG at 405 nm

Results and Discussion

Initial rSPA adsorption considerations

For all of these demonstration experiments, centrifugation was used to flow solution through the fiber tips as it allows for uniform flow through the fiber channels, yielding a more homogenous and reproducible surface modification than manual aspiration [15]. It is also advantageous because of parallel processing, allowing several tip constructs to be run at once. Two of the more basic considerations prior to quantitative determinations and evaluations of different chemistries is the assurance that all protein A binding is taking place on the fibers and understanding the kinetic trade-offs in the solution processing steps. In order to investigate the extent of protein A adsorption to the tip structural materials, rSPA was passed through a segment of empty FEP tubing affixed to a micropipette tip as well as a tip with no tubing present. In both cases, 100% of the rSPA was collected in the flow through, verifying no adsorption of rSPA to the tip assembly.

As with any adsorptive process in a flowing stream, there is a relationship between transit (exposure) time and the amount of ligand that can be transferred to the substrate surface. Initial adsorption studies involved passing 0.1 mL of a 0.1 mg mL^{-1} rSPA solution, effectively exposing the C-CP fiber tip to 10 µg of

protein across a range of centrifugation speeds. Optimum adsorption was found at maximum speed of this centrifuge, 1900 RCF; thus the fastest solution flow rate and shortest residence time. This is a counterintuitive result, as one would expect that longer exposure times would allow greater surface accumulation. However, the favorable mass transfer and high throughput properties of C-CP structures lead to optimal adsorption at the highest linear velocities.

Studies of protein surface adsorption under conditions of high shear (γ = linear velocity/channel gap) clearly indicate that adsorption rates and surface ordering increase as shear increases [22-24]. In practice, diffusion layer thicknesses decrease with $\gamma^{1/3}$ [25]. Previous protein separations on C-CP fiber columns reflected no loss in recoveries, nor diminished chromatographic performance, at linear velocities up to 75 mm s^{-1}, equating to shear rates of 75,000 s^{-1} [13]. The shear rates realized in this centrifugation processing (~10,000 – 50,000 s^{-1}) are far greater than are present in packed bed or monolithic columns. Here in lies the advantages of the basic C-CP column/tip structure; short diffusion distances to non-porous surfaces where convective diffusion (as found in monolithic materials [26,27]) likely controls mass transport [28]. While greater surface order has been documented under conditions of high shear, it is also clear that adsorption at low linear velocities (and thus longer exposure times) would increase the tendency for proteins to denature on the hydrophobic surfaces, limiting molar surface coverage and likely perturbing capture efficiencies.

Replicate adsorption experiments at the maximum centrifugal velocity at an rSPA concentration of 0.1 mL of 0.1 mg mL^{-1} resulted in initial capacities of 4.08 ± 0.40 µg per PP C-CP fiber tip (fiber mass = 4.0 mg, void volume = 8 µL) or ~1 µg mg^{-1} fiber. As might be expected based on the discussion above, narrowing of the inter-fiber spacing should improve the loading. As employed in microbore HPLC separations [21], radial compression of the fiber-packed microbore tubing results in more uniform packing as well. Radial compression applied before cutting the 2.54 cm tips results in a reduction of the interstitial fraction by ~10% (relative), yielding a void volume of ~7 µL. After radial compression, the amount of rSPA adsorbed per tip was determined to be 4.21 ± 0.08 µg (~1.1 µg mg^{-1} fiber), a slight increase in adsorption. Perhaps more importantly much improved reproducibility, from 9.8 %RSD down to 1.9% RSD, was realized.

Optimization of rSPA adsorption

To evaluate the maximum amount of rSPA adsorption onto the C-CP fiber tip surface, and hopefully IgG by extension, rSPA was loaded at various volumes and concentrations. The ~4 µg of protein adsorbed on 2.54 cm-long tips described in Section 3.1 agrees well with previous studies performed on 1 cm-long tips having “binding capacities” of ~1.5 µg for a range of proteins [29]. However, effects of increasing volume while retaining concentration and vise versa have not been evaluated for C-CP fibers. The relationship between the

extent of load rSPA concentration and eventual protein adsorption was first evaluated. In this case, no significant trend was observed as concentration was increased from 0.1 mg mL^{-1} to 0.8 mg mL^{-1} when the volume is kept constant at 0.1 mL. This is explained through the rapid passage of fluid through the C-CP fiber channels in a matter of a few seconds. Even with higher- concentration solutions, the flow (residence) time through the tip is not sufficiently long to yield greater levels of adsorption. Adsorption equilibrium considerations may also play a role in the lack of concentration dependence. Simply, the adsorption isotherm may have already reached its maximum at the lowest concentration and so has already met the maximum column efficiency for the fixed volume [30].

The alternative means to increase the amount of protein available to the C-CP fiber tips is to increase the load volume at the same protein concentration. Figure 3.2 shows the relationship between the protein adsorption and rSPA load volume when the concentration is kept constant at 0.1 mg mL^{-1}. As volume is increased from 0.1 mL to 1.2 mL, there is a significant increase in the amount of protein adsorbed. With increasing volume, the centrifugation (residence) time required for the entire solution to pass through the tips increases from 1 to 6 minutes, as such the time that the fibers are continuously wet by the load solution increases. The data in Fig. 3.2 clearly show that the adsorption processes are more favorable using a modest concentration with higher volumes. For example, the amount of protein A adsorbed for 0.8 mL of 0.1 mg mL^{-1} yields >3X higher loading than 0.1 mL of 0.8 mg mL^{-1}.

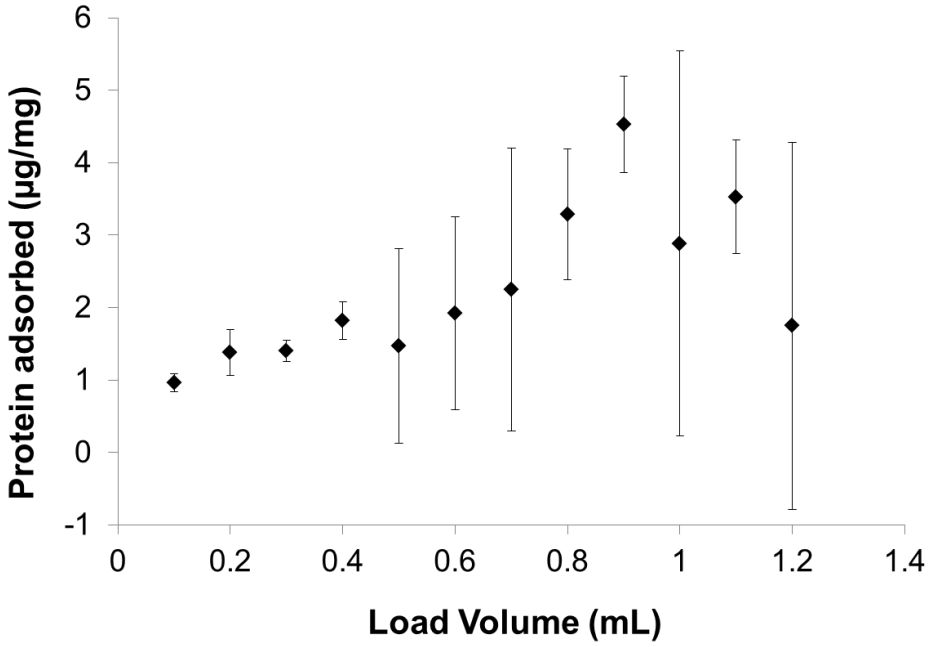

Figure 3.2 rSPA adsorption in µg protein per mg of PP C-CP fiber as a function of the load volume for a constant protein concentration of 0.1 mg mL^{-1}.

A somewhat surprising behavior is seen at load volumes of greater than 0.7 mL, where there is a definite loss in tip-to-tip binding precision and reproducibility and a rollover in binding capacity at volumes above 0.9 mL. When loading above this volume, the flow through time increases to ~6 min. With this increased time it is likely that the extent of protein relaxation and denaturing onto the hydrophobic PP surface begins to decrease the surface ordering and limits the available adsorption area. The decreased reproducibility is likely also reflective of this effect. The maximum rSPA adsorption is observed at a loading of 0.9 mL of 0.1 mg mL^{-1} rSPA. In this case, exposing 90 µg of protein to the fiber surfaces resulted in binding 17.1 ± 1.8 µg rSPA or 4.24 ± 0.44 µg mg^{-1} fiber for 6 replicate

tips, equating to a bed-volume binding capacity of 5.7 mg mL^{-1}. In terms of rSPA ligand capacity, this value is in very good agreement with literature values for other IgG purification phases, generally reporting recombinant protein A capacities of 1-6 mg mL^{-1} of bed volume [8,31,32].

Stability of adsorbed rSPA on C-CP fiber phases

A key issues in the bioprocessing of IgG using protein A affinity chromatography columns is the ability to purify multiple cycles of cell lysate on the same bed, ensuring successful regeneration without loss of capacity and no leakage of protein A from the support [33-35]. While an extensive cycling life time study is certainly warranted, it is informative to evaluate the rSPA-modified surface under solvent conditions common in HPLC and SPE methods as well as common IgG elution buffers. The stability of fiber-bound rSPA under several test solvents in shown in Table 3.1. As expected, the rSPA surface remains robust over a wide pH range, with no measurable leakage across pH 3 – 12. Likewise, acetic acid, citrate, acetate, and phosphate solutions of pHs commonly employed in IgG elution showed no protein A leaching. Of particular importance, wash solutions containing 1.0 M NaCl and 10 mM NaOH, most commonly used in CIP strategies, result in no ligand loss. The surfactant Tween 20 has been used as a washing agent to reduce non-specific binding of HCPs to affinity surfaces, but was disruptive to the rSPA surface even in low concentrations. Of other possible

IgG elution solvents examined, 0.1 M glycine, pH 3 and 0.01 M HCl caused rSPA to be removed.

Table 3.1 Stability of rSPA-modified surface under a variety of test solvents. Percentage removed reflects 0.9 mL of each solvent centrifuged through n = 6 tips.

Solvent	Adsorbed rSPA removed (%)
0.1 M Acetic Acid, pH 3	--*
50 % ACN	--
50% Methanol	30.5 ± 7.9
0.01 % Tween 20	65.4 ± 13.1
PBS, pH 3 - 12	--
1 M NaCl	--
10 mM NaOH	--
0.1 M Citrate Buffer, pH 3	--
0.1 M Sodium Citrate, pH 3-5	--
0.5 M Sodium Acetate, pH 3-5	--
0.1 M Sodium Phosphate, pH 5-7	--
0.1 M HCl	19.8 ± 8.7

* - no rSPA detected in elution solvent.

These results set a preliminary working space wherein there exist a number of potential intermediate wash and IgG elution solvents that will not appreciably cause rSPA elution from the PP C-CP fiber supports.

Adsorption of IgG and Myoglobin to native and rSPA-modified fibers

An obvious progression in evaluating species-specific surface interactions begins with an assessment of non-specific binding to the underlying support. In this case, myoglobin was chosen to simulate the potential effects of unwanted HCPs and other components of a broth supernatant. In these initial studies, it

was not critical to achieve the full binding capacity of the fiber surfaces, so the various loadings were performed with 0.1 mL of 0.1 mg mL^{-1} single component solutions of IgG and myoglobin. Table 3.2 presents the amount of the individual proteins adsorbed to the native PP C-CP tips as well as to the rSPA-modified C-CP tips.

Table 3.2 Amount of IgG and myoglobin adsorbed (10 µg exposure, individually) onto unmodified and rSPA-modified PP C-CP fiber tips

Analyte	Native PP (µg/mg)	rSPA-modified PP (µg/mg)
IgG	1.88 ± 0.05	1.82 ± 0.05
Myoglobin	1.38 ± 0.06	0.24 ± 0.03

As would be expected based on previous studies [29], both species adsorbed to the native PP fibers, as the hydrophobic PP surface readily adsorbs biomolecules in what would be called a non-specific way. The importance here is that when loaded onto the rSPA C-CP tips, a large disparity exists. In the case of the IgG, the amount of protein adsorbed is essentially unchanged, whereas there is a dramatic decrease in the amount of myoglobin retained on the tips. While the amount of IgG adsorbed remained the same, this is likely the maximum amount of IgG able to be captured solution (~7.5 µg/ 10 µg), and later results reflect a much higher adsorbed amount on rSPA-modified tips when more IgG is available. The reduced myoglobin retention on the protein A-modified surface is not surprising, with the amount that is retained perhaps being a reflection of

extent of the incomplete surface rSPA coverage, leaving exposed PP surfaces for myoglobin encroachment. However, it is more likely that there is some component of protein-protein (myoglobin-protein A) interactions, contributing to the total myoglobin retention. The consistent level of IgG binding on the rSPA surface seems to reflect a rather homogeneous protein A coverage.

At this point, it is clear that a fair level of selectivity would be achieved simply by impeding myoglobin retention. Indeed, an interesting situation occurs when the test solution is an equimass mixture of IgG and myoglobin, which would be an extreme case in bioprocesses. The protein concentrations were kept at 0.1 mg mL^{-1} with a 0.1 mL loading volume for both the native PP and rSPA-modified fibers. As presented in Table 3.3, the amount of IgG captured on the native fibers is essentially unchanged from the single-protein case, but there is slight decrease myoglobin binding (~22% by mass). This generally suggests a competitive binding situation wherein the IgG, which is far more hydrophobic and occupies more areal space, inhibits surface approach/retention at the native fiber surface.

Table 3.3 Amount of IgG and myoglobin adsorbed (as a mixture of 10 µg each) onto unmodified and rSPA-modified PP C-CP fiber tips

Analyte	Native PP (µg/mg)	rSPA-modified PP (µg/mg)
IgG	1.97 ± 0.04	1.98 ± 0.14
Myoglobin	1.16 ± 0.003	0.26 ± 0.05

As would be expected, by extension, the retention data for the mixture exposed to the rSPA-modified fibers reflects a situation where there is statistically little change in the IgG binding (relative to Table 3.2), yet the myoglobin retention is effectively the same as the single component case as shown in Table 3.2 (both appreciably reduced relative to the native fiber cases). Thus a situation is presented where there is perhaps access to the PP fiber surface, which results in surface binding of myoglobin in the presence of the rSPA layer, or indeed non-specific binding to the protein ligand. The retention of host proteins (surrogates here) means that there must either be better exclusion from being retained on exposed fiber surfaces or that highly effective wash steps must be implemented.

BSA block step

We have demonstrated that IgG adsorbs to the native PP as well as to the rSPA-modified PP, and so the issue arises as to the potential extent that IgG (or HCPs) is adsorbing non-specifically to unmodified regions of the fiber surface. In an attempt to investigate this, a BSA block step was implemented after rSPA adsorption to potentially "fill in" any remaining native areas of the fiber surface [36,37]. "Overloading" the rSPA surface with BSA was performed with 0.9 mL of a 0.2 mg mL^{-1} solution (180 μg total protein). On average, ~14 μg, or 3.5 μg mg^{-1}, BSA adsorbed to the fiber surface, which in fact is greater than the average of ~9 μg, or 2.3 μg mg^{-1}, BSA that adsorbs to the bare PP fibers. Thus, as

suggested in the myoglobin retention on the rSPA-modified tips, there is indeed appreciable non-specific binding to protein A itself. Indeed, BSA is known to be highly absorptive to a wide variety of surface types (e.g., hydrophobic and hydrophilic), with the variety of pathways and modalities being primary complicating features in surface treatment approaches [36,38,39].

To demonstrate the effect of the BSA blocking step on the adsorption of IgG and myoglobin, a 1:1 IgG:myoglobin mixture was passed through rSPA and BSA-modified tips and compared with passing the mixture through tips without the block. Again, the protein concentrations were kept at 0.1 mg mL^{-1} with a 0.1 mL loading volume. As shown in Table 3.4, the amount of IgG adsorbed remained the same regardless of the fact that the BSA block was applied.

Table 3.4 Amount of IgG and myoglobin adsorbed (as a mixture of 10 µg each) onto rSPA-modified C-CP fibers with and without the addition of a BSA block step (13.3 ± 1.7 µg or 3.32 ± 0.43 µg/mg fiber adsorbed)

Analyte	Without Block (µg/mg)	With Block (µg/mg)
IgG	1.98 ± 0.14	1.87 ± 0.01
Myoglobin	0.26 ± 0.05	0.32 ± 0.01

This further supports the idea that there is no non-specific binding of IgG to the fiber in the presence of protein A. However, unlike an expected decrease, the amount of myoglobin adsorbed remained the same, despite the use of the BSA block. Because most (if not all) of the PP fiber surface is modified with protein A and BSA, this further suggests that it is likely that myoglobin holdup is the result

of protein-protein interactions between myoglobin, protein A, and/or BSA. A recent presentation by Przybycien et al. provided evidence that non-specific binding of proteins to protein A is quite prominent [40]. Clearly, this general sort of non-specific binding must be addressed in a complete processing cycle in order to isolate IgG in high purity.

Binding capacity and isolation of IgG on rSPA C-CP fiber tips

Protein A contains five homologous domains for antibody binding, with two or three binding sites usually showing greater specificity for IgG. The stoichiometric relationship between IgG and protein A has been determined experimentally with varying results based on the subclass of IgG and the experimental parameters, with the general result of 3 – 3.3 molecules of IgG bound per molecule of protein A [41,42]. Covalent coupling of protein A to chromatography supports and sorbents usually occurs without restricting access to the active sites for IgG capture based on stoichiometric capture characteristics [43,44]. To evaluate this relationship, it was projected that, based on a binding stoichiometry of 3:1, the optimal rSPA adsorption of ~17 μg per C-CP fiber tip assembly should effectively bind ~140 μg of IgG. To utilize a more cell culture-relevant IgG concentration, 0.9 mL of 0.2 mg mL^{-1} was loaded, exposing 180 μg of IgG to each tip, with a 4:1 IgG:myoglobin (45 μg myoglobin) ratio employed to better reflect cell culture-relevant HCP concentrations [45]. Across this set of tests, 132.1 ± 5.9 μg of IgG (33.0 ± 1.5 μg mg^{-1} fiber) was captured, yielding a

protein/ligand stoichiometry of 2.9:1. Some myoglobin (10.0 ± 0.68 μg or 2.5 ± 0.17 μg mg^{-1} fiber) still adsorbed to each tip, despite the use of a block step, presumably through protein-protein interactions of myoglobin with BSA and/or protein A.

Intermediate wash steps are often used in purification protocols to remove unwanted cell proteins before IgG elution is performed [46]. Effective intermediate wash steps typically involve a buffer whose pH must be low enough to remove contaminants and unwanted HCPs but not so low as to begin to elute IgG (e.g., pH = 4-7). Figure 3.3 presents the recovery characteristics of the HCP surrogate myoglobin, as well as the target IgG, following wash steps involving passage of 1.8 mL volumes through the IgG:myoglobin exposed tips. The simplest option, of lowering the pH of the IgG loading buffer (20 mM di-basic sodium phosphate:150 mM sodium chloride) to 5, did not remove any myoglobin. Use of 0.5 M sodium acetate (pH = 5) resulted in a 39.3 ± 9.5% release of the adsorbed myoglobin, but at the cost of eluting 19.3 ± 7.9% of the bound target IgG. Use of 0.5 M sodium citrate (pH = 5) showed an even higher efficiency of 68.3 ± 9.4% removal, without any IgG leakage. Ultimately 0.5 M sodium citrate at pH = 4 demonstrated the ability to quantitatively remove myoglobin without any measureable loss of IgG.

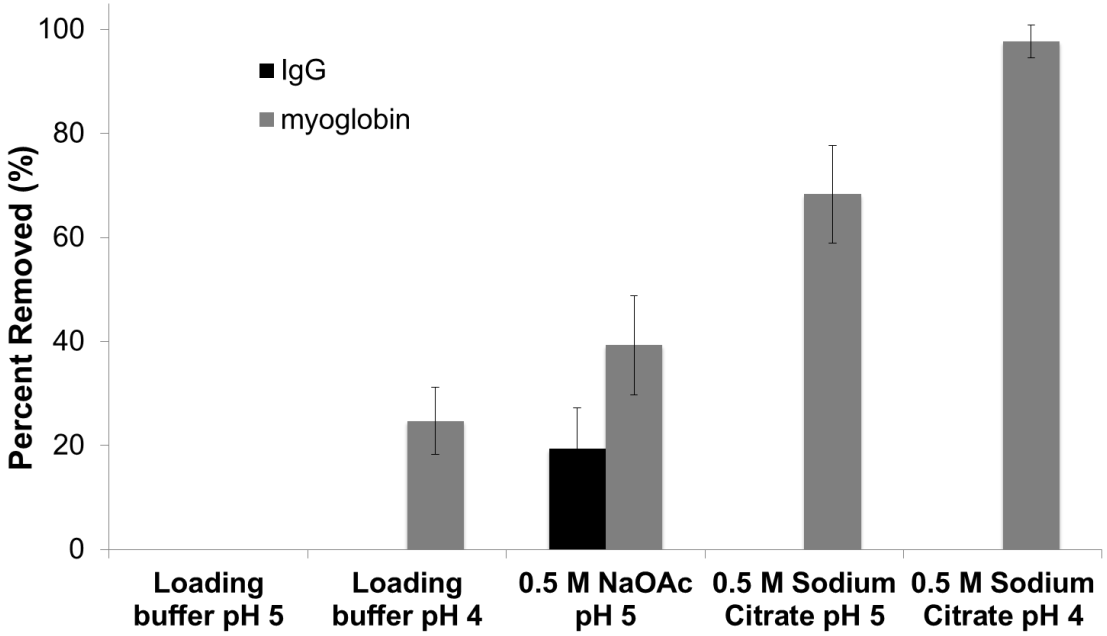

Figure 3.3 Percentage of adsorbed myoglobin and IgG removed from rSPA-modified C-CP fiber tips with the passage of 1.8 mL of different wash solvents.

IgG elution and recovery

There are many different elution solvents used throughout published protein A affinity chromatography studies [8,9,31,41,47,48]. In each case, there is always a consideration about the relative IgG recovery versus the potential of protein A column bleed. Most commonly, low pH is used alongside salts or other additives that prevent protein aggregation [47]. To ensure that leaking of rSPA off the C-CP fiber surface does not occur, only those IgG elution buffers that did not disrupt the rSPA-PP interaction as presented in Table 3.1 were examined here. Five elution buffers (0.1 M glycine, 0.5 M sodium acetate, 0.1 M sodium citrate, 0.1 M citric acid buffer, and 0.1 M acetic acid were evaluated initially by

passing 0.9 mL aliquots through the IgG-captured tips. The relative recoveries of each are presented in Fig. 3.4. Ultimately, the highest recovery was achieved using four times the loading volume (3.6 mL) of 0.1 mL acetic acid. This volume of eluent was capable of removing 117.8 ± 4.9 µg of IgG, corresponding to an 89.0 ± 4.6% recovery. Due to the use of the intermediate wash buffer, no myoglobin was seen in the elution volume.

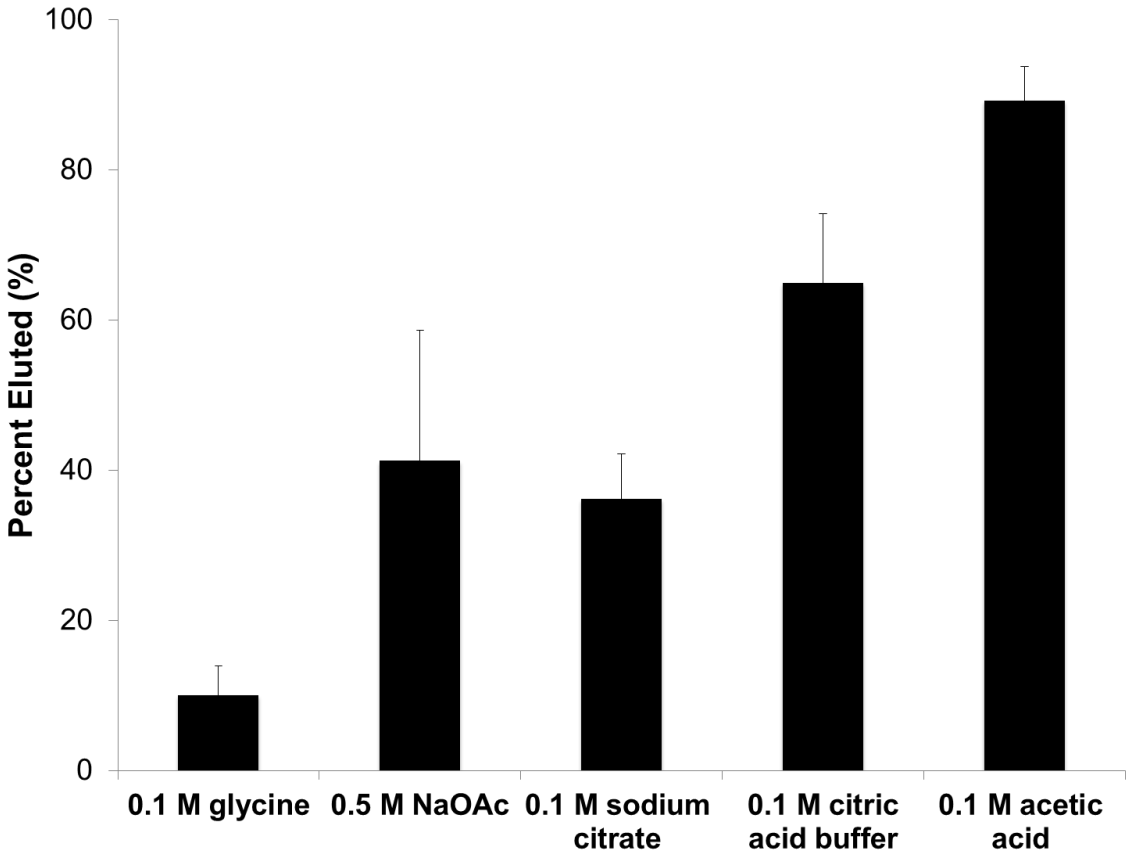

Figure 3.4 Percentage of adsorbed IgG eluted from rSPA-modified C-CP fiber tips with the passage of 3.6 mL of different solvents.

Certainly, the recoveries found here have room for improvement as the system is scaled up to a chromatographic platform. In addition, due to the acidity of the elution buffer, and because salts and detergents (i.e. urea, Tween-20) were unable to aid in elution, an immediate neutralization of the elution pool into a Tris-based solution or other basic buffer is necessary to prevent possible denaturation or aggregate formation [49-51]. This step is not out of line with what is commonly employed on other protein A phases.

Column Cleaning and Regeneration

With the high cost of commercial protein A resins, it is typical that a column is reused for many cycles of cell culture supernatant purification. To be able to reuse a column, however, residual IgG and other contaminants must be removed between cycles, commonly referred to as clean in place (CIP). CIP is most often affected with a low concentration of NaOH, which is inexpensive and easy to use [45,52]. The addition of NaCl to the caustic solution is thought to stabilize the immobilized protein A ligand and may also weaken ionic interactions. As depicted in Fig. 3.2, the rSPA surface is stable to a concentration of 0.01 M NaOH, though higher concentrations did lead to some leaching. As an initial investigation into the efficacy of this regeneration procedure, 3.6 mL of 10 mM NaOH + 1 M NaCl (effectively ~300 bed volumes) was used to clean/regenerate the r-SPA tips between immobilization/recovery cycles. Three tips were taken through the entirety of the r-SPA immobilization, BSA blocking,

and 4:1 IgG:myoglobin exposure steps. The average IgG binding was 105.7 ± 2.5 μg (26.4 ± 0.63 μg mg^{-1} fiber), with an average of 10.1 μg (2.5 μg mg^{-1} fiber) of myoglobin initially retained. The myoglobin washes occurred with unit efficiency, and the average IgG recovery was 89.2 %. The caustic wash removed 100% of the remnant IgG from two of the tips, while for the third only ~90% was removed. Subsequent washing of the structures with PBS and exposure to the IgG:myoglobin mixture revealed no loss in capacity for the first two tips (averaging 105.4 μg). In the case of the third tip, the amount of IgG captured, plus that remaining from the CIP step, was 105.8 μg. Thus, there was no loss in the actual IgG binding capacity following the caustic treatment. These results suggest that with full contaminant (residual IgG, HCPs) removal, the rSPA C-CP fiber surface retains 100% of its IgG binding capacity.

Concluding remarks

The results of this initial proof-of-concept work illustrate the potential of a novel protein A affinity chromatography support/stationary phase capable of recovering IgG from mixtures. Polypropylene C-CP fibers provide a stable and robust surface for adsorption of a recombinant protein A ligand, with a ligand capacity of 5.7 mg mL^{-1} (bed volume). As expected, binding stoichiometry of pure IgG to the protein A surface was found to be ~3:1. Elution of IgG resulted in 89% recovery and regeneration of the rSPA C-CP fibers in caustic media did not result in a loss in IgG capacity. It has already been shown that C-CP fibers yield

a highly advantageous chromatographic stationary phase due to very effective fluid movement, rapid mass transfer characteristics, and high recoveries. In comparison to currently available protein A resins, the C-CP fiber tips suggest possibilities for faster, more efficient antibody purification processing and ultimately, based on the cost of materials and high productivity a significant reduction in the cost of downstream processing.

While the micropipette tip format affords a very simple and versatile platform for initial investigations of C-CP fiber phase chemistries and basic performance characteristics, much work remains relative to implementation on scales of relevance to commercial applications. At this point, there are no immediate performance characteristics that would make further investigations unreasonable. Activities toward scale-up will include evaluations of the roles of fiber interstitial fraction and mobile phase linear velocity on the various adsorption, capture, and elution processes. There will certainly be finer tuning of the various process chemistries. As recently evaluated for protein processing via ion exchange on nylon 6 fiber columns, the throughput, yield, and productivity of IgG isolation from cell media will need to be determined [53]. Finally, the robustness of the chromatographic medium must be rigorously determined through isolation/recovery/regeneration cycles including any necessary CIP steps. It is believed that the basic transport properties of the C-CP fiber format, along with straightforward chemistries, offer practical advantages over current commercial formats.

Acknowledgments

This material is based upon work supported by the National Science Foundation Division of Chemistry under Grant No. 1011820 (co-funded by the MPS/CHE, ENG/CBET, and EPSCoR).

References

[1] G. Walsh, Nature Biotechnology 28 (2010) 917.

[2] B. Kelley, Mabs 1 (2009) 443.

[3] U. Gottschalk, Biotechnology Progress 24 (2008) 496.

[4] F. Wurm, Nature Biotechnology 22 (2004) 1393.

[5] A. Forsgren, J. Sjöquist, J Immunol 97 (1966) 822.

[6] H. Hjelm, K. Hjelm, J. Sjöquist, FEBS Lett 28 (1972) 73.

[7] S. Hober, K. Nord, M. Linhult, Journal of Chromatography B-Analytical Technologies in the Biomedical and Life Sciences 848 (2007) 40.

[8] R.L. Fahrner, D.H. Whitney, M. Vanderlaan, G.S. Blank, Biotechnol Appl Biochem 30 (Pt 2) (1999) 121.

[9] K. Swinnen, A. Krul, I. Van Goidsenhoven, N. Van Tichelt, A. Roosen, K. Van Houdt, Journal of Chromatography B-Analytical Technologies in the Biomedical and Life Sciences 848 (2007) 97.

[10] R.K. Marcus, W.C. Davis, B.C. Knippel, L. LaMotte, T.A. Hill, D. Perahia, J.D. Jenkins, Journal of Chromatography A 986 (2003) 17.

[11] D.M. Nelson, R.K. Marcus, Analytical Chemistry 78 (2006) 8462.

[12] R.D. Stanelle, C.A. Straut, R.K. Marcus, Journal of Chromatographic Science 45 (2007) 415.

[13] K.M. Randunu, R.K. Marcus, Anal. Bioanal. Chem. 404 (2012) 721.

[14] D.S. Fornea, Y. Wu, R.K. Marcus, Anal Chem 78 (2006) 5617.

[15] J.J. Pittman, V. Klep, I. Luzinov, R.K. Marcus, Analytical Methods 2 (2010) 461.

[16] B.T. Manard, R.K. Marcus, J Am Soc Mass Spectrom (2012).

[17] J.M. Randunu, R.K. Marcus, Anal. Bioanal. Chem. 404 (2012) 721.

[18] R.K. Marcus, J. Sep. Sci. 31 (2008) 1923.

[19] Z. Wang, R.K. Marcus, J. Chromatogr. A submitted for publication.

[20] A.J. Schadock-Hewitt, J.J. Pittman, K.A. Christensen, R.K. Marcus, Analyst submitted for publication.

[21] R.D. Stanelle, M. Mignanelli, P. Brown, R.K. Marcus, Analytical and Bioanalytical Chemistry 384 (2006) 250.

[22] C.F. Wertz, M.M. Santore, Langmuir 15 (1999) 8884.

[23] C.F. Wertz, M.M. Santore, Langmuir 17 (2001) 3006.

[24] P. Dejardin, E.N. Vasina, Colloids and Surfaces B-Biointerfaces 33 (2004) 121.

[25] M. Leveque, Ann. Mines 13 (1928) 284.

[26] S. Dimartino, C. Boi, G.C. Sarti, J. Chromat. A 1218 (2011) 1677.

[27] S. Dimartino, C. Boi, G.C. Sarti, J. Chromatogr. A 1218 (2011) 3966.

[28] J.M. Randunu, S. Dimartino, R.K. Marcus, J. Sep. Sci. 35 (2012) 3270.

[29] C.Q. Burdette, R.K. Marcus, Analyst 138 (2013) 1098.

[30] G. Carta, A. Jungbauer, Protein Chromatography: Process Development and Scale-Up, Wiley-VCH, 2010.

[31] R. Hahn, R. Schlegel, A. Jungbauer, Journal of Chromatography B-Analytical Technologies in the Biomedical and Life Sciences 790 (2003) 35.

[32] C. Boi, S. Dimartino, G. Sarti, Biotechnology Progress 24 (2008) 640.

[33] F. Steindl, C. Armbruster, R. Hahn, D. Armbruster, H. Katinger, Journal of Immunological Methods 235 (2000) 61.

[34] S. Lute, L. Norling, M. Hanson, R. Ernery, D. Stinson, K. Padua, G. Blank, Q. Chen, K. Brorson, Journal of Chromatography a 1205 (2008) 17.

[35] R. Hahn, K. Shimahara, F. Steindl, A. Jungbauer, Journal of Chromatography a 1102 (2006) 224.

[36] Y.L. Jeyachandran, J.A. Mielczarski, E. Mielczarski, B. Rai, J. Colloid Interface Sci. 341 (2010) 136.

[37] K. Reimhult, K. Petersson, A. Krozer, Langmuir 24 (2008) 8695.

[38] R. Kurrat, J.E. Prenosil, J.J. Ramsden, J. Colloid Interface Sci. 185 (1997) 1.

[39] R. Kurrat, J.J. Ramsden, J.E. Prenosil, J. Chem. Soc. Faraday Trans. 90 (1994) 587.

[40] T.M. Przybycein, in 9th Annual PEGS, Boston, MA, 2013.

[41] A. Jungbauer, R. Hahn, Current Opinion in Drug Discovery & Development 7 (2004) 248.

[42] S. Ghose, B. Hubbard, S.M. Cramer, Biotechnology and Bioengineering 96 (2007) 768.

[43] P. Thillaivinayagalingam, K. Reidy, A. Lindeberg, A. Newcombe, BioProcess International 10 (2012) 36.

[44] K. Huse, H.J. Bohme, G.H. Scholz, Journal of Biochemical and Biophysical Methods 51 (2002) 217.

[45] U. Gottschalk, Process Scale Purification of Antibodies, John Wiley & Sons, Hoboken, NJ, 2009.

[46] P. Hinckley, A.A. Shukla, in, Amgen, Inc., 2012.

[47] U. Gottschalk, Process Scale Purification of Antibodies, John Wiley & Sons, Incorporated, 2011.

[48] P.A. Marichal-Gallardo, M.M. Alvarez, Biotechnol. Prog. 28 (2012) 899.

[49] Y. Jiang, F. Li, M. Button, M. Cukan, R. Moore, N. Sharkey, H. Li, Protein Expression and Purification 74 (2010) 9.

[50] Y. Song, E. Dilger, J. Bell, W. Barton, X. Fang, Bmb Reports 43 (2010) 541.

[51] K. Sakamoto, Y. Ito, T. Hatanaka, P. Soni, T. Mori, K. Sugimura, Journal of Biological Chemistry 284 (2009) 9986.

[52] K. Brorson, J. Brown, E. Hamilton, K. Stein, Journal of Chromatography a 989 (2003) 155.

[53] K.M. Randunu, R.K. Marcus, Biotechnol. Progress 29 (2013) 1222.

CHAPTER FOUR

HEAD GROUP-FUNCTIONALIZED POLY(ETHYLENE GLYCOL)-LIPID (PEG-LIPID) SURFACE MODIFICATION FOR HIGHLY SELECTIVE ANALYTE EXTRACTIONS ON CAPILLARY-CHANNELED POLYMER (C-CP) FIBERS

Introduction

Polymeric stationary phases, specifically fiber-based polymers, have been under investigation for over fifty years for the separation of ions, small molecules, and macromolecules by high performance liquid chromatography (HPLC).[1-7] These polymeric phases generally offer common benefits over more widely applied porous silica-based HPLC stationary phases, including chemical robustness and ease of chemical derivatization.[3, 4, 8-12] In a fiber format, additional features include improved mass transfer due to their nonporous nature and convective diffusion throughout the column structure.[7, 13]

The specific polymer fiber form investigated here for applications in HPLC[5, 14-18] and solid phase extraction (SPE)[19-22] is the capillary-channeled polymer (C-CP) fiber. C-CP fibers are effectively non-porous (relative to the size of proteins), having average diameters of 35 - 50μm, and a very unique shape that includes 8 channels (Fig. 4.1a). These channels promote a self-alignment of the fibers when packed into an HPLC column (Fig. 4.1b), which results in a distribution of micron-sized open channels that run the length of the column. C-

CP fibers have 2-3x more surface area in comparison to circular cross section polymer fibers of the same nominal diameter.[14] The capillary channels of the C-CP column are very efficient at fluid transport, allowing for traditional HPLC column sizes to be operated at linear velocities of > 50 mm s^{-1}, while maintaining back pressures of < 2000 psi[5] without penalties of van Deemter C-term broadening.[18, 23] As a result, these C-CP columns provide for high throughput and high efficiency separation of biomacromolecules such as proteins.[24]

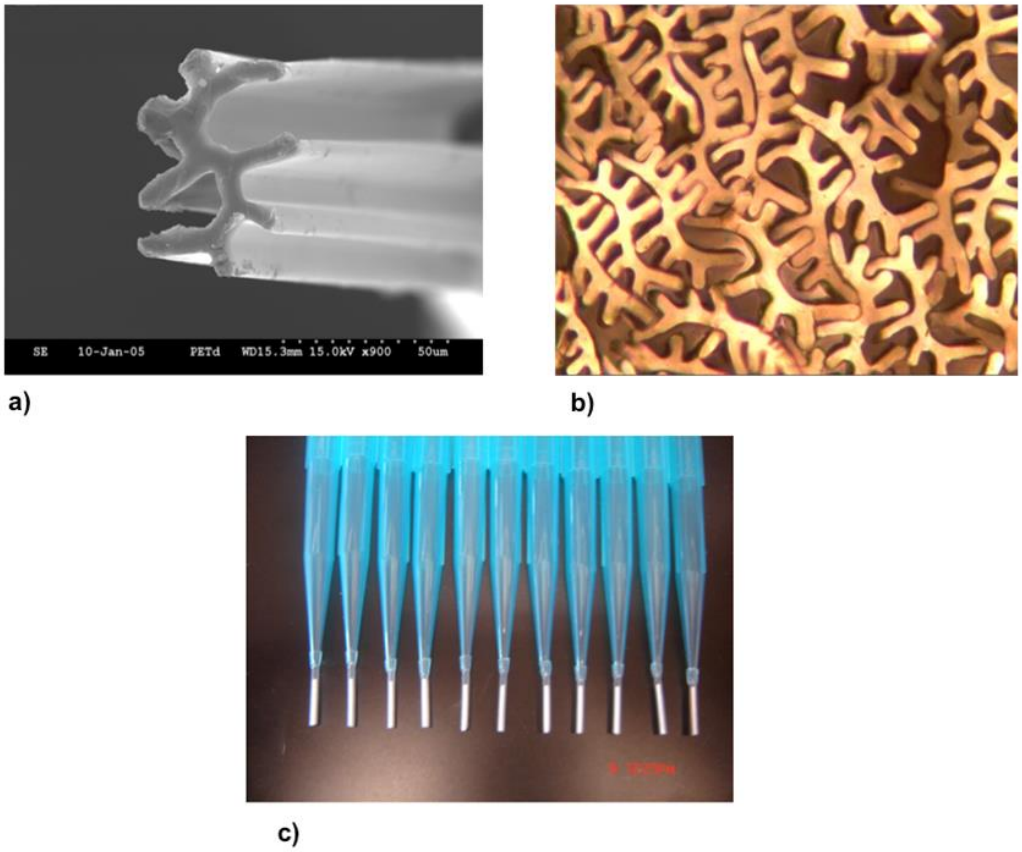

Figure 4.1 (a) Scanning electron micrograph (SEM) image of a C-CP fiber. (b) Image of a packed column of C-CP fibers demonstrating interdigitation. (c) Assembled C-CP fiber SPE tip format.

C-CP fibers used for macromolecule separations include nylon-6,[25, 26] polyester (PET),[6, 17] and polypropylene (PP),[18] allowing for applications in reversed phase (RP), ion-exchange (IEC), hydrophobic interaction (HIC) and affinity chromatography modalities. However, recent research has focused on the ability to modify the surface of the C-CP fibers, allowing for more specific analyte-surface interactions.[20, 27] There is a rich literature in the modification of polymer surfaces to affect chemical selectivity.[28, 29] Generally, most surface modifications found in textile chemistry literature can be achieved through active end group generation, including aminolysis, hydrolysis, and exposure to strong bases (i.e. NaOH or permanganate).[30-34] These straightforward approaches can produce high densities of –COOH, -NH, -OH, -CONH on the fiber surface for either analyte interaction or further modification under mild ambient conditions. However, these approaches to fiber modification are detrimental to the physical structure of fibers by breaking down the basic polymer/fiber backbone.[35] A more generalized approach, while still yielding high specificity and not compromising fiber integrity, would be desirable.

The on-column approach to functionalization reported here involves the simple adsorption of head group-functionalized poly(ethylene glycol) (PEG)-lipids, which are prominent in biologically-based research,[36-48] to the C-CP fiber surface. These amphipathic molecules (shown generically below) have been used in diverse applications including diagnostic assays,[45] coatings on hydrophobic nanoparticles,[41] and lipid bilayer modification of capillary

electrophoresis (CE).[38, 47, 48] The commercial availability of these functionalized PEG-lipids provides access to many potential surface modifications using one basic approach. Examples of common head groups include amines, carboxylic acids, maleimide, cyanur, and biotin. The use of functionalized PEG-lipids as means of modifying polymer surfaces for selective capture has not been described previously.

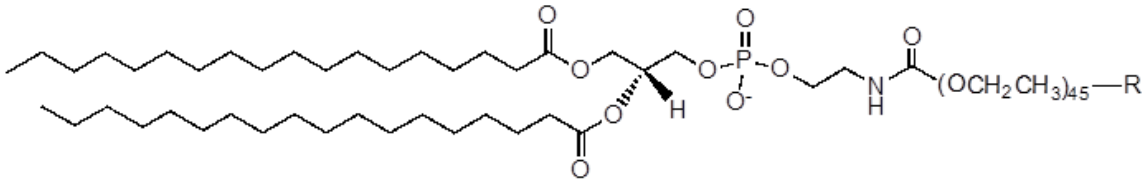

We demonstrate here the surface modification of PP C-CP fibers, using functionalized PEG-lipids to impart significantly greater selectivity than hydrophobic interactions between biomolecules and the fiber surface alone. C-CP fibers were modified with a biotin-PEG-lipid for the capture of streptavidin labeled with Texas Red (SaV-TR). In this case, the fluorescence intensity of Texas Red acted as a measure of streptavidin binding. Isolation of SAv-TR from an E. coli whole cell lysate from cells expressing recombinant tumor endothelial marker l 8 as an N-terminal fusion with a monomeric Citrine fluorescent protein (TEM8-mCit) demonstrates the efficacy of biotin-PEG-lipid C-CP fibers for extraction of target species from complex media. The diversity of functionalized lipid head groups, and further derivatization allowed by these headgroups, suggests broad chemical applicability to a variety of biomolecular recognition

moeities. It is envisioned that this approach can be implemented in many different formats, ranging from clinical diagnostics on fiber tips to C-CP fiber columns used in preparative chromatography. In fact, it is believed that this methodology could be implemented on virtually any hydrophobic support surface (e.g., polystyrene-divinyl benzene (PS-DVB)) to affect species-specific capture.

Experimental section

Chemicals and Reagents

PEG-lipids modified to contain either a biotin (1,2-Dimyristoyl-sy-Glycerol-3-phosphoethanolamine-N-[biotinyl (polyethylene glycol)-2000]) or methoxy (1,2-Dimyristoyl-sy-Glycerol-3-phosphoethanolamine-N-^{40}) head group (biotin-PEG-lipid, OMe-PEG-lipid), were purchased from Avanti Polar Lipids (Alabaster, AL). 5 µg mL^{-1} of each lipid were prepared in a 50:50 ethanol:water solution. Ethanol was obtained from Fisher Scientific (Pittsburgh, PA) and MilliQ water (18.2 MΩ cm^{-1}) was derived from a NANOpure Diamond Barnstead/Thermolyne Water System (Dubuque, IA). Bovine serum albumin (BSA) was obtained from Sigma Aldrich (Milwaukee, WI) and prepared to 5 µg mL^{-1} in phosphate buffered saline (PBS) consisting of 140 mM NaCl, 10 mM Na_2HPO_4, 1.8 mM KH_2PO_4, and 2.7 mM KCl at pH 7.3 (Sigma Aldrich). Two fluorescent proteins were utilized: streptavidin labeled with Texas Red (SAv-TR) (SouthernBiotech Birmingham, AL) was employed as the capture species on the PP C-CP fiber surfaces modified with biotin-PEG-lipid, and mCitrine (as TEM8-mCit), purified and in clarified cell

lysate, was used to assess non-specific binding. TEM8-mCit was expressed using T7 express, a BL21 strain of E. coli. Cells were grown in 1L of ECPM1 at 37 °C. Cells were induced at 37 °C with 0.8 mM IPTG for 3 hours. The cells were pelleted to remove the spent media and frozen in a -80 °C freezer. When ready to use, the pellet was re-suspended in approximately 20 mL 50 mM phosphate, 300 mM NaCl, 10 mM imidazole, and 0.1% Tween-20,pH 7.8-8). The solution was then lysed and sonicated briefly to reduce viscosity. The lysate was centrifuged to provide a cleared supernatant with minimal remaining cell debris. The concentration of TEM8-mCit in this cleared cell lysate (termed TEM8-*mCit lysate*) was determined, using a Nanovue Spectrophotometer (GE Healthcare, Little Chalfont, UK) at 516nm, to be ~14 nM. To yield purified TEM8-mCit (containing a hexahistidine tag), supernant was loaded onto a His column, and protein was eluted with 20-40 mM imidazole. The eluted protein was further purified by SEC and finally concentrated to 1 mL. The concentration of purified TEM8-mCit was determined to be ~200 nM. SAv-TR solutions were prepared in PBS solution or 0.1% Tween-20 (Rockland-inc.com, Gilbertsville, PA) PBS (PBST) solution. Experiments performed to illustrate non-specific binding of TEM8-mCit and selective capture of SAv-TR to the biotin-PEG-lipid fiber surface utilized protein concentrations of 0.4 µg/mL (~14 nM) in PBST or in the lysate.

C-CP Fiber Tip Preparation and Functionalization

The procedure for preparing microbore C-CP fiber columns, and subsequent implementation as SPE tips has been described previously.[19-21] Previous research has shown that interstitial volumes of $\varepsilon_i \approx 60\%$ (based on uracil retention) are optimal for macromolecule separations.[49] In this case, a total of 658 PP fibers were pulled to extend entirely through 300 mm long, 0.8 mm i.d. fluorinated ethylenepropylene (FEP) capillary tubing (Cole Palmer, Vernon Hills, IL), referred to here as the *fiber column*. The initial fiber column format is mounted in-line with an HPLC pump to clean the fibers from latent spin finish from the fiber extrusion and winding processes. To minimize chemical use in these demonstrations, the fiber column was segmented to 1 cm and the fibers used in a *tip* format. Following cleaning, the column was cut into 1 cm lengths with an additional 6 mm gap at one end. This gap allows the FEP tubing to be press-fit on to the end of the commercial low-retention micropipette tip (Redi-tip, Fisher Scientific, Pittsburgh, PA) as described previously,[19, 20] (Fig 4.1c).

Lipid solutions were prepared in a 50% water:ethanol solvent, balancing their solubility with the tendency for surface adsorption. After conditioning the tips with 1 mL 50% water:ethanol, 1 mL aliquots of the lipid solutions (biotin-PEG-lipid and OMe-PEG-lipid) were passed through at 1500 relative centrifugal force (RCF) (Clinical 50, VWR, West Chester, PA) for 2-3 minutes. This approach allows for the solvents to pass uniformly through the fiber interstices so that surface modification can occur homogenously. As noted above, chemical

modification of complete fiber columns would increase the fiber functionalization throughput.

Experimental Outline

Each experiment utilized three different fiber columns: an analyte specific column (modified with biotin-PEG-lipid), a control column (modified with OMe-PEG-lipid), and a bare PP column. Columns were first conditioned with 1 mL PBS or PBST, depending on the experiment. Initially, 1mL of the BSA solution was passed through the tips to presumably inhibit the adsorption of analyte, or other proteins, to the bare PP due to non-specific hydrophobic interactions. As seen, this “block” may be unnecessary if optimal PEG-lipid surface coverage is achieved. After a buffer wash, the fibers were exposed to 1 mL SAv-TR either in buffer (PBS or PBST), as a mixture with TEM8-mCit, or as a component (spiked) in clarified TEM8-mCit lysate. Finally, all tips were washed with buffer prior to fluorescence imaging to remove (any) residual non-specifically bound protein from the fiber tips.

Images and Statistical Data

Fluorescent images of the fiber tips were generated on an Olympus IX71, 4x/0.13 or 2x/0.08 UPlanFI (infinity corrected) objective (Olympus, Center Valley, PA). Fluorescent excitation was achieved using a Xe arc lamp with appropriate filters (Chroma, Bellows Falls, VT) for excitation 575/25 and emission 624/40 of SAv-

TR and excitation 494/20 for TEM8-mCit. For lysate experiments, fluorescence for both SAv-TR and TEM8-mCit bound to the fiber surface were captured in one image. An Ocra-ER (Hamamatsu) CCD camera was used for detection, images were processed and statistical data extracted using Slidebook 5.0 (Denver, CO).

Quantification of Protein Binding

After modification with PEG-lipid, the SAv-TR/TEM8-mCit load and wash solutions that had passed through the fiber tips were each collected individually. The amount of protein (SAv-TR and TEM8-mCit) bound to the C-CP fiber surfaces was determined through fluorescence measurements of the test solutions before and after passage through the tips. Response functions for SAv-TR and TEM8-mCit in PBST and in lysate were generated to determine concentration. A Tecan Genios fluorescence microplate reader (Tecan US, Inc. Durham, NC) utilizing a Nunc brand (Sigma Aldrich) black polystyrene 96-well microplate was used for measurement. The relative amounts of SAv-TR and TEM8-mCit adsorbed to the fiber surface was determined by subtracting the concentration observed in the solution exposed to the fiber surface from the concentration of the initial load solution. Any protein concentration in the wash was further subtracted from this number to give the final amount of analyte on the surface.

Results and discussion

C-CP fiber tips were evaluated for their ability to be functionalized utilizing the strong hydrophobic interaction of the lipid tails with the aliphatic structure of the PP surface. It is assumed that the lipid tail will lay along or imbed itself into the fiber surface while the PEG with functionalized head group will remain in solution, allowing for analyte interaction and reducing steric constraints at the fiber surface. Initial proof of concept was demonstrated utilizing the well understood interaction and high affinity of biotin and SAv. Two categories of control tips (OMe-PEG-lipid-coated fibers and bare PP fibers) were prepared to ensure that retained SAv-TR was from biotin-SAv specific interactions and not non-specific binding. Initially, a BSA block was applied for each category of tip before exposure to the SAv-TR solution. All tips were then exposed (through centrifugation) to 1 mL of 5 μg mL^{-1} SAv-TR solution followed by a 1 mL buffer wash. Figure 4.2 depicts representative fluorescence images of the tips for the three test cases. To minimize the impact of non-specific binding, the analyte capture experiment was performed in the presence of Tween-20. The use of Tween-20 in washing and blocking buffers is common in molecular recognition assays, including immunoassays, where the detergent adsorbs to hydrophobic supports and presents a hydrophilic surface to minimize potential non-selective interactions.[50, 51] In this experiment PBST buffer was used to prepare the fiber surface after lipid loading; additionally, the SAv-TR capture protein was loaded on the lipid-modified fibers in PBST buffer. No BSA block was performed.

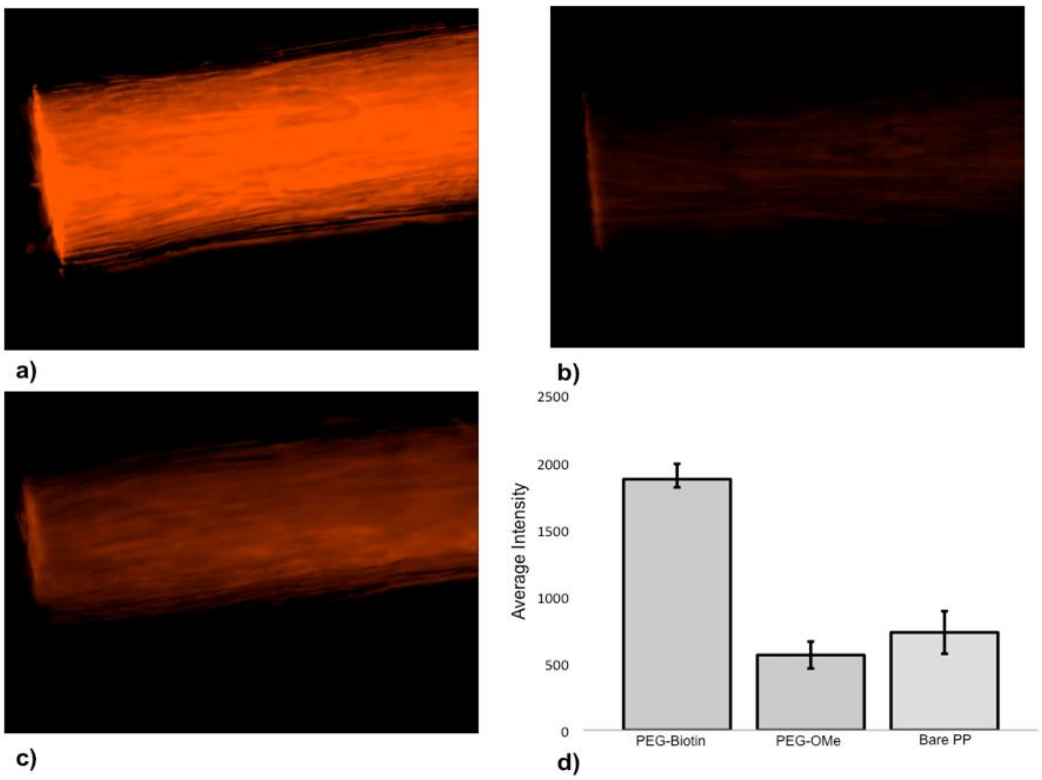

Figure 4.2 Fluorescent images of PP C-CP fibers after modification with modified PEG-lipids, BSA block, and passage of 1 mL of 5 µg mL^{-1} SAv-TR. (a) Biotin-PEG-Lipid modified (b) OMe-PEG-lipid modified (c) Native, unmodified PP C-CP fibers. (d) Average fluorescent responses for each column (n=3), collected from an identical-size mask down the center of each image. While only the first one-third of the fiber tips are imaged throughout this work, the uniformity of the capture process across the entire 1 cm tip is quite high, generally with a spatial variability of better than 10% relative.

As shown in Fig. 4.3, Tween-20 was successful at inhibiting non-specific binding of the SAv-TR on the two control surfaces. Tween-20 completely prevented non-specific binding from occurring while allowing uniform capture of the SAv-TR by the PEG-Biotin coated fibers (Fig. 4.3a). Clearly, the addition of Tween-20 in the sample matrix inhibits non-specific binding, even in the case of the highly hydrophobic polypropylene surface, eliminating the need for a BSA block.

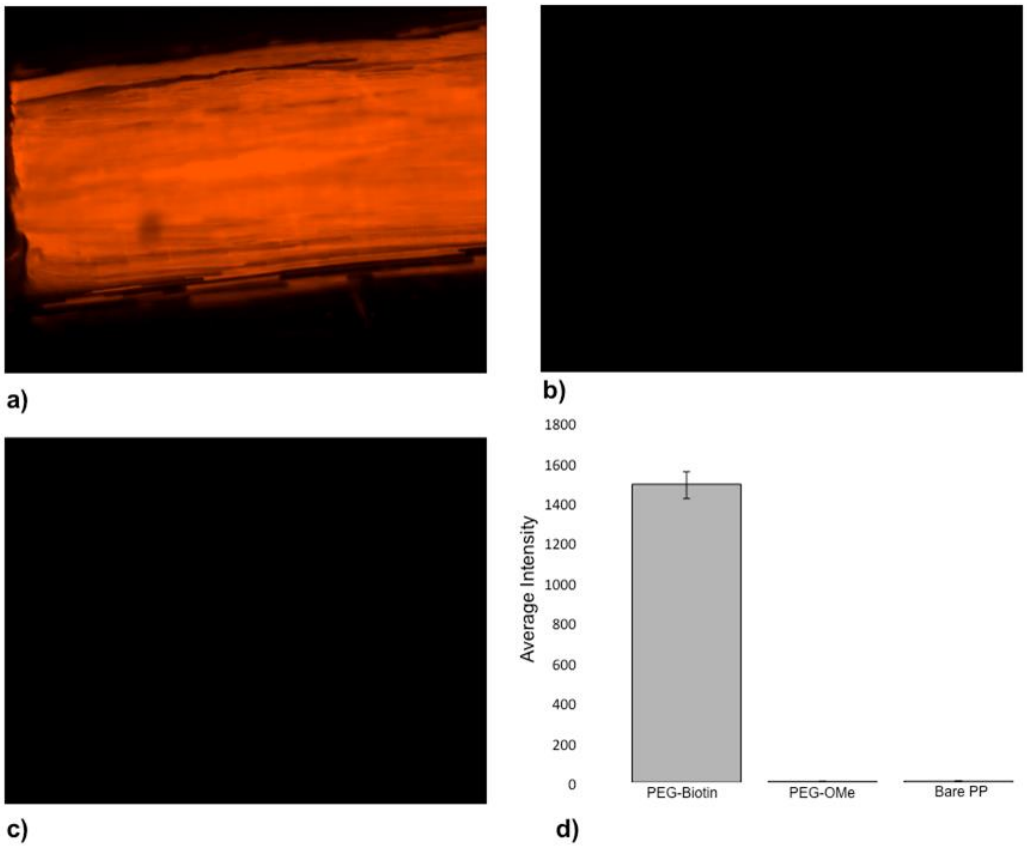

Figure 4.3 Fluorescent images of PP C-CP fibers after modification with modified PEG-lipids, PBST wash, and passage of 1 mL of 5 µg mL^{-1} SAv-TR in PBST to decrease non-specific binding. (a) Biotin-PEG-lipid modified, (b) OME-PEG-lipid modified, and (c) Native, unmodified PP C-CP fibers. (d) Average fluorescent responses for each column (n=3), collected from an identical-size mask down the center of each image.

To illustrate the ability of PEG-biotin modified C-CP fibers to capture SAv-TR from a complex lysate and to evaluate possible non-specific capture of other proteins, the capture of SAv-TR-out of TEM8-mCit lysate was evaluated. mCit is a variant of yellow fluorescent protein, and is used in this case as a tag for production of TEM8 in E. *coli*. Here we use m-Cit fluorescence from the fiber surface as an indication of non-specific protein binding in a practical system. In comparison to proteins in the PBST buffer, a cell lysate contains host-cell

proteins and other debris and is also more viscous, leading to the possibility of clogging stationary phases and high backpressures. However, the same volume of cell lysate required only 1 minute more of centrifugation time to pass through modified fiber tips than did analyte buffer solutions, clearly reflecting the advantageous fluid flow properties of C-CP fibers. Fiber tips treated with biotin-PEG-lipid and bare fibers were loaded with TEM8 mCit lysate spiked with SAv-TR to make a 0.4 μg mL^{-1} solution. A lower concentration of SAv-TR was chosen than used in previous experiments (12.5-fold less), with the goal of reducing the concentrations to reflect the same order of magnitude as the competing TEM8-mCit. The lysate His buffer included 0.1% Tween-20, so no BSA-blocking modification step was needed for prevention of non-specific binding. Images were collected with SAv/TR and TEM8-mCit excitation/emission simultaneously, so if both proteins were present, both green and red fluorescence would result. As shown in Fig. 4.4a, while the SAv-TR signal is evident on the biotin-PEG-lipid fiber tips, there is no visible TEM8-mCit fluorescence. The results of the imaging experiments are presented graphically in Fig. 4.4c. We note that absolute values for non-specific fluorescence observed here are similar to those observed in Figure 4.3. These data demonstrate that specificity is imparted by the biotin-PEG-lipid fiber coating.

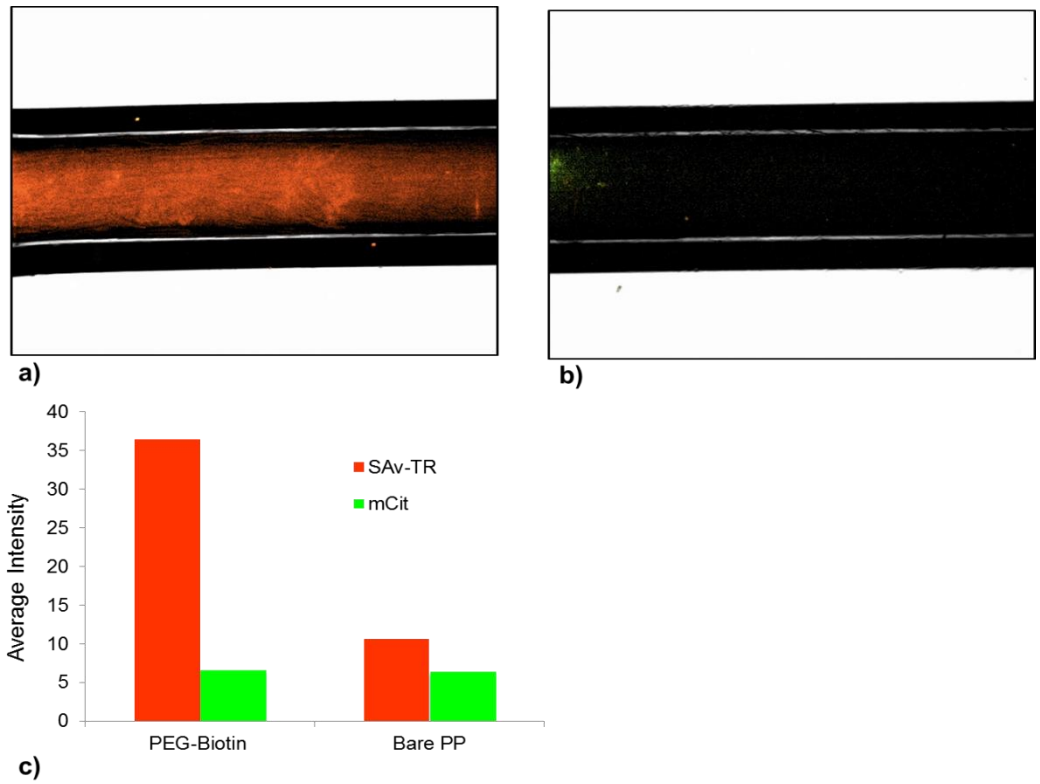

Figure 4.4 Fluorescent images of PP C-CP fibers after modification, PBST wash, and exposure to TEM8-mCit lysate spiked with 0.4 µg mL^{-1} SAv-TR. Presence of SAv-TR indicated in red and mCit in green. (a) Biotin-PEG-lipid modified, and (b) Native, unmodified PP C-CP fibers. (c) Average fluorescent responses for each column (n=3), collected from an identical-sized mask down the center of each image.

In order to determine the actual amount of SAv-TR and TEM8-mCit binding, fluorescence measurements were performed on the pass-through lysate solutions. Unfortunately, due to the imidazole present in the TEM8-mCit lysate, measurements of SAv-TR were complicated by imidazole fluorescing in the SAv-TR spectral window. Therefore, the relative retention of the two proteins was determined from a mixture of the purified TEM8-mCit and SAv-TR in PBST buffer. Table 4.1 shows the quantitative amount of SAv-TR and TEM8-mCit in the load mixtures before and after passage through the PEG-biotin modified and

bare PP C-CP fiber tips. These data indicate that only SAv-TR is binding to the C-CP fiber tips, and that ~70% of the applied SAv is captured on the biotin-PEG-lipid surfaces. Non-specific binding is not evident for TEM8-mCit on either bare or biotin-PEG-lipid fiber tips under these conditions.

Table 4.1 Fluorescently-determined masses of proteins exposed to C-CP fiber tips and recovered in the flow-through (1 mL volume). Protein solutions (14 nM) of each of SAv-TR and TEM8-mCIT were prepared in PBST

Solution	µg SAv-TR in solution	µg mCit in solution
SAv-TR/mCit load mixture	0.26 ± 0.06	0.37 ± 0.01
PEG-Biotin tip flow through	0.08 ± 0.02	0.35 ± 0.01
Bare PP tip flow through	0.27 ± 0.01	0.38 ± 0.01

Clearly, the addition of the Tween-20 in the sample matrix inhibits non-specific binding, even in the case of the highly hydrophobic polypropylene surface, eliminating the need for a BSA blocking layer.

Conclusions and Future Work

Presented here is a straightforward approach to modification of PP C-CP fibers with functionalized PEG-lipids to affect highly selective separations. Modification of the fiber surface with biotin-PEG-lipid was able to capture SAv-TR from a complex lysate with no non-specific binding in the presence of Tween-20. Advantages include modification occurring homogenously on-column, under ambient conditions, with vast possibilities due to the wide array of available lipid

head groups. The results presented here suggest the utility of this methodology as any lipid should be absorbable to the PP C-CP fibers, thus generating a modified fiber surface in a single step. The ability to change the analyte-specific interaction is as easy as a head group substitution (or derivatization on-column).

Paths forward will look at the more practical aspects of this generalized methodology. For example, one potential limitation to this approach involves the chemical robustness of the PEG-lipid modification. Preliminary studies in this regard have involved use of a FITC head group PEG-lipid that was fluorescently imaged on the fiber surfaces prior to and following exposure to common chromatographic solvents. Only in the case of solvent compositions >90% ACN and hexanes (which are not relevant in bio-separations) was any surface elution observed. The total binding capacity, first of the lipids and then of captured proteins, will be a particular issue in terms of larger-scale preparative chromatography. More fundamental studies will look towards gaining greater insights into factors controlling protein accessibility to the active lipid head groups, such as primary lipid orientation and use of linker molecules of varying length and chemical makeup between the lipid tails and the functional head group. Ultimately, we believe that the combination of the physical attributes of the C-CP fiber column/tips coupled with the general utility of the lipid surface modification methodology holds a great deal of promise in fields ranging from clinical diagnostics to downstream protein processing. This general methodology has potential applications in species-selective immobilization on virtually any

hydrophobic support phase, including plastic lab-on-a-chip devices and chromatographic supports such as polystyrene-divinyl PS-DVB.

Acknowledgments

This material is based upon work supported by the National Science Foundation Division of Chemistry under Grant No. 1011820 (co-funded by the MPS/CHE, ENG/CBET, and EPSCoR) to R.K.M. and the National Science Foundation EFRI Grant No. 0937985 to K.A.C.

References

1. R. D. Kirby and D. M. Cates, *Textile Res. J.*, 1983, **53**, 586-591.
2. L. Q. Chen, W. Zhang and Z. Zhen, *J. Chromatogr. A*, 1996, **740**, 195-199.
3. C. M. Ladisch, Y. Yang, A. Velayudhan and M. R. Ladisch, *Textile Res. J.*, 1992, **62**, 361-369.
4. Y. Kiso, K. Jinno and T. Nagoshi, *HRC- J. High Res. Chromatogr.*, 1986, **9**, 763.
5. D. M. Nelson and R. K. Marcus, *Protein Peptide Letts.*, 2006, **13**, 95-99.
6. K. J. Hilbert and R. K. Marcus, *J. Sep. Sci.*, 2010, **33**, 3571-3577.
7. R. K. Marcus, *J. Sep. Sci.*, 2008, **31**, 1923-1935.
8. H. B. Ding, M. C. Yang, D. Schisla and E. L. Cussler, *AICHE J.*, 1989, **35**, 814-820.
9. R. D. Hegedus, *.J. Chromatogr. Sci.*, 1988, **26**, 425-431.
10. K. Hamaker, J. Y. Liu and C. M. Ladisch, *Biotechnol. Prog.*, 1998, **14**, 21.
11. A.Singh and N.G.Pinto, *React. Polym.*, 1995, **24**, 229-242.
12. Y. Kiso, K. Takayama and K. Jinno, *HRC- J. High Res. Chromatogr.*, 1989, **12**, 169-173.
13. R. K. Marcus, *J. Sep. Sci.*, 2009, **32**, 695-705.
14. R. K. Marcus, W. C. Davis, B. C. Knippel, L. LaMotte, T. A. Hill, D. Perahia and J. D. Jenkins, *J. Chromatogra. A*, 2003, **986**, 17-31.
15. D. K. Nelson and R. K. Marcus, *J. Chromatogr. Sci.*, 2003, **41**, 475.

16. R. D. Stanelle, C. A. Straut and R. K. Marcus, *J. Chromatogr. Sci.*, 2007, **45**, 415-421.

17. D. M. Nelson and R. K. Marcus, *Anal. Chem.*, 2006, **78**, 8462-8471.

18. J. M. Randunu and R. K. Marcus, *Anal. Bioanal. Chem.*, 2012, **404**, 721-729.

19. D. S. Fornea, Y. Wu and R. K. Marcus, *Anal. Chem.*, 2006, **78**, 5617-5621.

20. J. J. Pittman, V. Klep, I. Luzinov and R. K. Marcus, *Anal. Methods*, 2010, **2**, 461-469.

21. C. Q. Burdette and R. K. Marcus, *Analyst*, 2013, **138**, 1098-1106.

22. B. T. Manard and R. K. Marcus, *J. Am. Soc. Mass Spectrom.*, 2012, **23**, 1419-1423.

23. Z. Wang and R. K. Marcus, *J. Chromatogr. A*, **submitted for publication**.

24. K. M. Randunu and R. K. Marcus, *Biotechnol. Prog.*, 2013, **29**, 1222-1229.

25. R. D. Stanelle and R. K. Marcus, *Anal. Bioanal. Chem.*, 2009, **393**, 273-281.

26. A. J. Schadock-Hewitt, J. J. Pittman, K. A. Stevens and R. K. Marcus, *J. Appl. Polym. Sci.*, 2013, **128**, 1257-1265.

27. A. J. Schadock-Hewitt and R. K. Marcus, *J. Sep. Sci.*, 2014, **in press**.

28. J. M. Goddard and J. H. Hotchkiss, *Prog. Polym. Sci.*, 2007, **32**, 698-725.

29. M. Phaneuf, E. R. Deutsch, F. LoGerfo, W. Quist, M. Bide and T. Zhong, *AATCC Rev.*, 2005, 39-43.

30. M. Bide, T. Zhong, J. Ukponmwan, M. Phaneuf, W. Quist and F. LoGerfo, *AATCC Rev.*, 2003, 24-28.

31. E. S. Kim, C. H. Lee and S. H. Kim, *J. Appl. Polym. Sci.*, 2009, **112**, 3071-3078.

32. W. Chen and T. J. McCarthy, *Macromolecules*, 1998, **31**, 3648-3655.

33. A. Papra, H. G. Hicke and D. Paul, *J. Appl. Polym. Sci.*, 1999, **74**, 1669-1674.

34. X. Jia, M. Herrera-Alonso and T. J. McCarthy, *Polymer*, 2006, **47**, 4916-4924.

35. M. S. Ellison, L. D. Fisher, K. W. Alger and S. H. Zeronian, *J. Appl. Polym. Sci.*, 1982, **27**, 247-257.

36. S. Zalipsky, *Bioconjugate Chem.*, 1995, **6**, 150-165.

37. L. Schmitt, C. Dietrich and R. Tampe, *J. Am. Chem. Soc.*, 1994, **116**, 8485-8491.

38. E. Mansfield, E. E. Ross and C. A. Aspinwall, *Anal. Chem.*, 2007, **79**, 3135-3141.

39. T. J. Pappas and L. A. Holland, *Sensors. Actuators B*, 2008, **128**, 427-434.

40. M. C. Sandstrom, E. Johansson and K. Edwards, *Langmuir*, 2007, **23**, 4192-4198.

41. P. K. Kandel, L. P. Fernando, P. C. Ackroyd and K. A. Christensen, *Nanoscale*, **3**, 1037-1045.

42. D. T. Auguste, J. Kirkwood, J. Kohn, G. G. Fuller and R. K. Prud'homme, *Langmuir*, 2008, **24**, 4056-4064.

43. Z. P. Chen, J. B. Zhu, H. X. Chen, Y. Y. Xiao, M. S. Feng, H. Cai, J. Chen and B. C. Cai, *Drug Devel. Ind. Pharm.*, 2010, **36**, 657-665.

44. Y. Hao, X. Yang, S. Song, M. Huang, C. He, M. Cui and J. Chen, *Nanotechnology*, 2012, **23**, 045103.

45. J. A. A. Ho, C. H. Hung, L. C. Wu and M. Y. Liao, *Anal. Chem.*, 2009, **81**, 5671-5677.

46. F. Kitagawa, T. Hasegawa, H. Taji, S. Onoue, Y. Tsuda and K. Otsuka, *Anal. Sci.*, 2008, **24**, 155-159.

47. J. M. Cunliffe, N. E. Baryla and C. A. Lucy, *Anal. Chem.*, 2002, **74**, 776-783.

48. L. A. Holland and A. M. Leigh, *Electrophoresis*, 2003, **24**, 2935-2939.

49. J. M. Randunu, S. Dimartino and R. K. Marcus, *J. Sep. Sci.*, 2012, **35**, 3270-3280.

50. D. E. Rebeski, E. M. Winger, Y.-K. Shin, M. Lelenta, M. M. Robinson, R. Varecka and J. R. Crowther, *J. Immunol. Methods*, 1999, **226**, 85-92.

51. M. Steinitz, *Anal. Biochem.*, 2000, **282**, 232-238.

CHAPTER FIVE

LOADING CHARACTERISTICS AND CHEMICAL STABILITY OF HEAD GROUP-FUNCTIONALIZED PEG-LIPID LIGAND TETHERS ON POLYPROPYLENE CAPILLARY-CHANNELED POLYMER FIBERS

Introduction

High performance liquid chromatography (HPLC) is the prevailing analytical separation technique for the characterization of complex biomedia, as well as the purification of biomolecules, such as proteins, in downstream processing applications. More specifically, affinity chromatography is perhaps the most powerful method of isolating target species due to the use of highly-specific ligands. The use of highly-specific capture chemistries reduces the number of steps required to yield a pure product. A continuous focus is placed on innovation toward novel support phases, which allow for increased throughput and efficiency, while also reducing the costs associated with these purification steps. Traditional resin beads and porous silica-based HPLC stationary phases are reliable and can afford high *analytical* efficiencies, yet suffer from high pressure drops and low throughput and yield for downstream protein purification processes. In addition, problems with phase stability and non-specific protein-surface interactions cause difficulties. For these reasons, alternative phases for preparative protein separations are desirable. Polymeric stationary phases offer

benefits to these traditional phases due to their chemical robustness and ease of chemical derivatization [1-5]. Relevant here, polymer fiber stationary phases offer additional advantages, as described in detail by Marcus [6, 7].

The polymer fiber stationary phase discussed here is the capillary-channeled polymer (C-CP) fiber [6, 7]. C-CP fibers have been investigated over the past decade as a stationary phase in HPLC [8-13] and solid phase extraction (SPE) [14, 15] applications, particularly of proteins. C-CP fibers are unique in shape, having average diameters of 35-50 µm, with eight channels running the entire length of the fiber. They have 2 – 3x more surface area than a circular cross section diameter of the same nominal diameter [8]. When packed into a column structure, the fibers self-align to form micron-sized open channels running the length of the column. Due to very efficient fluid movement, separations can be performed at high linear velocities (> 75 mm s^{-1}) with low backpressures (< 2000 psi). Another advantage is the result of their non-porous surface (relative to protein size) structure, yielding improved mass transfer via convective diffusion [5, 11, 16]. For these reasons, C-CP fiber columns yield high throughput and efficient macromolecule separations in applications utilizing reversed phase (RP) [12], ion exchange (IEC) [9], hydrophobic interaction (HIC) [10], and affinity chromatography [13, 17].

Recent focus in the use of C-CP fibers has been in the modification of the polymer surface chemistries to generate analyte-specific stationary phases [13, 17, 18]. As described previously [6, 7], several surface modification techniques

for polymers are known [19-24]. Unfortunately, many of these techniques can be harmful to the physical structure of the polymer/fiber by breaking down the polymer backbone leaving the fiber brittle and structurally unstable. Thus, the ability to generate an analyte specific surface while maintaining the physical properties of the fibers is a focus of current activities. A straightforward approach has been realized with the on-column modification of C-CP fiber surfaces with head group-functionalized poly(ethylene glycol) (PEG)—lipids (Fig. 5.1). PEG-lipids are very well known in biological literature for incorporation into liposomes or particles to facilitate *in vivo* processes, such as drug delivery and cell imaging [25-33].

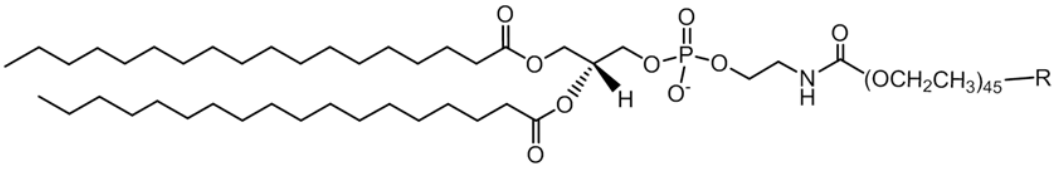

Figure 5.1 Base chemical structure of a head group-functionalized PEG-lipid

The novel surface modification occurs by virtue of the strong hydrophobic interaction between the lipid tails and the polypropylene (PP) fiber surface, with the hydrophilic PEG extending away from the surface and acting as a spacer arm. In this way, steric constraints at the surface are reduced, allowing for the analyte of interest to interact with the functional group/ligand. Overall, this allows for a straightforward on-column adsorption of PEG-lipids. Essentially, the lipid

moiety is used to tether a ligand to the C-CP fiber surface, and we have termed this general methodology as lipid tethered ligands (LTL). The variable head group (R) provides either its own degree of chemical specificity (as in the use of biotin as the head group), or for the subsequent on-column modification to implement further modification. PEG-lipids are commercially available with a range of functional groups including amine, carboxylic acid, maleimide, cyanuric chloride, succinimidyl ester, and biotin. Previously, we have demonstrated on a solid phase extraction (SPE) tip format, the modification of PP C-CP fibers with biotin-PEG-lipid for the capture of streptavidin from complex mixtures [17]. By use of Texas Red-labelled streptavidin, fluorescence imaging demonstrated that a uniformly modified biotin-PEG-lipid surface could be generated. The addition of Tween-20 to the sample eliminated almost all non-specific binding. In a complex lysate expressing mCitrine fluorescent protein, only SAv-TR was captured on the biotin-PEG-lipid modified PP C-CP fibers, yielding a highly selective stationary phase. With the concept of LTL to modify C-CP fibers as an affinity phase methodology demonstrated, the obvious next steps involve the practical aspects of affecting productive preparative phases. Critical in this process is an understanding the loading characteristics and chemical robustness of PEG-lipids on PP C-CP fibers, looking towards their applications in various protein separations.

Presented here, a fluorescein (FITC) head-group modified PEG-lipid was used as a model LTL, yielding a fluorescent surface in one modification step.

The objective of this research was to determine the parameters wherein the highest-density lipid modified surface could be generated in the most efficient way. In this way, a better understanding of how the PEG-lipid best dynamically interacts with the PP C-CP fiber surface will be revealed, also providing a general protocol for practical LTL modifications. The dynamic loading characteristics of the FITC-PEG-lipid on a PP C-CP fiber column were determined at seven concentrations and six volumetric flow rates through frontal analysis of breakthrough measurements. A second study evaluated the chemical robustness of the surface modifications by exposure to several common chromatography solvents as well as other solvent systems. The fate of the modification was assessed through fluorescence imaging before and after solvent exposure. Overall, the modification of C-CP fibers with head-group functionalized lipids demonstrates a straightforward, one-step surface modification, yielding a surface with the potential for high selectivity towards the analyte of interest. Overall, this modification methodology suggests a diverse set of possibilities due to the variety of head groups and further derivatizations available.

Experimental

Materials

PEG-lipid functionalized to contain a fluorescein head group (1,2-distearoyl-sn-glycero-3-phosphoethanolamine-N-[poly(ethylene glycol)5000-N'-

fluorescein) (FITC-PEG-lipid) was purchased from Nanocs Inc. (New York, NY) and prepared to necessary concentrations in 50:50 ethanol:water solution. HPLC-grade acetonitrile (ACN), methanol, and ethanol were purchased from EMD Millipore (Darmstadt, Germany). Hexanes were purchased from Fisher Scientific (Pittsburg, PA). Milli-Q water (18.2 MΩ-cm) was derived from a Millipore water system (Billerica, MA) and used to prepare all aqueous solutions. Phosphate buffered saline (PBS) was prepared as 140 mM NaCl, 10 mM Na_2HPO_4, 1.8 mM KH_2PO_4, and 2.7 mM KCl at pH 7.4 (Sigma Aldrich, Milwaukee, WI). Along with the above-mentioned solutions, 0.1% Tween-20, 5% sodium dodecyl sulfate (Sigma Aldrich), 75 mM imidazole (Alfa Aesar, Ward Hill, MA) and 20 mM Tris-HCl (Teknova, Hollister, CA) were used as test solutions to test the surface stability of FITC-PEG-lipid modified C-CP fibers.

C-CP Fiber Column Assembly and Instrumentation

C-CP fibers were manufactured though a melt extrusion process from polypropylene pellet feedstock and obtained from the Clemson University School of Materials Science and Engineering (Clemson, SC). The general procedure for preparing C-CP fiber columns has been described previously [8, 13, 14]. Based on the desired column interstitial fraction, the set number of fibers are wound from the initial spool onto a rotary counter, collected on a yarn stretcher bar, rinsed with ACN, methanol, and Milli-Q water, and then pulled through column tubing. Here, columns are prepared in two separate forms. For adsorption

capacity and breakthrough characteristic studies, 100 mm x 0.8 mm i.d. PEEK was used as the column tubing (Cole Parmer). The column was packed to yield an interstitial volume of $\varepsilon_i \approx 0.64$ (based on uracil retention), which has been found optimal for macromolecule separations [11]. The weight of C-CP fiber stationary phase per 100 mm was 17.5 ± 0.2 mg. Chromatographic experiments were performed on an HPLC system consisting of a Waters (Milford, MA, USA) Model 600S controller, a Waters Model 600 HPLC pump connected to a Rheodyne 7725i six-port injector valve (Rohnert Park, CA, USA) fit with a 300 µL stainless steel injection loop, and a Waters Model 2487 dual wavelength absorbance detector at 230 nm. Chromatograms were collected using the Waters Empower 2 data acquisition system and processed with Microsoft Excel (Seattle, WA, USA). All presented data are representative of triplicate injections.

The stability of the modified surface was evaluated via fluorescent imaging experiments using 0.8 mm i.d. fluorinated ethylene propylene (FEP) as the column tubing (Cole Parmer, Vernon Hills, IL), thus providing an optically clear conduit for imaging. In this case, the micropipette tip format developed for solid phase extraction (SPE) applications was employed [14, 15], providing a simple format for spin-down processing and fluorescent imaging. The column was cut into 1 cm segments with a ~4 mm section of empty tubing left at one end allowing the FEP tubing to be press-fit on to the end of a 1000 µL low-retention pipette tip (Molecular BioProducts, Fisher Scientific, Waltham, MA). Solution exposure to tips occurred through centrifugation spin-down (Clinical 50, VWR, West Chester,

PA) at 1900 relative centrifugal force (RCF). Fluorescent images of modified fiber tips were taken on an Olympus IX71, 2x/0.08 UPlanFI (infinity corrected) objective (Olympus, Center Valley, PA) with an excitation wavelength of 494 nm and emission monitoring at 535 nm achieved with appropriate filters (Chroma, Bellow Falls, VT). An Ocra-ER (Hamamatsu) CCD camera was used for detection. Slidebook 5.0 (Denver, CO) was used to process images and produce statistical data.

Dynamic binding capacity and adsorption isotherm

The dynamic binding capacity (DBC) for FITC-PEG-lipid on the PP C-CP fibers was determined through frontal analysis of breakthrough curves on a 100 mm x 0.8 mm i.d. PP C-CP fiber column. Throughout the course of DBC experiments, one single column was used. First, the column was conditioned with ~ 20 column volumes (CVs) of 50:50 ethanol:water. FITC-PEG-lipid solution was introduced to the column until the concentration in the effluent (C) equaled the concentration of the load solution (C_o), based on the UV-Vis absorbance maximum determined in previous injections performed with no column. Second, adsorbed FITC-PEG-lipid was eluted from the fiber phase by the continuous introduction of 100% ACN until a steady baseline was observed. Finally, the column was re-equilibrated with ~20 CVs of 50:50 ethanol:water before the next injection. Breakthrough curves were generated at 7 different concentrations (0.005, 0.05, 0.25, 0.5, 1, 2, and 3 mg mL^{-1}) and 6 different volume flow rates

covering 0.15 – 1.0 mL min^{-1} (linear velocities (U_o) = 8.6, 17.1, 25.7, 34.2, 42.8, and 57.1 mm s^{-1}). The amount of adsorbed FITC-PEG-lipid under each set of experimental conditions was calculated at 50% breakthrough, where the effluent concentration is 50% of the influent concentration (C/C_o = 0.50), using the following equation [34]:

$$q = C_o(V_b - V_{dead}) / W \qquad [1]$$

where q represents the amount of bound ligand (mg PEG-lipid/g stationary phase), V_b is the effluent volume at 50% breakthrough (mL), V_{dead} is the dead volume of the system (mL), C_o is the load concentration of PEG-lipid (mg mL^{-1}), and W is the dry mass of the fibers in the column (g). The loading values are reported as an average of triplicate injections.

Evaluation of the stability of the PEG-lipid modification

Each of the various solutions were centrifuged through 1 cm-long PP C-CP fiber tips in 1 mL aliquots for 3 minutes. Tips were first conditioned with 50:50 ethanol:water, and then loaded with 5 µg mL^{-1} FITC-PEG-lipid to affect the common modified surface. After a wash with 50:50 ethanol:water to remove any un-adsorbed lipid, three tips were exposed to each challenge solution. In order to ensure that the surface environment was consistent for the imaging experiments, a final wash with 50:50 ethanol:water was necessary, as this established the same pH and thus the same fluorescence yields. Fluorescent images were taken before and after exposure to the challenge solutions, with the

original image fluorescence intensity used as the control to determine percentage of ligand lost when compared to the image taken after solution exposure. Mean intensities are reported for triplicate trials.

Results and Discussion

Dynamic PEG-lipid binding characteristics and adsorption isotherms

In terms of chromatography media, the dynamic binding capacity is the amount of target product that will bind to the stationary phase under normal flow conditions. It is calculated based on the amount of target protein, with a known concentration, that can be loaded under defined flow conditions before a significant amount of non-retained solute is detected in the flow through (i.e. breakthrough) [35]. Such measurements are the primary means of determining the optimal parameters for capture processes on phases under development, providing a straight forward means of comparison. To be clear, in this case, we are using this method to assess the density of capture ligands on the fiber surface, which is not necessarily a direct reflection of the eventual protein loading capacity for a specific application. The goal here is to determine the role that the parameters of solute concentration and flow velocity have on yielding the most efficient PEG-lipid modification on the PP C-CP fiber column.

Breakthrough curves were generated on microbore format C-CP fiber columns as these have shown high efficiency for rapid analytical scale protein

separations [12], taking advantage of high linear velocities, achieved at low volume flow rates, without experiencing solute mass transfer limitations. This is also an advantageous platform for method development as these columns require relatively small amounts of solvent and analyte. Breakthrough curves were obtained for FITC-PEG-lipid concentrations of 0.005 to 3 mg mL^{-1}. The amount of adsorbed lipid was calculated according to Eq. 1 at each concentration, with the resulting adsorption isotherm shown in Figure 5.2. In a literal sense, adsorption isotherms are used to assess surfaces under equilibrium conditions.

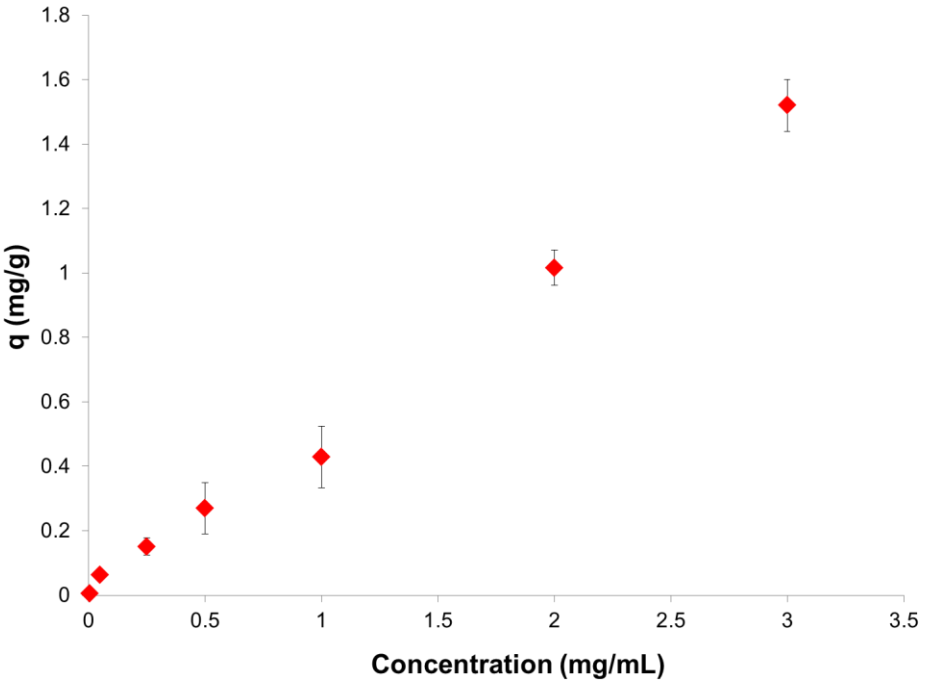

Figure 5.2 Adsorption isotherm of FITC-PEG-lipid adsorbed onto PP C-CP fibers at load concentrations 0.005 – 3 mg mL^{-1}. Calculations were done at 50% breakthrough. Each concentration was run in triplicate.

As such, stationary phase adsorption isotherms are usually generated as a static (equilibrium) measurement or at relatively low flow rates because common porous phases often suffer mass transfer limitations at increased flow rates. However, the *dynamic* isotherm was generated here at the highest flow rate used, 1 mL min^{-1} (U_o = 57.1 mm s^{-1}) as C-CP fibers have consistently shown enhanced performance in terms of chromatographic resolution and process throughput and yield as flow rates are increased [12, 36, 37]. The data clearly remain linear across this relatively broad concentration range. The dynamic adsorption data was fit to a linear isotherm, as well as the common Langmuir and Freundlich isotherms using Matlab [37]. All three yielded excellent fits, with correlation coefficients (R^2) of 0.9957 for the linear, 0.9948 for the Langmuir, and 0.9952 for the Freundlich models. The fact that the data fit each model well infers that the “non-linear” adsorption phenomena reflective of surface heterogeneity or multi-layering are not present [38] . This contrasts the case for protein (lysozyme) adsorption onto nylon 6 C-CP fibers, where the dynamic isotherms begin to level off at concentrations of ~1.5 mg mL^{-1} [37]. The broad linear range of response is particularly surprising as the critical micelle concentrations of this sort of PEG-lipid are cited at between 0.03 and 0.07 mg mL^{-1} [39, 40]. Attempts to extend the isotherm to higher solute concentrations were restricted due to a 5 mg mL^{-1} lipid stock concentration. The fact that the isotherm remains linear up to 3 mg mL^{-1} highlights the efficient mass transfer characteristics of C-CP fiber columns.

As described above, preparative separations on porous media are limited by the diffusion rates of macromolecules in terms of accessing the available surface area. In the case of the C-CP fiber phase, the lack of porosity alleviates this kinetic limitation, though admittedly at the expense of equilibrium binding capacities due to their low specific surface area. To evaluate the effect of linear velocity on FITC-PEG-lipid binding capacity, the volume flow rate was varied from 0.15 – 1 mL min^{-1} (U_o = 8.6 – 57.1 mm s^{-1}), using a solute concentration of 3 mg mL^{-1} as this was the highest point in the Fig. 5.2 isotherm. Fig. 5.3a shows the full breakthrough curves for FITC-PEG-lipid adsorption on the PP C-CP fiber column as a function of the volume flow rate. The shapes of these curves do not vary significantly across the flow rates. There are two boundary situations that might be expected in such plots: decreasing slopes in the transition regions affected by slow mass transfer kinetics or sharpening in the case where no limitations exist. Clearly, mass transfer limitations are not evident here. In fact, as shown in Fig. 5.3b, there is very little qualitative difference in the transition region of the breakthrough curves in the region of $C/C_o \approx 0.5$ of the curves, where the loading is calculated. As seen in Fig. 5.3c, there is a slight difference in the binding capacity across this range of linear velocities, initially increasing from 0.15 to 0.6 mL min^{-1} and then decreasing above this point. The general shape of the response here suggests that there are kinetic limitations to the system. These limitations are not due to intrapore adsorption-desorption kinetics, but the solute residences times on-column.

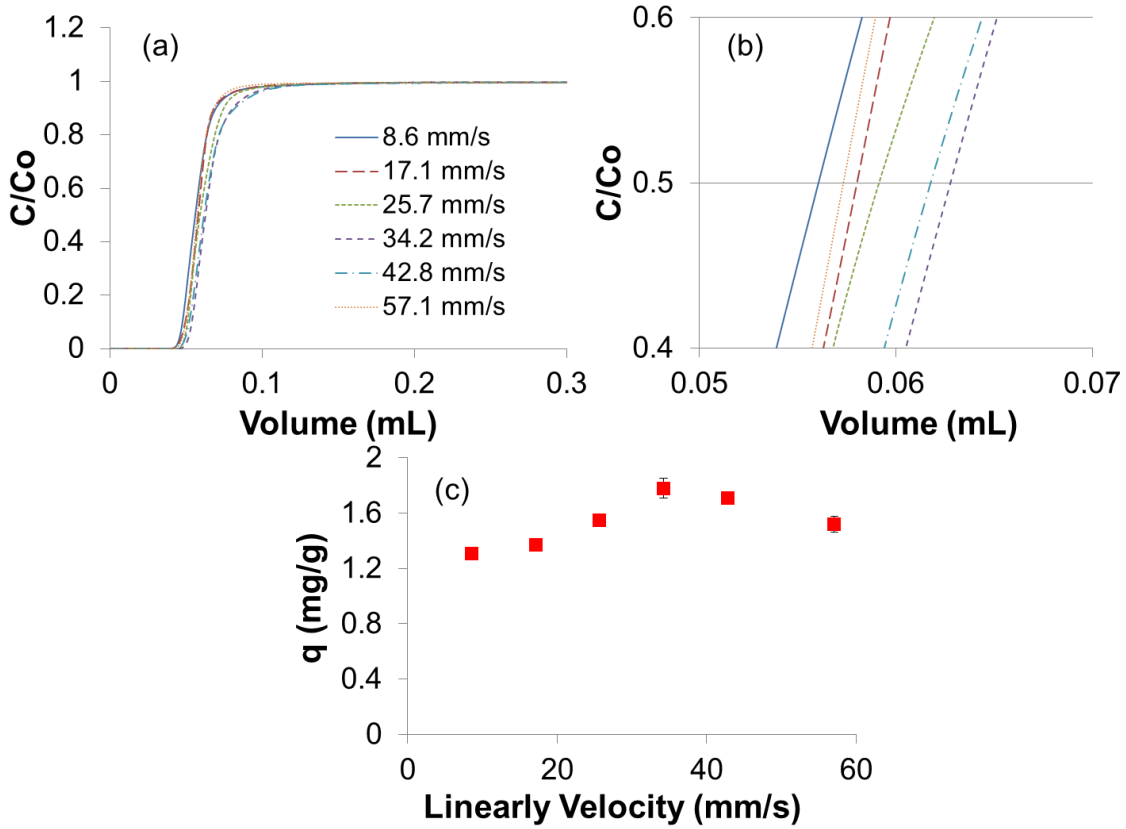

Figure 5.3 Breakthrough curves of 3 mg mL^{-1} FITC-PEG-lipid at different linear velocities. (b) gives an up-close look at 50% breakthrough and (c) shows the loading capacity at each linear velocity when calculated at 50% breakthrough.

As the linear velocity increases, there is less residence time across the column, leading to the slight decrease in column binding capacity as flow rates increase above 0.6 mL min^{-1}.

The maximum ligand binding capacity was found at 0.6 mL min^{-1} to be 1.78 mg of FITC-PEG-lipid per gram of fiber (1.9 mg mL^{-1} fiber, $3.25x10^{-4}$ mg cm^{-1}). In comparison to other affinity phases under development, such as those modified with glutathione for the purification of GST-tagged proteins [41] and

those modified with lectins for the purification of glycoproteins [42, 43] , there is 3-6 times less ligand concentration on PEG-lipid modified PP C-CP fiber columns**.** It is interesting to compare the obtained ligand density to what might be expected on a first-principles basis. Lee *et al.* determined that the cross sectional area of a single hydrocarbon lipid chain was 23.27 Å based on measurements of Langmuir monolayers of fatty acids and phospholipids at a liquid surface [44], and literature agrees that the theoretical molecular area of a phospholipid is around 46 Å [45]. While these reported values suggest that there could be ~2 PEG-lipid molecules per nm^2 of surface area, the experimental data presented above yields ~0.3 PEG-lipid molecules per nm^2. However, the theoretical values are based only on the area occupied by the lipid chain, and do not take into consideration the 5000 Da PEG attached to the head of the phospholipid. Allen *et al.* reported on the incorporation of PEG-lipids into liposomes, where the lipid incorporates itself into the bilayer, and PEG remains on the surface to prevent serum protein binding *in vivo* [46]. As the PEG molecular weight was increased from 350 to 2000 Da, the area occupied per PEG molecule increased from 4.68 nm^2 to 37.18 nm^2. Thus, at 2000 Da, there are 0.03 molecules per nm^2. The PEG group on FITC-PEG-lipid employed here has a molecular weight of 5000 Da, thus the theoretical density would be ~0.012 molecules per nm^2. What is seen in these studies is a value closer to the case of the lipid binding limit than what is seen with the PEG-lipids in bilayers. Clearly, it may be the large PEG group that is limiting the binding capacity of PEG-lipid onto

the C-CP fibers. Future studies will be directed at evaluating how the lipid tail is interacting with the fiber surface. It is believed that the hydrocarbon chain is burying itself into the PP fiber structure, with the PEG group affecting access as the layer approaches saturation. Due to the linear trend of the adsorption isotherm, it is also likely that the maximum capacity of the C-CP fiber column has not actually been reached. Performing frontal analysis with a PEG-lipid having a much smaller PEG group would be necessary to increase the binding capacity. In either case, as discussed previously [36], C-CP fiber columns compensate for lower surface area/coverage in the ability to operate at much higher loading rates, yielding higher throughput and yield.

Chemical stability of FITC-PEG-lipid on PP C-CP fibers

The stability of any stationary phase modification is a key characteristic as is defines the useable lifecycle of that phase. Ligand loss affects not only the capture capacity of a phase, but also limits the ultimate purity of the derived product if ligand is leached during the course of the elution step. As the PEG-lipid modification occurs through adsorption to the C-CP fiber surface, it is important to evaluate the stability and robustness of the interaction between the lipid tail and the PP surface. Here, the use of the FITC head group is used to advantage as C-CP fiber tips prepared in clear FEP tubing can be imaged after both the adsorption and challenge steps [17]. Figure 5.4 demonstrates the types

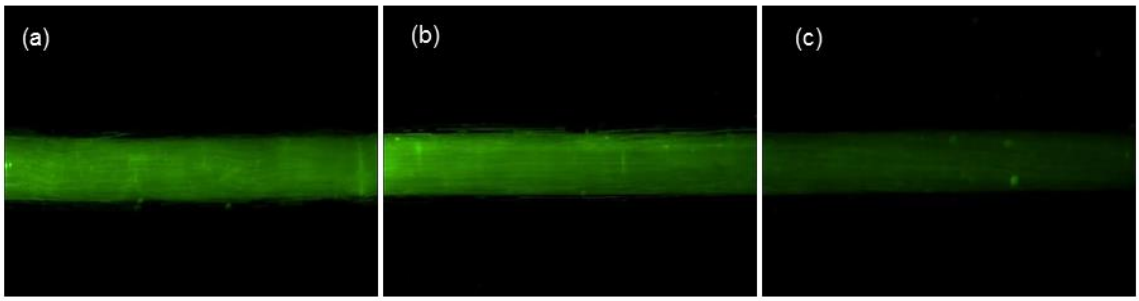

Figure 5.4 Fluorescence images of FITC-PEG-lipid modified PP C-CP fibers still in FEP tubing. Images were taken with a 2x objective and show ~5 mm of column. FITC fluorescence was measured with 494 nm excitation and 531 nm emission. Images shows FITC-PEG-lipid fluorescence after exposure to (a) 50% ethanol (b) 0.1% Tween-20 (c) 50% ACN

of fluorescent images recovered in these experiments. The three images reflect individual tips exposed to: a) 50% ethanol (the load solvent), b) 0.1 % Tween -20, and c) 50% ACN. As fluorescein has pH dependence in its fluorescence intensity [47], the tips were washed several times with 50% ethanol (pH ~7) before imaging to have the same solvent environment across all images. As can be seen, exposure to the first two solvents shows very little difference, while the third reflects a loss of the FITC-PEG-lipid.

Figure 5.5 presents the quantitative results of triplicate FITC-PEG-lipid modified tips following exposure to each of the challenge solvents. The solvents were chosen as being reflective of those commonly used for HPLC separations, and a few which might be expected to solubilize the hydrophobic lipid tail in favor of remaining adsorbed to the fiber surface. As can be seen, there is no statistical difference between the fluorescence response found for tips that were imaged immediately after surface modification (first entry) and those which were washed with the common HPLC solvents. Only in the case of the exposing the modified

fibers to the 50% ACN and mixed hexanes is a loss (~40 %) in ligand density seen; interpreted as a solubilization and elution of the lipid. Of course there would be no situation wherein modified fibers/columns would be exposed to these two solvents.

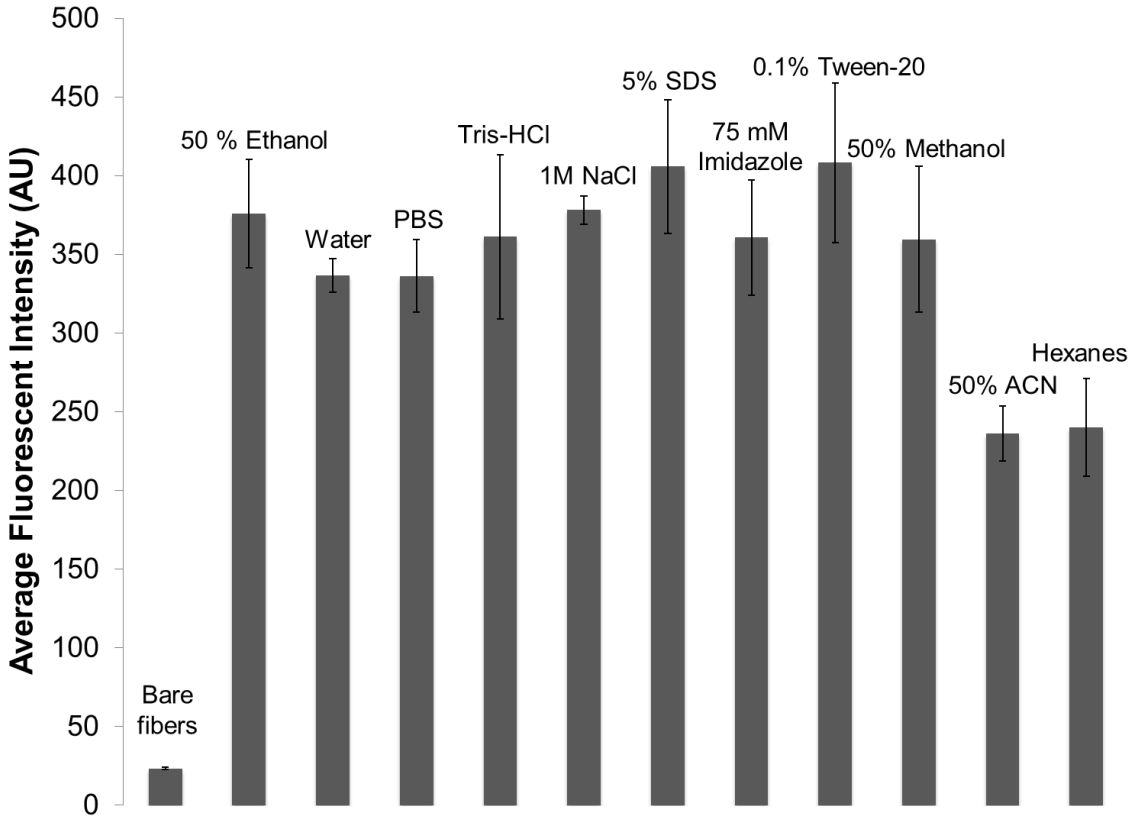

Figure 5.5 Change in mean fluorescence intensity of FITC-PEG-lipid modified PP C-CP fibers tips after exposure to test solutions. The intensity of the 50% ethanol (loading solvent) bar is used as the control. Bare fibers represents native, unmodified PP C-CP fibers.

Certainly, the robustness of the PEG-lipid modified surfaces must be evaluated in greater detail under process conditions, but the results of these studies are a very encouraging outcome.

Concluding remarks

The modification of C-CP fibers with head group-functionalized PEG-lipids provides a straightforward surface modification with almost limitless possibilities due to the many functional groups available and secondary modifications that can be affected. Indeed, the LTL methodology in general should be applicable to almost any hydrophobic surface. The adsorption characteristics of PEG-lipid onto PP C-CP fibers were evaluated via breakthrough curves and frontal analysis. Linear adsorption isotherms were realized across a concentration range 0.005 to 3 mg mL^{-1}, suggesting the creation of a very uniform monolayer of ligand. The qualitative and quantitative nature of the breakthrough curves as a function of mobile phase linear velocity (U_o = 8.6 – 57.1 mm s^{-1}), highlight the rapid mass transfer and efficient fluid movement that are characteristic of C-CP fiber columns. While the dynamic binding capacity of 1.8 mg g^{-1}, found at 0.6 mL min^{-1} of 3 mg mL^{-1} FITC-PEG-lipid, is small in comparison to commercially available affinity ligand stationary phases, the physical properties of C-CP fibers allow them to perform at much higher linear velocities providing higher throughput and yields in protein separations. Finally, the PEG-lipid surface modifications remain stable after exposure to several test solvents, with only 50% ACN and hexanes able to disrupt the surface, suggesting that the PEG-lipid modification of C-CP fibers is chemically robust.

Future work is focused on gaining a better understanding of how PEG-lipid interacts with the PP C-CP fiber surface. As discussed above, it is clear that a

maximum binding capacity isn't being reached due to several possible factors including low solute concentration or the large PEG group taking up too much area. Recently, work has focused on creating synthetic PEG-lipids to remove the unstable phosphate group and allow for a tailorable PEG chain length. It is possible that with a shorter PEG group, binding capacity can significantly increase. PEG-lipid with 7-nitrobex-2-ozo-1,3-diazole-4-yl (NBD) functionalized on the head group or to end of the tail allows for a fluorescent surface and utilizes the unique optical properties of NBD to determine if the tail is burying itself into the fiber structure. Along the same lines, other important parameters to address include determining an optimum loading solvent for PEG-lipid, as there is a tradeoff between the PEG-lipid solubility, the formation of micelles, and the affinity towards the PP fiber surface. Additionally, while PEG-lipid binding on a 1-inch column showed consistent binding across the entire length, the binding capacity, efficiency, and consistency across longer columns, which would be needed for preparative situations, should be determined. This work will lead to a better-characterized and optimized stationary phase for various situations.

Acknowledgment

This material is based upon work supported by the National Science Foundation Division of Chemistry under grant CHE-1307078.

References

[1] Ladisch, C. M., Yang, Y. Q., *Textile Research Journal* 1992, *62*, 481-486.

[2] Kiso, Y., Jinno, K., Nagoshi, T., *J. High Resolute Chromat. Chromat. Comms.* 1986, *9*, 763.

[3] Ding, H. B., Yang, M. C., Schisla, D., Cussler, E. L., *Aiche Journal* 1989, *35*, 814-820.

[4] Hegedus, R. D., *Journal of Chromatographic Science* 1988, *26*, 425-431.

[5] Hamaker, K., Liu, J. Y., Ladisch, C. M., *Biotechnol. Progress* 1998, *14*, 21.

[6] Marcus, R. K., *Journal of Separation Science* 2008, *31*, 1923-1935.

[7] Marcus, R. K., *Journal of Separation Science* 2009, *32*, 695-705.

[8] Marcus, R. K., Davis, W. C., Knippel, B. C., LaMotte, L., Hill, T. A., Perahia, D., Jenkins, J. D., *Journal of Chromatography A* 2003, *986*, 17-31.

[9] Stanelle, R. D., Straut, C. A., Marcus, R. K., *Journal of Chromatographic Science* 2007, *45*, 415-421.

[10] Stanelle, R. D., Marcus, R. K., *Analytical and Bioanalytical Chemistry* 2009, *393*, 273-281.

[11] Randunu, K. M., Dimartino, S., Marcus, R. K., *J Sep Sci* 2012, *35*, 3270-3280.

[12] Randunu, J. M., Marcus, R. K., *Anal. Bioanal. Chem.* 2012, *404*, 721-729.

[13] Schadock-Hewitt, A. J., Marcus, R. K., *J Sep Sci* 2014, *37*, 495-504.

[14] Fornea, D. S., Wu, Y., Marcus, R. K., *Analytical Chemistry* 2006, *78*, 5617-5621.

[15] Manard, B. T., Marcus, R. K., *J Am Soc Mass Spectrom* 2012.

[16] Dimartino, S., Herigstad, M., Boi, C., Sarti, G., *Journal of Biotechnology* 2010, *150*, 78.

[17] Schadock-Hewitt, A. J., Pittman, J. J., Christensen, K. A., Marcus, R. K., *Analyst* 2014, *139*, 2108-2113.

[18] Jiang, L., Marcus, R. K., *Analytical and Bioanalytical Chemistry* 2014, *submitted for publication*.

[19] Bide, M., Zhong, T., Ukponmwan, J., Phaneuf, M., Quist, W., LoGerfo, F., *AATCC Review* 2003, 24-28.

[20] Kim, E. S., Lee, C. H., Kim, S. H., *Journal of Applied Polymer Science* 2009, *112*, 3071-3078.

[21] Chen, W., McCarthy, T. J., *Macromolecules* 1998, *31*, 3648-3655.

[22] Papra, A., Hicke, H.-G., Paul, D., *Journal of Applied Polymer Science* 1999, *74*, 1669-1674.

[23] Jia, X., Herrera-Alonso, M., McCarthy, T. J., *Polymer* 2006, *47*, 4916-4924.

[24] Ellison, M. S., Fisher, L. D., Alger, K. W., Zeronian, S. H., *Journal of Applied Polymer Science* 1982, *27*, 247-257.

[25] Zalipsky, S., *Bioconjugate Chemistry* 1995, *6*, 150-165.

[26] Sandstrom, M. C., Johansson, E., Edwards, K., *Langmuir* 2007, *23*, 4192-4198.

[27] Auguste, D. T., Kirkwood, J., Kohn, J., Fuller, G. G., Prud'homme, R. K., *Langmuir* 2008, *24*, 4056-4064.

[28] Chen, Z. P., Zhu, J. B., Chen, H. X., Xiao, Y. Y., Feng, M. S., Cai, H., Chen, J., Cai, B. C., *Drug Development and Industrial Pharmacy* 2010, *36*, 657-665.

[29] Hao, Y., Yang, X., Song, S., Huang, M., He, C., Cui, M., Chen, J., *Nanotechnology* 2012, *23*, 045103.

[30] Ho, J. A. A., Hung, C. H., Wu, L. C., Liao, M. Y., *Analytical Chemistry* 2009, *81*, 5671-5677.

[31] Kandel, P. K., Fernando, L. P., Ackroyd, P. C., Christensen, K. A., *Nanoscale*, *3*, 1037-1045.

[32] Kitagawa, F., Hasegawa, T., Taji, H., Onoue, S., Tsuda, Y., Otsuka, K., *Analytical Sciences* 2008, *24*, 155-159.

[33] Smith, A. M., Duan, H., Rhyner, M. N., Ruan, G., Nie, S., *Phys Chem Chem Phys* 2006, *8*, 3895-3903.

[34] Vera-Avila, L., Gallegos-Perez, J., Camacho-Frias, E., *Talanta* 1999, *50*, 509-526.

[35] Do, T., Ho, F., Heidecker, B., Witte, K., Chang, L., Lerner, L., *Protein Expr Purif* 2008, *60*, 147-150.

[36] Randunu, K. M., Marcus, R. K., *Biotechnology Progress* 2013.

[37] Wang, Z., Marcus, R. K., *Biotechnology Progress* 2014, *submitted for publication*.

[38] Guiochon, G., Golshan-Shirazi, S., Katti, A. M., *Fundamenatals of Preparative and Nonlinear Chromatography, 2nd Ed.*, Academic Press 2006.

[39] Sezgin, Z., Yüksel, N., Baykara, T., *Eur J Pharm Biopharm* 2006, *64*, 261-268.

[40] Lukyanov, A. N., Torchilin, V. P., *Adv Drug Deliv Rev* 2004, *56*, 1273-1289.

[41] Huang, Y., Zhang, R., Li, J., Li, Q., Su, Z., Ma, G., *Protein Expr Purif* 2014, *95*, 84-91.

[42] Bedair, M., Oleschuk, R. D., *Analyst* 2006, *131*, 1316-1321.

[43] Fukushima, K., Satoh, T., Baba, S., Yamashita, K., *Glycobiology* 2010, *20*, 452-460.

[44] Lee, K., Gopal, A., von Nahmen, A., Zasadzinski, J., Majewski, J., Smith, G., Howes, P., Kjaer, K., *Journal of Chemical Physics* 2002, *116*, 774-783.

[45] Kuhl, T. L., Leckband, D. E., Lasic, D. D., Israelachvili, J. N., *Biophys J* 1994, *66*, 1479-1488.

[46] Allen, C., Dos Santos, N., Gallagher, R., Chiu, G. N., Shu, Y., Li, W. M., Johnstone, S. A., Janoff, A. S., Mayer, L. D., Webb, M. S., Bally, M. B., *Biosci Rep* 2002, *22*, 225-250.

[47] Diehl, H., Markuszewski, R., *Talanta* 1989, *36*, 416-418.

CHAPTER SIX

EDIVDENCE FOR THE INTERCALATION OF PEG-LIPID ACYL CHAINS INTO POLYPROPYLENE FIBER MATRICES

Introduction

Complex biological samples can contain thousands of compounds of diverse function and concentration. Biomarkers of potential interest in proteomics and clinical research are often in low abundance,[1] while those overexpressed in fermentation/culture batches for therapeutic drug production require large-scale purification procedures that are time-consuming and costly.[2] Thus, the development and improvement of chromatographic stationary phases is in a constant state of evolution to yield greater separation selectivity and column efficiency for the separation of proteins. For application in downstream processing, this means developing novel stationary phases that address the need for improvements in physical robustness, chemical stability and flexibility, binding capacity, and mass transfer kinetics.[3,4] To this end, polymeric phases in various formats (e.g., beads, fibers, and monoliths) are attractive alternatives to silica-based materials. Of course, chemical selectivity of the phase toward capture of the target protein is driven by solute-surface interactions, or more correctly with surface-bound ligands of high specificity. As such, a good deal of stationary phase development falls under the topic of polymer surface modification chemistry, where technologies developed across diverse fields of

use may find general utility. For example, novel ligand tethering chemistries developed for protein separations may be equally valid to prevent biofouling of polymer surfaces as well as in *in vivo* drug delivery applications.[5-10]

For macromolecule separations, where particulate phases suffer kinetic disadvantages due to solute diffusion within the porous structure, monolithic and fibrous polymer stationary phases excel. Monoliths have a unique pore channel structure, with very short diffusion distances, allowing operation at high linear velocities with minimal kinetic limitations.[11-14] However, the fabrication costs and engineering challenges for large-format monoliths have been problematic to this point. As an alternative, fibrous stationary phases have similar physical and chemical advantages to monoliths, but are inexpensive and provide a more straightforward approach in the large-scale preparative realm of chromatography. Marcus has reviewed the physical and chemical attributes that underlie their use for protein separations on the analytical and preparative scales.[15,16] Natural (e.g., cotton and wool) and synthetic (e.g., polyester, nylon, and polypropylene) polymers present a variety of basic surface chemistries, with an incredibly rich toolbox of surface modification strategies dating back to biblical times.

Capillary-channeled polymer (C-CP) fibers are a novel fibrous stationary phase which has been under investigation in this laboratory for protein separations in reserved phase (RP), ion exchange (IEC), and affinity chromatography (AC) modes.[17-23] They have also been applied as sorbents for solid phase extraction (SPE) processing for protein analytics.[24-26] C-CP fibers are

melt-extruded from nylon 6, poly (ethylene terephthalate) (PET), or polypropylene (PP) to form solid polymer fibers that are unique due to eight capillary channels that extend along the axis of the fiber.[17] This unique shape gives them approximately three times more surface area than a fiber of the same nominal diameter having a circular cross section. When packed into a column, the fibers self-align to form 1-5 μm open, parallel channels running the length of the column. These channels allow for C-CP fiber columns to have excellent fluid transport and solute mass transfer properties. Separations on traditional-sized HPLC columns packed with C-CP fibers can be performed at high linear velocities (> 100 mm s^{-1}) with low backpressures (< 2000 psi). The surface of C-CP fibers is non-porous relative to the size of a protein,[27] and thus rapid mass transfer via convective diffusion allows for high linear velocity separations without significant contribution to van Deemter C-term broadening.[18,20,28] As such, C-CP fiber columns yield high throughput and yield necessary for efficient large-scale protein separations.[21]

Taking these physical (hydrodynamic) advantages a step further, recent focus on C-CP fibers has been on surface modification to generate an analyte-specific stationary phase without disrupting the physical fiber attributes.[22,23,29,30] To this end, a new modality of ligand tethering has been developed, wherein phospholipids modified with poly(ethylene glycol) spacer arms and terminated with chem-reactive head groups provide a very simple, yet robust modification strategy. These head-group functionalized PEG-lipids are well known in

biological science literature,[31-39] but their use as a means of affixing ligands for chemical separations has only recently been reported, termed lipid tethered ligands (LTL).[22,40,41] This modification occurs due to the strong hydrophobic interaction between the lipid tail and the polypropylene (PP) C-CP fiber surface. Potential steric constraints at the surface are reduced as the hydrophilic PEG group extends away from the surface to allow for interaction between the functional group and analyte of interest. This one-step modification occurs on column under ambient conditions. PEG-lipids are commercially available with a number of functional head groups including amine, carboxylic acid, maleimide, cyanuric chloride, succinimidyl ester, fluorescein (FITC), and biotin.

The initial demonstration of the modification of PP C-CP fibers employed a biotin-PEG-lipid for the selective capture of streptavidin labeled with Texas-red (SAv-TR) from a complex cell lysate mixture containing a green fluorescent protein, mCitrine.[22] Biotin-PEG-lipid modified fibers captured SAv-TR with minimal non-specific binding, yielding a highly selective affinity phase. In a subsequent study, FITC-PEG-lipid was used to study ligand loading characteristics and the chemical stability of the PEG-lipid modification.[40] PEG-lipid adsorption isotherms performed at a linear velocity of 57 mm s^{-1} remained linear across the concentration range of 0.005 to 3 mg mL^{-1}, suggesting uniform monolayer coverage. Breakthrough curves generated at linear velocities ranging from 8.6 to 57.1 mm s^{-1} were very similar, attributed to the C-CP fibers' efficient mass transfer and fluid movement. However, the dynamic ligand capacity was

low based of the projected area taken up by a phospholipid. It was hypothesized that the lipid tail that may be adsorbed onto the PP fiber surface, was hindering the amount of PEG-lipid that could reach the surface, rather than allowing formation of an ordered brush-like structure dictated by the 5000 Da (n = 113) PEG groups. The chemical stability of the PEG-lipid adsorption was evaluated across a broad range of common chromatographic solvents, including phosphate buffered saline (PBS), Tris-HCl, sodium dodecyl sulfate (SDS), imidazole, Tween-20, and methanol; none of which removed measureable amounts of PEG-lipid. Only in the case of 50% acetonitrile and pure hexanes was appreciable (~30%) ligand loss observed. As such, the adsorption to the PP fiber surface is very robust. Clearly, more information is needed to determine how the lipid tail is interacting with the PP fiber structure. Specifically, as presented in Fig. 6.1, do the hydrophobic lipid chains lie along the fiber surface, or do they intercalate into the fiber pore structure? Indeed, the question being posed here is analogous to those posed in the generation of PEGylated surfaces employed across many fields of research.

A labeled lipid probe is employed here to evaluate the PEG-lipid/polypropylene interaction via fluorescent microcopy. In membrane and cell biology, fluorescent lipid probes are used to study important processes in membranes and live cells where these probes are easily integrated.[42] Phospholipids synthesized with the 7-nitro-2-1,3-benzoxadiazol-4-yl (NBD) fluorophore attached to either the head group or the fatty acyl chain are versatile

probes due to the unique properties of the NBD group, which fluoresces weakly in water and strongly in organic solvents or hydrophobic environments. NBD-labeled lipids have been particularly useful for monitoring membrane organization and dynamics due to their high degree of environmental sensitivity.[43-47] The NBD group exhibits a red edge excitation shift (REES), a phenomenon where slow solvent reorientation, relative to fluorescence lifetime, around the excited state of fluorophore causes an increase in the wavelength of maximum emission as the excitation wavelength is shifted towards the red edge of the absorption band.[48] NBD fulfills the necessary conditions for a fluorophore to exhibit REES as it is polar and gives a large change in dipole moment when excited, so significant solvent relaxation can occur. Overall, when the solvent molecules in close proximity to the NBD group are motionally-restricted and REES is observed, it is a reflection of the local environment.

In this work, NBD-labeled PEG-lipids are employed as probes to determine the modality of the adsorption to the PP C-CP fiber surface; whether with the alkyl chains resting along the fiber surface or intercalating into the bulk fiber. Environmental differences were monitored through fluorescence microscopy, reflecting whether or not the ligand was exposed to the solvent or imbedded in the fiber polymer matrix. These findings provide insight into the high chemical stability of this surface modification and a surface orientation that allows for high ligand capacity. It is also believed that the phenomena presented here

have relevance to diverse technological areas where surface-bound PEG functionality is important.

Experimental Section

Chemicals and Reagents

4-Chloro-7-nitrobenzofurazan (NBD-chloride) was obtained from Sigma Aldrich (St. Louis, MO), 1,2-dipalmitoyl-*sn*-glycero-3-phosphoethanolamine-N-(7-nitro-2-1,3-benzoxadiazol-4-yl) (ammonium salt) (16:0 NBD-PE) and 1-acyl-2-{12-[(7-nitro-2-1,3-benzoxadiazol-4-yl)amino]dodecanoyl}-*sn*glycero-3-phosphoethanolamine (acyl 12:0 NBD-PE) were obtained from Avanti Polar Lipids, Inc. (Alabaster, Al). NBD-Cl, NBD-PE, and acyl NBD-PE were prepared to 20 μg mL^{-1} 50:50 (v/v) ethanol:water (EtOH:H_2O). The structures of the three probe species are depicted in Fig. 6.2. HPLC-grade acetonitrile (ACN), methanol, and ethanol (190 proof) were obtained from EMD Millipore (Darmstadt, Germany). Hexanes were purchased from Fisher Scientific (Pittsburg, PA). MilliQ water (18.2 MΩ-cm) was derived from a Millipore water system (Billerica, MA) and used to prepare all aqueous solutions.

C-CP Fiber Tip Preparation and Modification

C-CP fibers are obtained from the Clemson University School of Materials Science and Engineering (Clemson, SC).[49] The procedure for preparing microbore C-CP fiber columns and then formatting them as SPE tips has been described previously.[22,24] In this study, a total of 720 nylon 6 fibers or 480 PP fibers were pulled through 300 mm long, 0.8 mm i.d. fluorinated ethylene propylene (FEP) capillary tubing (Cole Parmer, Vernon Hills, IL). These columns were packed to yield an interstitial void volume of $\varepsilon_i \approx 0.61$ (based on uracil retention), which had previously been found optimal for macromolecule separations.[28] After packing, columns were washed with ACN, methanol, and MilliQ water to remove any latent spin finish from the fiber manufacture process. The fiber columns were cut into 1 cm lengths with a gap at one end to allow for the FEP tubing to be press-fit on to the end of a commercial low-retention micropipette tip. Solution exposure was affected through solvent spin-down at 2000 x g relative centrifugal force (RCF) on a VWR Symphony Centrifuge (West Chester, PA) for 3-4 minutes. This approach allows for minimized chemical use and a quick modification of the fiber surface. C-CP fiber tips were modified in three steps: condition, load, and wash with 1 mL of the relevant solvent. Nylon 6 tips were modified with NBD-Cl and PP tips were modified with NBD-PE or acyl NBD-PE. Either 50:50 EtOH:H_2O or hexanes was used as the condition/load/wash solvent. After modification, tips were stored in a sealed, light-tight container.

Imaging

The C-CP fiber-containing tips were pulled from the micropipette and placed in a tray for fluorescence imaging. As the FEP tubing is optically clear, spectra were generated with fibers in the tubing without contributions from background signals. Fluorescence spectral images of the modified fiber tips were acquired on a Leica SP8X Multiphoton Confocal Microscope System (Leica Microsystems, Buffalo Grove, IL) with a Leica HC PL APO 10x/0.40NA CS dry objective, using a white light laser at 70% power. Spectra were collected using a lambda scan, where a narrow detection window is used to measure the emission signal as a function of the excitation wavelength. The wavelength was increased from 470 nm to 510 nm in 10 nm increments. At each excitation wavelength, fluorescent spectra were recorded from 530 - 590 nm with a step size of 3.93 nm (15 steps), using the high quantum efficiency GaAsP hybrid detection system (Leica HyD) in standard mode, gated from 0-12 ns with 94% gain. The detection bandwidth was 10 nm. Due to low light levels, the pinhole size was increased to 6.68 AU. The operation software was the Leica application suite advanced fluorescence (LAS AF) version 3.2.0.9652. Imaging conditions were kept constant for all samples.

Results and Discussion

While there may be several approximations as to how the hydrophobic PEG-lipid tail is interacting with the PP fiber structure, the two most simplistic cases are shown in Figure 6.1 where a) the lipid tail is laying on top of the fiber surface or b) the lipid tail is intercalating into the PP polymer matrix.

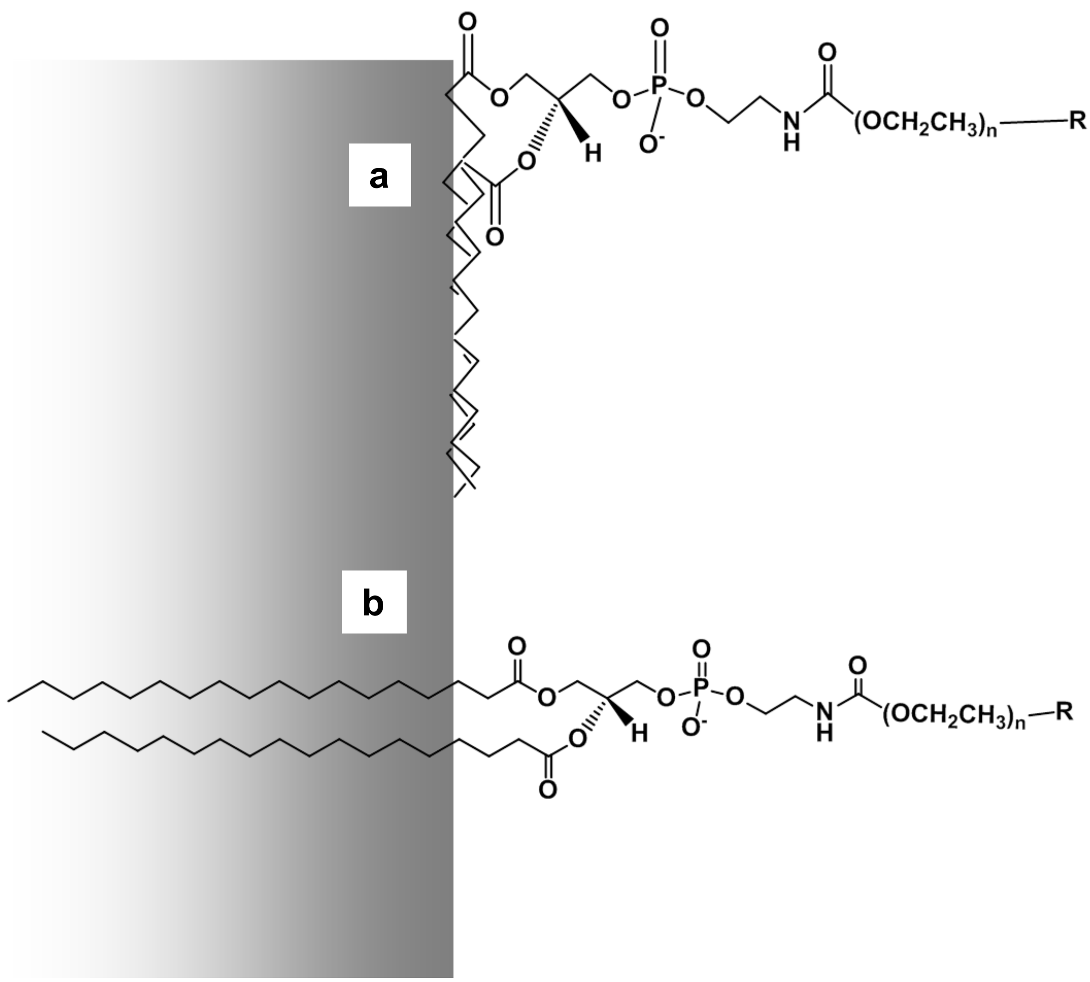

Figure 6.1 General representations of the possible interactions of PEG-lipid tails with hydrophobic fiber surfaces: a) lipid tail lays along the fiber surface and b) lipid tail intercalates into the fiber structure.

While PEG-lipids are most often incorporated into liposomes and other vesicles containing lipid bilayers, there have been some accounts of PEG-lipid being incorporated into polymer nanoparticles.[37,39,50] In each of these instances, the PEG-lipid was added as a component in the nanoparticle synthesis as the particles are condensed from the solution phase, where the lipid portion is incorporated into the matrix and the hydrophilic PEG group is residing in the aqueous phase. There are related works in terms of the interactions of lipid-like species and fabric materials. Some studies have focused on the use of polypropylene non-woven textiles as oil absorbents for oil-spill cleanup,[51,52] and the lipid distribution on soiled cotton textiles described "penetration of lipids into textile structures".[53] In neither of these cases, though, is the precise means of adsorption elucidated. Indeed, intercalation of a lipid tail *into* any sort of polypropylene (or other hydrophobic solid) structure cannot be found in the literature.

The NBD-labeled lipids are an excellent way to probe the interaction of PEG-lipids with the PP C-CP fiber structure due to the changes in fluorescence behavior of NBD, reflecting whether or not the ligand exited in a motionally-restricted environment. Based on the robustness of the lipid-PP interactions,[40] it was hypothesized that the lipid tail intercalates into the PP fiber structure (Fig. 6.1b). Inverse size exclusion chromatography (iSEC) measurements reflect pores on the order of 4 nm in diameter, and so lipid penetration can be imagined.[27] The three forms of the NBD molecule shown in Fig. 6.2 allow for the

evaluation of this hypothesis. In NBD-PE, the NBD group is covalently attached to the head group of a phosphatidylethanolamine molecule, which is expected to be fully solvated. In the acyl NBD-PE, the NBD group is covalently attached to the end of one fatty acid chain of the phosphatidylethanolamine, and so the spectral response would reflect its physical location. In order to assess the spectral response of the NBD, should it be located at the surface of the fiber (but not necessarily within it), the singular NBD-Cl molecule is exposed to the nylon 6 C-CP fiber, where it covalently binds to amine groups on the surface.

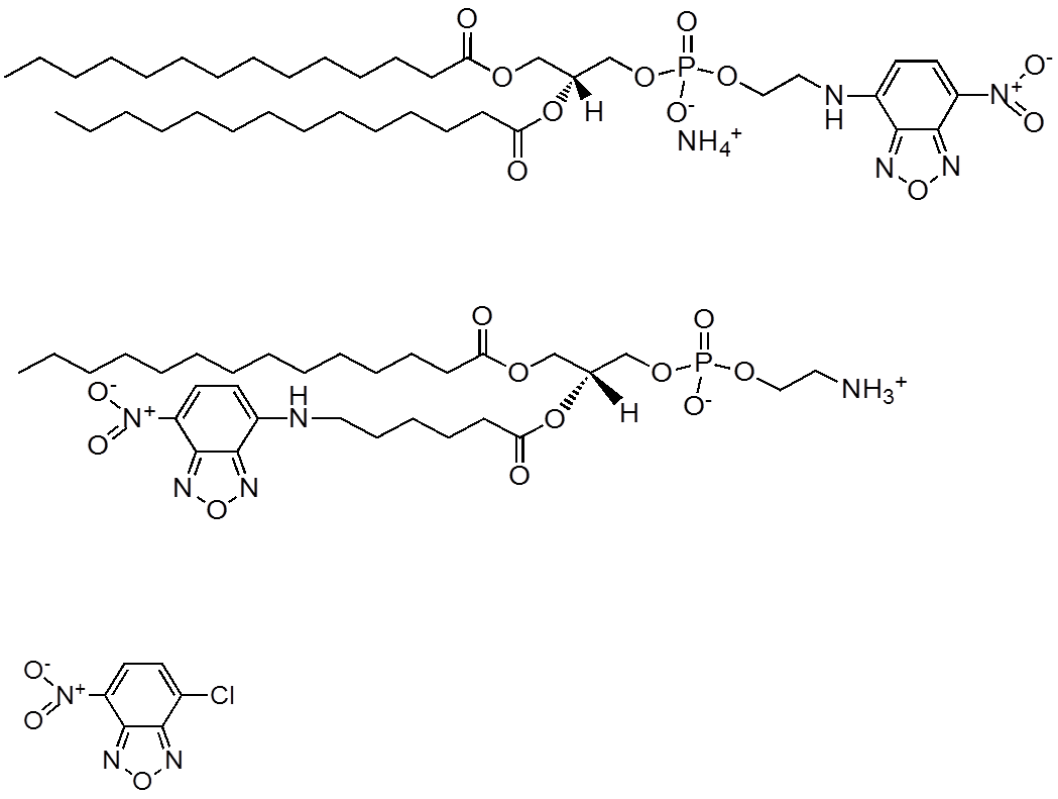

Figure 6.2 Chemical structures of NBD-labeled lipids and the NBD-Cl molecule used to modify C-CP fibers.

Thus the potentialities of the PEG-lipid interactions depicted in Fig. 6.1 can be assessed based on the occurrence, or not, of a REES fluorescence response.

All three molecules were prepared to 20 µg mL^{-1} in 50:50 (v/v) EtOH:H_2O, as it has been a very effective loading solvent for PEG-lipid modifications to create chromatographic stationary phases.[22,40]

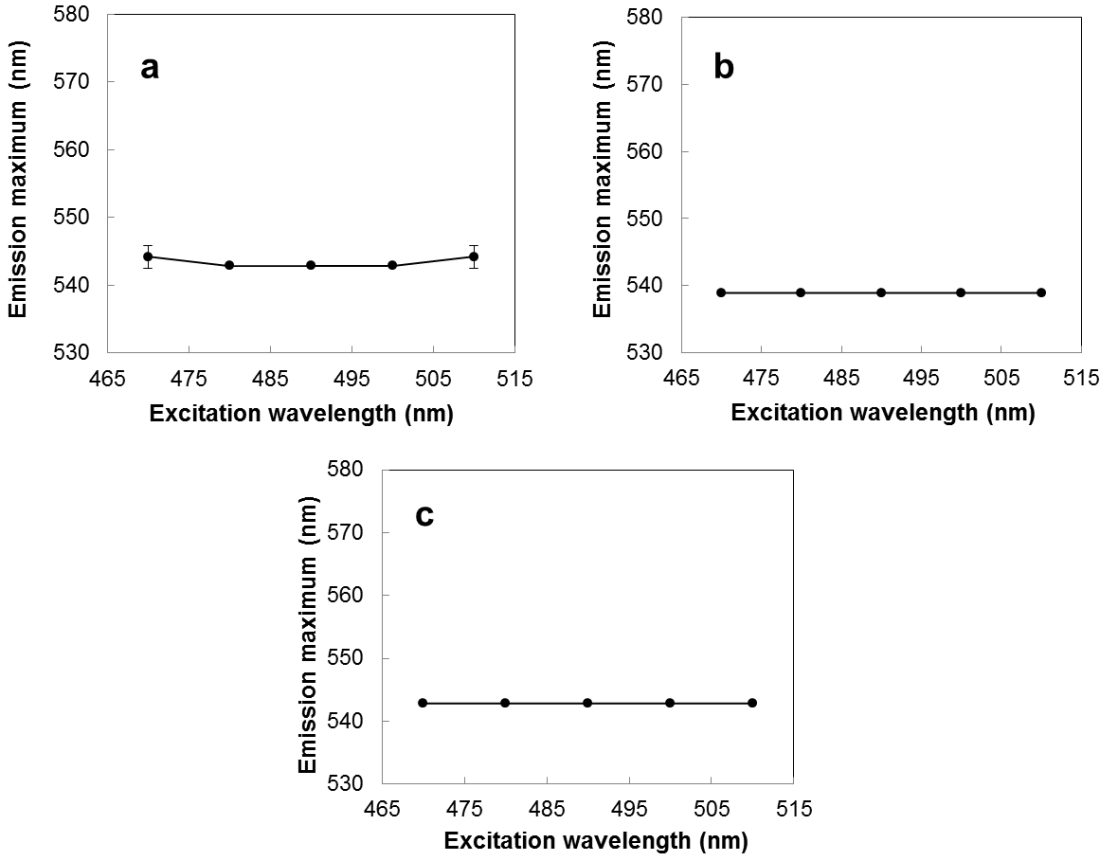

Figure 6.3 The effect of changing excitation wavelength on the wavelength of maximum emission (REES) of a) NBD-Cl, b) NBD-PE, and c) acyl NBD-PE modified C-CP fibers. Loading and wash steps were performed in 50:50 EtOH:H_2O.

The manufacturer recommends a 1:1 mixture of ethanol and water to dissolve lipids, as this decreases the polarity of the solution (over a purely aqueous phase) to prevent aggregation or formation of micelles. As seen in Fig. 6.3, there is no change observed in the emission wavelength maximum as the excitation wavelength is increased from 470 nm to 510 nm for a) NBD-Cl (bound to nylon 6), b) NBD-PE, or the c) acyl NBD-PE modified PP C-CP fibers. The lack of a spectral shift reflects the fact that the NBD group in each instance exists in a well-solvated, motionally-unrestricted environment. However, due to the flexibility of the acyl chain and the polarity of the NBD group, it is possible that the lipid tail is actually intercalating into the polymer structure but then looping back so that the NBD resides in the polar solvent environment as depicted in Fig. 6.4.

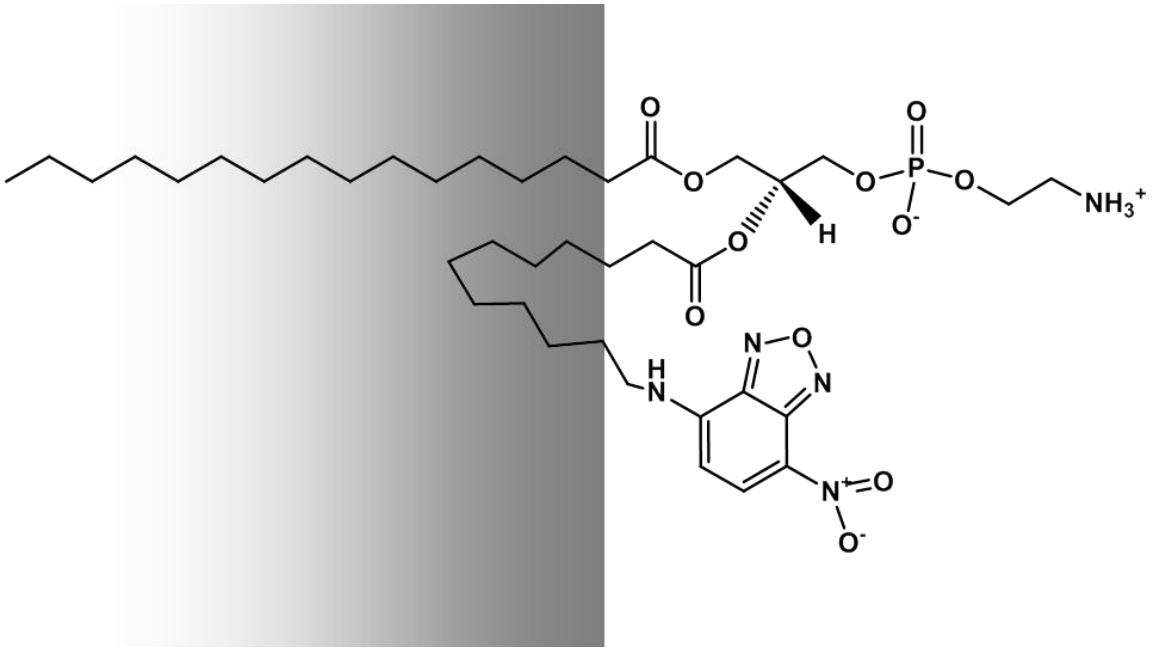

Figure 6.4 Diagrammatic representation of acyl-NBD group solvation in the case of a 50:50 EtOH:H_2O deposition solvent.

This precise situation has been reported for acyl NBD-PE located in membranes, where the polar NBD group affixed to the hydrocarbon tail loops back towards the lipid/water interface instead of penetrating deeper into the hydrophobic lipid bilayer, as would be favored for a purely aliphatic chain.[54-57] Again, this is attributed to the polar NBD group's affinity for the polar solvent environment and the flexible acyl chain allowing it to loop. Clearly, a nonpolar loading solvent is necessary to reduce the propensity of the NBD group to migrate back to the solvent environment.

In terms of non-polar solvents, n-hexane presents an environment for which the polar NBD group will have a very low propensity to remain solvated; or at least will be far less likely to affect the lipid adsorption processes. Schadock-Hewitt and Marcus demonstrated that out of many solvents tested, ACN and hexanes were the only solvents able to remove adsorbed PEG-lipid molecules from PP C-CP fiber surfaces.[40] Hexanes removed ~30% of the adsorbed lipid, and so while there is a driving force for the solvation of the alkyl lipid chains and their removal from the fiber, there is sufficient affinity for strongly adsorbed species to remain. The PEG-lipids were loaded in hexanes, with adsorption confirmed through absorbance measurements of the load solutions post exposure to the fiber media. Figure 6.5 presents the emission wavelength of maximum intensity as a function of the excitation wavelength from 470 nm to 510 nm on the a) NBD-Cl, b) NBD-PE, and c) acyl NBD-PE-modified PP C-CP fibers

loaded in hexanes. Tips modified with NBD-Cl and NBD-PE, where the NBD group should be un-restricted in the solvent environment, showed no increase in the maximum emission wavelength. Tips modified with acyl NBD-PE, where the NBD group is attached to the lipid tail and hypothesized to intercalate into the PP backbone structure, definitively exhibited REES, showing a 32 nm increase in wavelength of maximum emission.

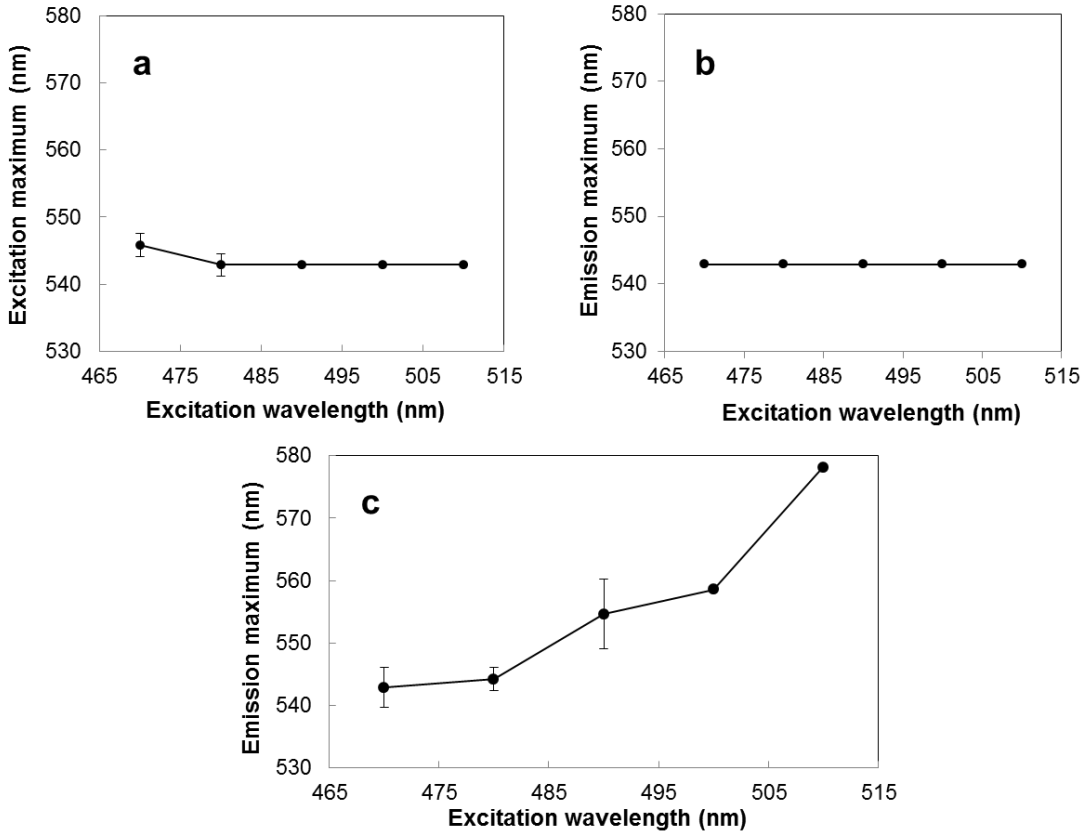

Figure 6.5 The effect of changing excitation wavelength on the wavelength of maximum emission (REES) of a) NBD-Cl, b) NBD-PE, and c) acyl NBD-PE modified C-CP fibers. Loading and wash steps were performed in 100% hexanes.

This confirms that the NBD probe is located in the motionally-restricted environment of the polymer fiber matrix. The intensity-normalized spectra presented in Fig. 6.6 show emission scans of acyl NBD-PE modified fibers when loading in a) 50:50 ethanol:water and b) 100% hexanes at 470 nm, 490 nm, and 510 nm. The emission spectra are consistently composed of three distinct peaks, at ~545 nm, ~558 nm, and ~578 nm.

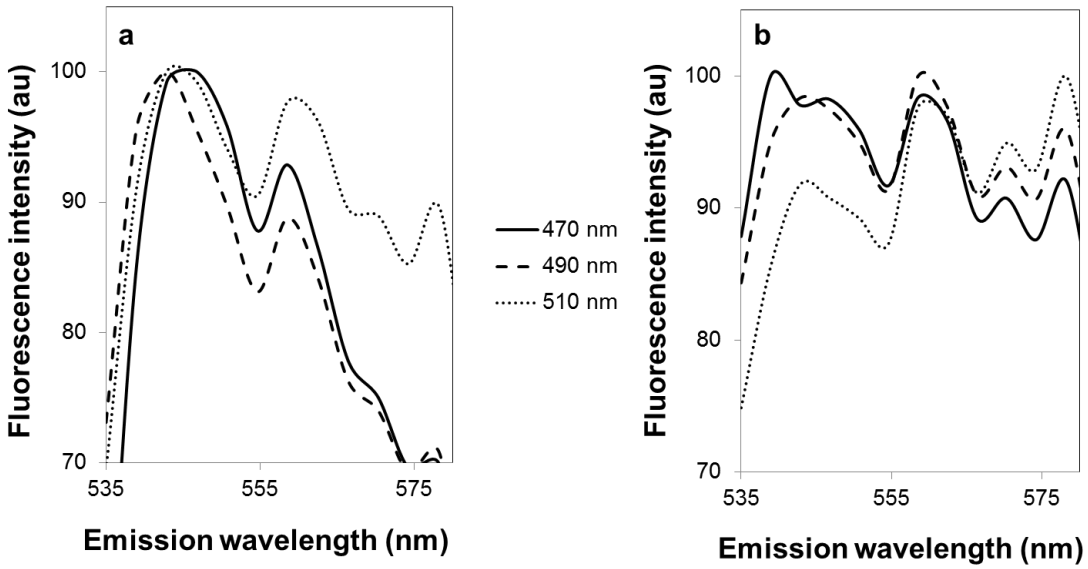

Figure 6.6 Intensity-normalized fluorescence emission spectra of acyl NBD-PE at increasing excitation wavelengths. a) loading in 50:50 EtOH:H_2O, b) loading in 100% hexanes. Spectra are the average of triplicate experiments.

Emission spectra of NBD-PE modified fibers when loading in 50:50 ethanol:water gave no indication of REES with an emission maximum of ~545 nm for each excitation wavelength. The emission spectra of acyl NBD-PE modified fibers

when loading in 100% hexanes exhibit REES with an increase in emission maximum from ~545 nm at 470 nm excitation, ~558 nm at 490 nm excitation, and ~578 nm at 510 nm excitation. Thus, it is concluded that modifications of PP C-CP fibers with PEG-lipids involves intercalation of the lipid tail *into* the intrafiber structure. This creates a very robust surface modification relative to most solvents encountered in liquid chromatography or other biomolecule processing situations. Referring to Fig. 6.1, this mode of adsorption suggests that the surface loading of PEG-lipids will be dictated by the crowding of the PEG and head group moieties, and not the lipid anchors.

Conclusions

Evidence for the intercalation of lipids chains into polypropylene fibers has been presented. The environmentally-sensitive NBD fluorophore was used to probe the interaction of PEG-lipids with the fiber, as it is commercially available covalently attached to the head group (NBD-PE) or the acyl chain (acyl NBD-PE) of a lipid. Fibers modified with NBD-PE or the NBD-Cl molecule did not display REES. Modification performed in hexane solvent was necessary to drive the polar NBD group into the fiber. When fibers were modified with acyl NBD-PE in hexane solvent, REES was observed, confirming the hypothesis that the lipid tail is intercalating into the fiber structure. Overall, these results explain the robustness and stability of head group functionalized PEG-lipid modified PP C-CP fibers in their use in lipid tethered ligand (LTL) systems.

It is believed that the system evaluated here has relevance to many other fields wherein surface modification of hydrophobic substrates is desired. In many of these, there exists a deep literature involving the immobilization of PEG groups. These include the creation of surfaces of high resistance to biofouling, surfaces of spatio-specific differences in hydrophobicity, and the use of polymeric nanoparticles for time-released drug delivery.

Acknowledgment

This material is based upon work supported by the National Science Foundation Division of Chemistry under grant CHE-1307078. The authors would like to thank Dr. Terri Bruce, Director of the Clemson Light Imaging Facility, and Charlie Hemphill from Leica Microsystems, for their assistance and expertise with acquiring images from the Leica SP8X Multiphoton Confocal Microscope System

References

(1) Nice, E. C.; Rothacker, J.; Weinstock, J.; Lim, L.; Catimel, B. *J. Chromatogr. A* **2007**, *1168*, 190.

(2) Linhult, M.; Gülich, S.; Hober, S. *Protein Pept. Lett.* **2005**, *12*, 305.

(3) Ladisch, M. R. *Bioseparations engineering: Principles, practice, and economics*; Wiley, 2001.

(4) Carta, G.; Jungbauer, A. *Protein Chromatography: Process Development and Scale-Up*; Wiley-VCH, 2010.

(5) Leckband, D.; Sheth, S.; Halperin, A. *J. Biomater. Sci. Polym. Ed.* **1999**, *10*, 1125.

(6) Vermette, P.; Meagher, L. *Colloids Surf. B* **2003**, *28*, 153.

(7) Bi, H.; Zhong, W.; Meng, S.; Kong, J.; Yang, P.; Liu, B. *Anal. Chem.* **2006**, *78*, 3399.

(8) Duncanson, W. J.; Figa, M. A.; Hallock, K.; Zalipsky, S.; Hamilton, J. A.; Wong, J. Y. *Biomaterials* **2007**, *28*.

(9) Pai, S. S.; Tilton, R. D.; Przybycien, T. M. *AAPS J.* **2009**, *11*, 88.

(10) Rabanel, J.-M.; Hidgen, P.; Banquy, X. *J. Controlled Release* **2014**, *185*, 71.

(11) Jungbauer, A.; Hahn, R. *J. Sep. Sci.* **2004**, *27*, 767.

(12) Jungbauer, A.; Hahn, R. *Journal of Chromatography A* **2008**, *1184*, 62.

(13) Rodrigues, A.; Mata, V.; Zabka, M.; Pais, L. In *Monolithic Materials: Preparation, Properties, and Applications*; Svec, F., Tennikova, T. B., Deyl, Z., Eds.; Elsevier Science: Amsterdam, 2003.

(14) Lee, D.; Svec, F.; Fréchet, J. M. *J. Chromatogr. A* **2004**, *1051*, 53.

(15) Marcus, R. K. *J. Sep. Sci.* **2008**, *31*, 1923.

(16) Marcus, R. K. *J. Sep. Sci.* **2009**, *32*, 695.

(17) Marcus, R. K.; Davis, W. C.; Knippel, B. C.; LaMotte, L.; Hill, T. A.; Perahia, D.; Jenkins, J. D. *J. Chromatogr. A* **2003**, *986*, 17.

(18) Nelson, D. M.; Marcus, R. K. *Anal. Chem.* **2006**, *78*, 8462.

(19) Stanelle, R. D.; Straut, C. A.; Marcus, R. K. *J. Chromatogr. Sci.* **2007**, *45*, 415.

(20) Randunu, J. M.; Marcus, R. K. *Anal. Bioanal. Chem.* **2012**, *404*, 721.

(21) Randunu, K. M.; Marcus, R. K. *Biotechnol. Prog.* **2013**, *29*, 1222.

(22) Schadock-Hewitt, A. J.; Pittman, J. J.; Christensen, K. A.; Marcus, R. K. *Analyst* **2014**, *139*, 2108.

(23) Schadock-Hewitt, A. J.; Marcus, R. K. *J. Sep. Sci.* **2014**, *37*, 495.

(24) Fornea, D. S.; Wu, Y.; Marcus, R. K. *Analytical Chemistry* **2006**, *78*, 5617.

(25) Burdette, C. Q.; Marcus, R. K. *Analyst* **2012**, *138*, 1098.

(26) Manard, B. T.; Marcus, R. K. *J. Am. Soc. Mass Spectrom.* **2012**.

(27) Wang, Z.; Marcus, R. K. *J. Chromatogr. A* **2014**, *1351*, 82.

(28) Randunu, K. M.; Dimartino, S.; Marcus, R. K. *J. Sep. Sci* **2012**, *35*, 3270.

(29) Pittman, J. J.; Klep, V.; Luzinov, I.; Marcus, R. K. *Anal. Methods* **2010**, *2*, 461.

(30) Jiang, L.; Marcus, R. K. *Anal. Bioanal. Chem.*, *in press*.

(31) Zalipsky, S. *Bioconjugate Chem.* **1993**, *4*, 296.

(32) Sandstrom, M. C.; Johansson, E.; Edwards, K. *Langmuir* **2007**, *23*, 4192.

(33) Auguste, D. T.; Kirkwood, J.; Kohn, J.; Fuller, G. G.; Prud'homme, R. K. *Langmuir* **2008**, *24*, 4056.

(34) Chen, Z. P.; Zhu, J. B.; Chen, H. X.; Xiao, Y. Y.; Feng, M. S.; Cai, H.; Chen, J.; Cai, B. C. *Drug Dev. Ind. Pharm.* **2010**, *36*, 657.

(35) Hao, Y.; Yang, X.; Song, S.; Huang, M.; He, C.; Cui, M.; Chen, J. *Nanotechnol.* **2012**, *23*, 045103.

(36) Ho, J. A. A.; Hung, C. H.; Wu, L. C.; Liao, M. Y. *Anal. Chem.* **2009**, *81*, 5671.

(37) Kandel, P. K.; Fernando, L. P.; Ackroyd, P. C.; Christensen, K. A. *Nanoscale* **2011**, *3*, 1037.

(38) Kitagawa, F.; Hasegawa, T.; Taji, H.; Onoue, S.; Tsuda, Y.; Otsuka, K. *Anal. Sci.* **2008**, *24*, 155.

(39) Smith, A. M.; Duan, H.; Rhyner, M. N.; Ruan, G.; Nie, S. *Phys. Chem. Chem. Phys.* **2006**, *8*, 3895.

(40) Schadock-Hewitt, A. J.; Marcus, R. K. *J. Sep. Sci.*, *in press*.

(41) Jiang, L.; Schadock-Hewitt, A. J.; Marcus, R. K. *Anal. Chem.*, *submitted for publication*.

(42) Maier, O.; Oberle, V.; Hoekstra, D. *Chem. Phys. Lipids* **2002**, *116*, 3.

(43) Haldar, S.; Chaudhuri, A.; Chattopadhyay, A. *J. Phys. Chem. B* **2011**, *115*, 5693.

(44) Haldar, S.; Chattopadhyay, A. In *Fluorescent Methods to Study Biological Membranes*; Springer: 2013, p 37.

(45) Chattopadhyay, A.; Mukherjee, S. *Biochemistry* **1993**, *32*, 3804.

(46) Chattopadhyay, A.; Mukherjee, S. *J. Phys. Chem. B* **1999**, *103*, 8180.

(47) Mukherjee, S.; Raghuraman, H.; Dasgupta, S.; Chattopadhyay, A. *Chem. Phys. Lipids* **2004**, *127*, 91.

(48) Lakowicz, J. R.; Keating-Nakamoto, S. *Biochemistry* **1984**, *23*, 3013.

(49) Brown, P. J.; M., M.; Sinclair, K.; Tucker, E.; Inam, A. In *Southeast Regional Meeting of the American Chemical Society* 2004.

(50) Yu, W. W.; Chang, E.; Falkner, J. C.; Zhang, J.; Al-Somali, A. M.; Sayes, C. M.; Johns, J.; Drezek, R.; Colvin, V. L. *J. Am. Chem. Soc.* **2007**, *129*, 2871.

(51) Wei, Q. F.; Mather, R. R.; Fotheringham, A. F.; Yang, R. D. *Mar. Pollut. Bull.* **2003**, *46*, 780.

(52) Zhao, J.; Xiao, C.; Xu, N. *Environ. Sci. Pollut. Res. Int.* **2013**, *20*, 4137.

(53) Obendorf, S. K.; Varanasi, A.; Mejldal, R.; Nielsen, V. *J. Surfactants Deterg.* **2003**, *6*, 1.

(54) Chattopadhyay, A.; London, E. *Biochemistry* **1987**, *26*, 39.

(55) Abrams, F. S.; London, E. *Biochemistry* **1993**, *32*, 10826.

(56) Huster, D.; Müller, P.; Arnold, K.; Herrmann, A. *Biophys. J.* **2001**, *80*, 822.

(57) Loura, L. M.; Ramalho, J. P. *Biochim. Biophys. Acta* **2007**, *1768*, 467.

CHAPTER SEVEN

SUMMARY

The research presented in this dissertation utilized capillary-channeled polymer (C-CP) fibers as a stationary phase for HPLC applications. As explained in detail, C-CP fibers provide an excellent alternative to costly silica or polymer bead-based phases that can lead to inefficient protein separations. The overall goal for industrial protein separations is generating the fastest, least expensive, and most efficient separation and purification. To enhance the efficiency of C-CP fibers, generating a high surface density of selective functional groups is essential. Thus, the focus of this dissertation was on the modification of C-CP fibers to generate an analyte specific stationary phase while still maintaining the advantageous physical properties of the fibers. The overall mode of modification here was surface adsorption. A hydrophobic polypropylene surface strongly adsorbs hydrophobic proteins and other molecules. This simple approach leads to many possible chemically reactive functional groups available for protein capture. The chapters of this dissertation highlight the advantageous physical properties of the C-CP fibers while evaluating the enhancements that a surface modification brings.

In Chapter II, the physical properties of polyamide (nylon 6) C-CP fibers were evaluated and give a general overview of why these unique fibers are important. Nylon 6 C-CP fibers were used as the stationary phase for the HPLC

separation of a protein suite. However, differences in chromatographic behavior between two (presumably identical) nylon 6 fibers, revealed previously unknown differences between the two. In the protein separations on a capillary column, three proteins separated in under 2 min. on one nylon 6 fiber column, but did not separate on the second nylon 6 fiber column. An extensive list of testing was performed, leading to the discovery that the differences between the fibers lie in their solid, extruded forms. In other words, during the melt-extrusion process that formed the fiber, differences in molecular weight, and thus end group density (which determined separation quality) were made. Other fiber differences are noted, with the overall conclusion being that C-CP fiber characteristics are dependent on the extrusion process and the exact base polymer they were made with.

Chapter III described a novel affinity chromatography stationary phase developed from polypropylene (PP) C-CP fibers modified with a recombinant protein A ligand. The application of protein A affinity chromatography is the selective capture of immunoglobulin G (IgG) antibody, used for drug therapeutics. This affinity phase was used in an SPE micropipette tip format so that solvent and analyte use was minimized. The adsorption of protein A onto the PP fiber surface was evaluated at differing load concentrations and volumes to generate an optimally modified surface. Exposure to a mixture of human IgG and myoglobin (used as a surrogate host cell protein) evaluated the selective capture ability of the affinity phase, and how well non-specific binding was

minimized. The efficacy of selective binding to the protein A ligand was demonstrated by an optimal 2.9:1 (IgG:protein A) binding stoichiometry. A wash buffer removed all nonspecifically bound species, and IgG was successfully eluted from the surface with high yield. Overall, strong initial results show promise for protein A modified C-CP fibers to be used for protein A affinity chromatography.

Chapter IV described another novel stationary phase with head group-functionalized poly(ethylene glycol)-lipid (PEG-lipid) modified PP C-CP fibers. The aliphatic lipid tails adsorbs strongly to the hydrophobic fiber surface , with the hydrophilic PEG group extending towards the more polar mobile phase, thus allowing for the chemically reactive head group to be free in solution to interact with the desired analyte. Again, an initial proof-of-concept was achieved by adsorption of a biotin-PEG-lipid to the PP C-CP fiber surface. Surface modification and uniformity was evaluated by binding streptavidin labeled with Texas Red (SAv-TR) to the biotin. Isolation of SAv-TR from a mixture in neat buffer and in cleared lysate demonstrated the capability of the modified fibers to extract an analyte of interest from a complex viscous mixture. It is believed that this surface modification approach is generally applicable to a diversity of selective protein immobilization applications, including clinical diagnostics and preparative scale HPLC on C-CP fibers as well as to other hydrophobic supports.

Chapter V expanded on the proof-of-concept study in Chapter IV with the evaluation of ligand loading to generate a ligand dense surface. In order to study

ligand binding characteristics, a fluorescein-labeled polyethylene glycol-lipid was used as a model system. Breakthrough curves and frontal analysis were employed to characterize the surface loading characteristics across a range of lipid concentrations and mobile phase flow rates. Efficient mass transfer and fluid transport yield a linear adsorption isotherm up to the maximum loading concentration of 3 mg mL^{-1}, at a linear velocity of 57.1 mm s^{-1}. Under these conditions, the dynamic binding capacity was found to be 1.52 mg g^{-1} of fiber support. Variation of the linear velocity from 8.6 – 57.1 mm s^{-1} showed only small changes in breakthrough volume. The maximum ligand capacity of 1.8 mg g^{-1} is found under conditions of a load velocity of 34.2 mm s^{-1} and a concentration of 3 mg mL^{-1} lipid. Exposure of the lipid modified fibers to several challenge solvents reveals a chemically robust system, with only 50% ACN and hexanes able to disrupt the lipid adsorption. Overall, the straightforward C-CP fiber surface modification with head group-functionalized lipids provides both a diverse yet practically robust ligand tethering system.

Chapter VI looked at exactly how the PEG-lipid modification, or lipid tethered ligand (LTL) system (from Chapter IV and V) was occurring. This basic methodology has promise in many areas where robust polymer surface modifications are desired. In order to understand the mode of adsorption of the lipid tail to the polypropylene surface, lipids labeled with the environmentally-sensitive 7-nitro-2-1,3-benzoxadiazol-4-yl (NBD) fluorophore were used, with NBD covalently attached to the head group (NBD-PE) or the acyl chain (acyl

NBD-PE) of the lipid. When modified with the acyl NBD-PE, fluorescence imaging of the fiber at excitation wavelengths increasing from 470 – 510 nm caused a 32 nm shift in emission towards the red edge of the absorption band, indicating that the NBD molecule (and thus the lipid tail) is motionally-restricted. Fluorescence imaging on fibers modified with NBD-PE or the free NBD-Cl dye molecule yielded no change in the emission response. The results of these fluorescence imaging studies provided evidence that the acyl chain portions of the PEG-lipids intercalate into the polypropylene fiber structure, yielding a robust means of surface modification and the potential for high ligand densities.

The future of C-CP fibers lies in surface modification to generate an analyte specific surface. Specifically, as described above, surface modification with PEG-lipids provides a robust surface modification with potentially high ligand densities. As the specific surface area of C-CP fibers is smaller than other competing and commercially available phases, a greater number of surface ligands available for analysis will yield higher binding capacities. Higher binding capacities combined with the physical advantages of C-CP fibers (fast, efficient separations), will make C-CP fibers a viable phase. As most studies have been done at analytical scale, future experiments will increase the scale towards the preparative side, where the advantages of C-CP fibers should really shine. Specifically, the protein A ligand modification in Chapter III will be performed at a semi-preparative scale and look at IgG capture from complex cell lysates. As the PEG-lipid surface modifications have seen great outcomes, the Marcus

laboratory has been synthesizing PEG-lipids to be specifically tailored to the application. This includes removing the phosphate group, which could potentially be hydrolyzed, and reducing the PEG chain length significantly, which has been found to hinder surface adsorption when available at n = 50 to 100 monomer lengths. With the base knowledge of these surface modifications fully understood, their application as stationary phases for HPLC can be fully evaluated and realized.

APPENDICES

Appendix A

Supplementary Information for Chapter II

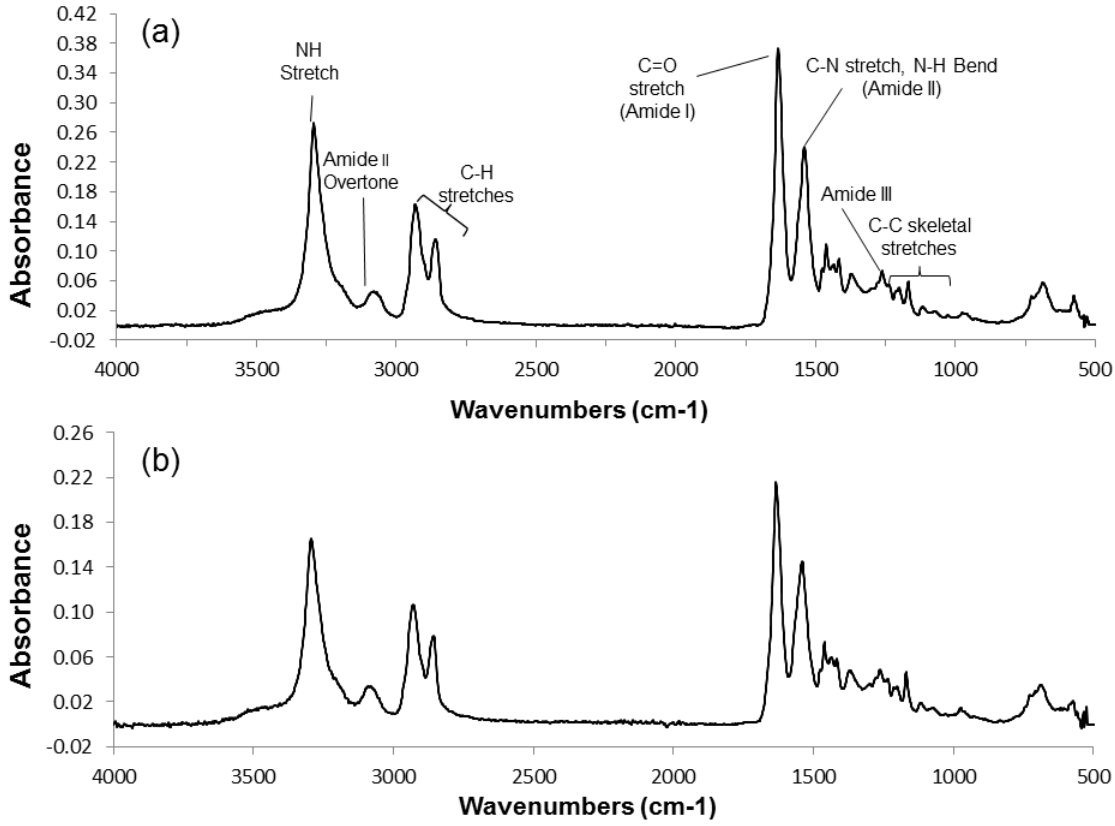

Figure A-1. ATR-FTIR of spectra of (a) nylon 6A and (b) nylon 6B C-CP fibers. Labels indicate characteristics IR bands of nylon 6 and confirm the basic identity of each C-CP fiber sample.

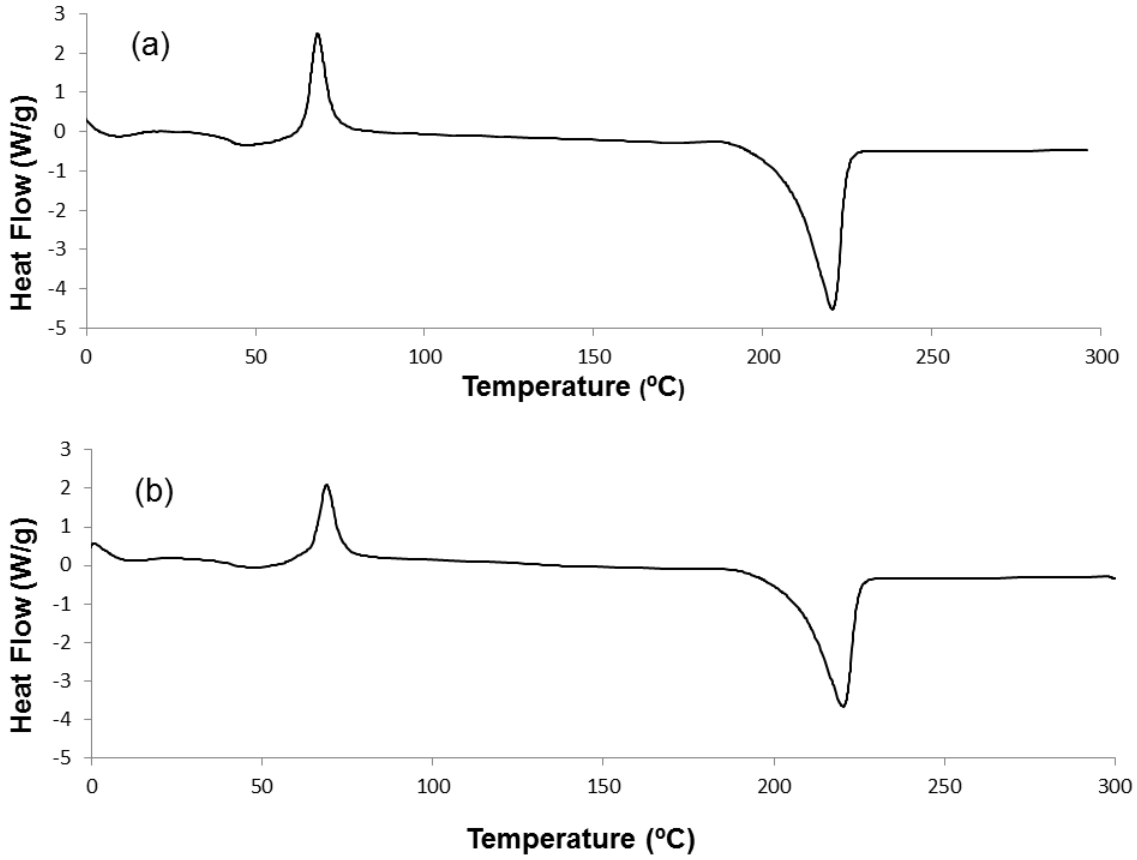

Figure A-2. DSC curves of a) nylon 6A and b) nylon 6B after a quench-cool treatment. The samples were initially heated from 0-300 °C at a rate of 20 °C min^{-1} before being quench-cooled on a liquid nitrogen cooled steel bar and reintroduced into the heating chamber.

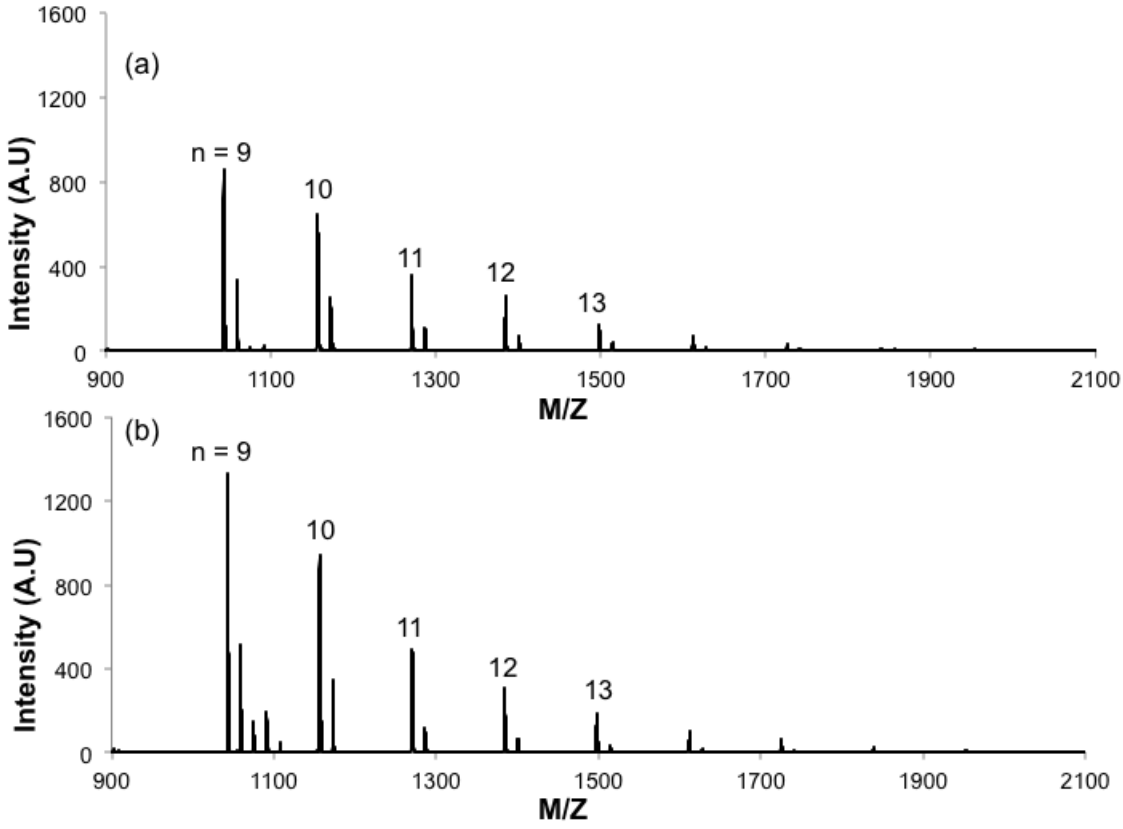

Figure A-3. MALDI-TOF mass spectra of a) nylon 6A and b) nylon 6B C-CP fibers dissolved in 2,2,2-trifluoroethanol.

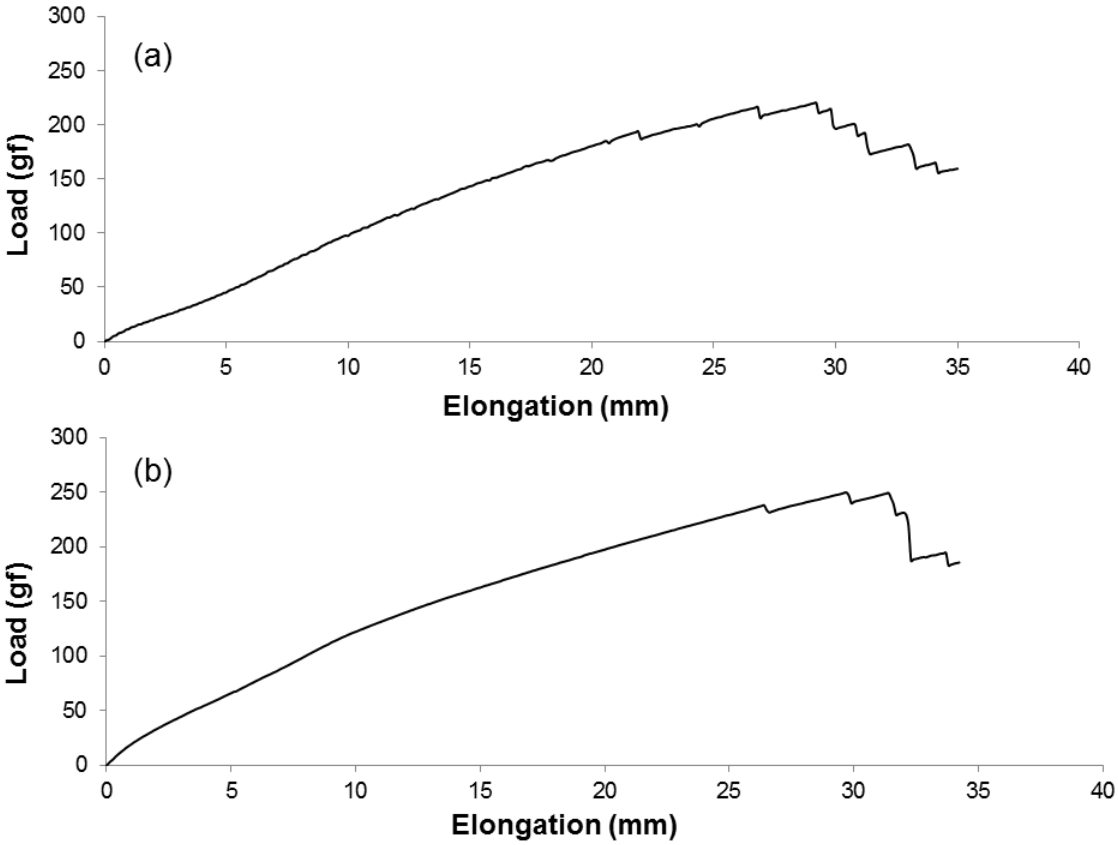

Figure A-4. Tensile testing on a) nylon 6A and b) nylon 6B C-CP fibers showing maximum strain and load before breakage

Appendix B

Reuse Permission for Chapter II

JOHN WILEY AND SONS LICENSE TERMS AND CONDITIONS

Oct 01, 2014

This is a License Agreement between Abby J Schadock-Hewitt ("You") and John Wiley and Sons ("John Wiley and Sons") provided by Copyright Clearance Center ("CCC"). The license consists of your order details, the terms and conditions provided by John Wiley and Sons, and the payment terms and conditions.

All payments must be made in full to CCC. For payment instructions, please see information listed at the bottom of this form.

License Number	3480300743786
License date	Oct 01, 2014
Licensed content publisher	John Wiley and Sons
Licensed content publication	Journal of Applied Polymer Science
Licensed content title	Extrusion-based differences in two types of nylon 6 capillary-channeled polymer (C-CP) fiber stationary phases as applied to the separation of proteins via ion exchange chromatography
Licensed copyright line	Copyright © 2012 Wiley Periodicals, Inc.
Licensed content author	Abby J. Schadock-Hewitt,Jennifer J. Pittman,Kathryn A. Stevens,R. Kenneth Marcus
Licensed content date	Sep 17, 2012
Start page	1257
End page	1265
Type of use	Dissertation/Thesis
Requestor type	Author of this Wiley article
Format	Print and electronic
Portion	Full article
Will you be translating?	No
Title of your thesis / dissertation	SURFACE MODIFICATIONS OF CAPILLARY-CHANNELED POLYMER (C-CP) FIBER STATIONARY PHASES: IMPROVING THE EFFICIENCY OF HIGHLY SELECTIVE ANALYTE SEPARATIONS
Expected completion date	Dec 2014

Appendix C

Reuse Permission for Chapter III

JOHN WILEY AND SONS LICENSE TERMS AND CONDITIONS

Oct 01, 2014

This is a License Agreement between Abby J Schadock-Hewitt ("You") and John Wiley and Sons ("John Wiley and Sons") provided by Copyright Clearance Center ("CCC"). The license consists of your order details, the terms and conditions provided by John Wiley and Sons, and the payment terms and conditions.

All payments must be made in full to CCC. For payment instructions, please see information listed at the bottom of this form.

License Number	3480301087480
License date	Oct 01, 2014
Licensed content publisher	John Wiley and Sons
Licensed content publication	Journal of Separation Science
Licensed content title	Initial evaluation of protein A modified capillary-channeled polymer fibers for the capture and recovery of immunoglobulin G
Licensed copyright line	© 2014 WILEY-VCH Verlag GmbH & Co. KGaA, Weinheim
Licensed content author	Abby J. Schadock-Hewitt,R. Kenneth Marcus
Licensed content date	Jan 25, 2014
Start page	495
End page	504
Type of use	Dissertation/Thesis
Requestor type	Author of this Wiley article
Format	Print and electronic
Portion	Full article
Will you be translating?	No
Title of your thesis / dissertation	SURFACE MODIFICATIONS OF CAPILLARY-CHANNELED POLYMER (C-CP) FIBER STATIONARY PHASES: IMPROVING THE EFFICIENCY OF HIGHLY SELECTIVE ANALYTE SEPARATIONS
Expected completion date	Dec 2014

Appendix D

Reuse Permission for Chapter V

JOHN WILEY AND SONS LICENSE TERMS AND CONDITIONS

Nov 04, 2014

This is a License Agreement between Abby J Schadock-Hewitt ("You") and John Wiley and Sons ("John Wiley and Sons") provided by Copyright Clearance Center ("CCC"). The license consists of your order details, the terms and conditions provided by John Wiley and Sons, and the payment terms and conditions.

All payments must be made in full to CCC. For payment instructions, please see information listed at the bottom of this form.

License Number	3501961174989
License date	Nov 04, 2014
Licensed content publisher	John Wiley and Sons
Licensed content publication	Journal of Separation Science
Licensed content title	Loading characteristics and chemical stability of headgroup-functionalized poly(ethylene glycol)-lipid ligand tethers on polypropylene capillary-channeled polymer fibers
Licensed copyright line	© 2014 WILEY-VCH Verlag GmbH & Co. KGaA, Weinheim
Licensed content author	Abby J. Schadock-Hewitt,R. Kenneth Marcus
Licensed content date	Nov 2, 2014
Start page	n/a
End page	n/a
Type of use	Dissertation/Thesis
Requestor type	Author of this Wiley article
Format	Print and electronic
Portion	Full article
Will you be translating?	No
Title of your thesis / dissertation	SURFACE MODIFICATIONS OF CAPILLARY-CHANNELED POLYMER (C-CP) FIBER STATIONARY PHASES: IMPROVING THE EFFICIENCY OF HIGHLY SELECTIVE ANALYTE SEPARATIONS
Expected completion date	Dec 2014